

**Climate change effects on soil carbon dynamics:
CO₂ flux from water-repellent and
fire-affected soils**

Carmen Sánchez-García

Submitted to Swansea University in fulfilment of the
requirements for the Degree of Doctor of Philosophy

Swansea University

2021



Summary

Climate change is increasing the frequency and intensity of droughts and this is expected to enhance the development of soil water repellency: a very common property of both dry and fire-affected soils. In some regions climate change is also increasing the occurrence and severity of wildfires. Large pulses of CO₂ flux from soil to the atmosphere caused by heavy rainfall events (i.e. the Birch effect) can contribute substantially to annual C emissions from soils. However, the effect of the first rainfall after a drought on water-repellent soils and the first post-fire rainfall event on soil CO₂ flux remain poorly understood.

To address these knowledge gaps this research focuses on: i) investigating the effects of soil water repellency on the CO₂ pulse after wetting; ii) improving understanding of the effects of vegetation fires on post-fire soil CO₂ flux; and iii) studying the role of ash produced naturally during vegetation fires in post-fire soil CO₂ flux.


The results from this research clearly indicate that water repellency is a key controller of the CO₂ pulse following the wetting of dry and fire-affected soils. Both the amount of water and the increase in soil water content after wetting are used as indicators of the magnitude of the Birch effect, but this research suggests that their application in water-repellent soils should be re-evaluated. The findings presented here challenge the conceptual notion that the Birch effect is comprised of one large pulse of CO₂ and highlights the need to incorporate high-frequency observations during the period following wetting to capture the entire CO₂ response to wetting. The results from this thesis suggest that ash is a key player in post-fire C fluxes and should be considered in post-fire C investigations in order to make realistic predictions of the impacts of vegetation fires on C dynamics.

Declarations and statements

Declaration

This work has not previously been accepted in substance for any degree and is not being concurrently submitted in candidature for any degree.

Signed:




Date: 12/03/2021

Statement 1

This thesis is the result of my own investigations, except where otherwise stated. Where correction services have been used, the extent and nature of the correction is clearly marked in a footnote(s). Other sources are acknowledged by footnotes giving explicit references. A bibliography is appended.

Signed:



Date: 12/03/2021

Statement 2

I hereby give consent for my thesis, if accepted, to be available for photocopying and for inter-library loan, and for the title and summary to be made available to outside organisations.

Signed:



Date: 12/03/2021

Authorship declarations

Published article 1: Water repellency reduces soil CO₂ efflux upon rewetting

Located in: Chapter 2

Candidate contribution: The candidate led all aspects of the publication, from conception and design to the acquisition, analysis and interpretation of data. The publication was solely drafted by the candidate.

Co-authors contributions:

1) *Dr Bruna R. F. Oliveira:* Contributed to the acquisition of field data, interpretation of the data and revision of the manuscript.

2) *Dr Jan Jacob Keizer:* Contributed to the acquisition of field data, interpretation of the data and revision of the manuscript.

3) *Prof. Stefan H. Doerr:* Contributed to the design of the work, interpretation of the data and made substantial contribution to revising the manuscript.

4) *Dr Emilia Urbanek:* Contributed to the design of the work, interpretation of the data and made substantial contribution to revising the manuscript.

All the authors approved the final manuscript before publication.

We, the undersigned, agree with the above stated contributions for the published peer-review manuscript contributing to this thesis:

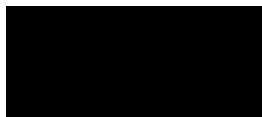
Candidate:



Co-author 1:



Co-author 2:



Co-author 3:



Co-author 4:



Published article 2: The effect of water repellency on the short-term release of CO₂ upon soil wetting

Located in: Chapter 3

Candidate contribution: The candidate led all aspects of the publication, from conception and design to the acquisition, analysis and interpretation of data. The publication was solely drafted by the candidate.

Co-authors contributions:

1) *Prof. Stefan H. Doerr:* Contributed to the design of the work, interpretation of the data and made substantial contribution to revising the manuscript.

2) *Dr Emilia Urbanek:* Contributed to the design of the work, interpretation of the data and made substantial contribution to revising the manuscript.

All the authors approved the final manuscript before publication.

We, the undersigned, agree with the above stated contributions for the published peer-review manuscript contributing to this thesis:

Candidate: 

Co-author 1: 

Co-author 2: 

Article 3 (under second journal revision): Wildland fire ash enhances short-term CO₂ flux from soil in a Southern African savannah

Located in: Chapter 4

Candidate contribution: The candidate led all aspects of the publication, from conception and design to the acquisition, analysis and interpretation of data. The publication was solely drafted by the candidate.

Co-authors contributions:

1) *Dr Cristina Santín:* Contributed to the acquisition of field data by conducting the fieldwork, contributed to the design of the work, interpretation of the data and made substantial contribution to revising the manuscript.

2) *Prof. Stefan H. Doerr:* Contributed to the acquisition of field data by conducting the fieldwork, contributed to the design of the work, interpretation of the data and made substantial contribution to revising the manuscript.

3) *Ms Tercia Strydom:* Contributed to the acquisition of field data by conducting the fieldwork, and to the revision of the manuscript.

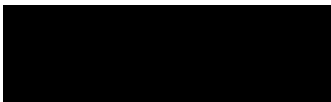
4) *Dr Emilia Urbanek:* Contributed to the design of the work, interpretation of the data and made substantial contribution to revising the manuscript.

All the authors approved the final manuscript before publication.

We, the undersigned, agree with the above stated contributions for the published peer-review manuscript contributing to this thesis:

Candidate: 

Co-author 1: 

Co-author 2: 

Co-author 3: 

Co-author 4: 

Contents page

Summary	ii
Declarations and statements	iii
Authorship declarations.....	iv
Contents page	vii
Acknowledgements.....	ix
List of tables	x
List of figures.....	xii
Abbreviation	xv
Chapter 1. Introduction	1
1.1. Introduction and thesis outline.....	2
1.2. Soil CO ₂ flux.....	3
1.2.1. Sources of CO ₂ in soil	5
1.2.2. Transport of soil CO ₂ to the atmosphere.....	6
1.2.3. Main environmental controllers of soil CO ₂ flux.....	7
1.2.3.1. Effect of temperature on soil CO ₂ flux.....	8
1.2.3.2. Effect of soil moisture on soil CO ₂ flux.....	9
1.2.4. CO ₂ flux upon wetting: the “Birch effect” and mechanisms underlying the CO ₂ pulse following wetting.....	10
1.3. Soil water repellency.....	12
1.3.1. Origins, implications and measurement methods.....	12
1.3.1.1. Implications for soil hydro-geomorphological processes	13
1.3.1.2. Implications for organic matter and soil respiration	14
1.3.2. Soil water repellency and climate change	15
1.4. Fire effect on soil.....	16
1.4.1. Fire effects on relevant soil properties.....	16
1.4.1.1. Physical properties.....	17
1.4.1.2. Chemical properties.....	18
1.4.1.3. Biological properties	20
1.4.2. Effect of ash on fire-affected soils	21
1.4.3. Fire effects on soil CO ₂ flux	23
1.5. Synthesis of research gaps, thesis objectives and structure	24
1.5.1. Research design	26
1.5.2. Research structure.....	26
Chapter 2. Water repellency reduces CO₂ efflux upon rewetting	31
2.1. Introduction	32
2.2. Research design and methods	34
2.2.1. Laboratory methods	37
2.2.2. Field methods	39
2.2.3. Data analysis	40
2.3. Results.....	40
2.3.1. CO ₂ efflux prior to and after wetting	40
2.3.2. Water repellency distribution prior to wetting	46
2.3.3. Soil moisture prior to and after wetting	49
2.4. Discussion.....	53
2.5. Conclusions	57
Chapter 3. The effect of water repellency on the short-term release of CO₂ upon soil wetting	58
3.1. Introduction	59
3.2. Research design and methods	60

3.2.1. Soil sampling and preparations.....	61
3.2.2. Soil wetting and CO ₂ efflux measurements	63
3.3. Results.....	65
3.3.1. CO ₂ efflux before and after wetting.....	65
3.3.2. Cumulative CO ₂ efflux	69
3.3.3. Effect of SWR on wetting, drainage and retained water	70
3.4. Discussion.....	73
3.5. Conclusions	77
Chapter 4. Wildland fire ash enhances short-term CO ₂ flux from soil in a Southern African savannah	79
4.1. Introduction.....	80
4.2. Research design and methods	82
4.2.1. Study sites	82
4.2.3. Laboratory experiments and analysis	85
4.2.4. Data analysis	87
4.3. Results.....	87
4.3.1. CO ₂ flux evolution with time	87
4.3.2. Cumulative CO ₂ flux and respired C.....	89
4.3.3. Chemical properties of soil and ash.....	93
4.3.4. Differential scanning calorimetry (DSC) and thermogravimetry (TG) analysis	97
4.4. Discussion.....	98
4.5. Conclusions	103
Chapter 5. General discussion	104
5.1. Soil water repellency and the Birch effect.....	106
5.1.1. Preferential flow and limited wetting: the main controllers of the Birch effect	106
5.1.2. Further implications of SWR on soil CO ₂ flux.....	106
5.2. Sources of the Birch effect and the importance of high frequency observations.....	108
5.2.1. A dual response to wetting.....	108
5.2.2. Capturing the entire CO ₂ response to drying-wetting events	109
5.3. Wildland fire ash is a key player in post-fire CO ₂ fluxes	110
5.4. Recommendations for future work	112
Chapter 6. Conclusions	114
Appendices.....	116
i) Supplementary material: Chapter 2	116
ii) Supplementary material: Chapter 4	118
Bibliography	121

Acknowledgements

I have many people to thank who have supported me through this work in many different ways:

Special thanks to my supervisors Emilia Urbanek and Stefan Doerr. I am extremely grateful for your continuous support, inspiration and reliability, and for all the great opportunities that you have given me over the past 4 years. Thank you for challenging me and for your always positive and constructive supervision.

Thanks to the Earth Surface Processes Team in Aveiro University, in particular to Bruna Oliveira and Jan Jacob Keizer, for a fun and productive collaboration.

Thanks to Cris Santín for your support and generosity in the Kruger experiment, and to Josie Duffy and Julia Kelly for kindly proofreading long sections of this thesis.

To Danny McCarroll for the help and advice with the statistical analysis, and to the College of Science's technicians for the crucial help during my lab experiments, in particular to Grahame Walters.

To the many wonderful people from the Wallace building that I have been so lucky to share this journey with. I have learned so much from all of you, both personally and professionally. I feel lucky to call many of you friends and to finish this stage with so many great memories and experiences that have made it all worth it. I will not name you all for fear of forgetting someone but finishing this thesis remotely because of the pandemic has not been the same. I have missed our office breaks, lunches at El Pondo, beach barbecues, house warming parties, cinema trips, walks, hundreds of coffees and many other gatherings.

Last but not least, I cannot thank Stewart enough for the unconditional support. To my wonderful Lana for giving me perspective, I adore you. To my Rita, for taking us on countless dog walks around the amazing Swansea and Gower locations regardless of the weather. And to my family in Spain and Scotland who have helped me in so many ways.

List of tables

Table 2.1:	General characteristics of the topsoil (0-5 cm depth) at the two recently burned soils with ash (BwA) and with ash removed (BnoA).	36
Table 2.2:	Average SWC (measured volumetrically (% v v ⁻¹) in the field and gravimetrically (% g g ⁻¹) in the intact cores) before and after wetting with water (water-repellent scenario) and wetting with water and wetting agent (wetable scenario).	49
Table 2.3:	Time to drainage (min after the start of wetting) and drainage as a percentage of total water added under laboratory conditions in burnt soils with ash (BwA) and ash removed (BnoA) under water-repellent (wetted with water) and wettable (wetted with water and wetting agent) conditions.	50
Table 3.1:	General characteristics of the soil from the two study sites (CB: Cefn Bryn, SG: Southgate) before autoclaving.	61
Table 3.2:	Soil water repellency tests results (Doerr, 1998) before and after autoclaving both soils CB and SG at air dry, intermediate and high SWC (% g g ⁻¹).	63
Table 3.3:	Average water retained in soil (expressed as volume in cm ³ and as % of total water applied) and SWC after wetting (% g g ⁻¹) for autoclaved wettable and water-repellent soils from CB and SG.	72
Table 4.1:	Experimental fire characteristics including atmospheric conditions (wind speed, air temperature (Air T) and relative humidity (RH)), maximum temperature range (Tmax) registered in the soil surface and grass (n = 12), residence times > 300 °C, and details of fire impacts on vegetation.	84
Table 4.2:	Carbon (C) respired as CO ₂ (CO ₂ -C; g C m ⁻²) during the 28 day observation period and during the CO ₂ pulse expressed in g of C and as a percentage of the total C (TC).	90

Table 4.3:	Spearman's rank correlation (Spearman's rho) between CO ₂ flux (size of the pulse and cumulative flux) and selected characteristics of the PreF, PostF and PostF_wA samples in mg kg ⁻¹ (total C and N, and dissolved organic carbon (DOC), NH ₄ ⁺ , NO ₃ ⁻ and PO ₄ ; n = 9).	91
Table 4.4:	Chemical properties of the pre-fire (PreF) and post-fire (PostF) soils and of the ash.	94
Table 4.5:	Elemental analysis (mg kg ⁻¹) of the pre-fire (PreF) and post-fire (PostF) soil and the ash.	96
Table 4.6:	Main TG-DSC parameters for the pre-fire (PreF) and post-fire soil (PostF) and in the ash. T50 _Q : temperature at which sample has released half of its total stored energy; Q1, Q2 and Q3: percentage of heat released in each group of thermal oxidation (150 – 375 °C; 375 – 475 °C; 475 – 600 °C respectively).	98

List of figures

Fig. 1.1:	Schematic representation of the perturbation of the global carbon cycle caused by anthropogenic activities and the active carbon cycle.	4
Fig. 1.2:	Schematic illustration of the effect of different moisture conditions on microbial respiration. A) Very dry conditions, B) intermediate moisture availability and C) saturated conditions.	10
Fig. 1.3:	Contour plot showing soil water content distribution and preferential flow in a silt loam water-repellent soil.	14
Fig. 1.4:	Fire effects on biological, chemical and physical soil properties and the estimated temperature ranges at which the changes occur.	17
Fig. 1.5:	Diagram of research design.	26
Fig. 1.6:	(A) CO ₂ analyser system measuring in the site in which the ash layer was left untouched (burnt with ash, BwA), and (B) Burnt site in which the ash layer was removed before the experiments (burnt without ash, BnoA).	27
Fig. 1.7:	Location of the study area from Chapter 2 in Portugal (star).	28
Fig. 1.8:	Map of the sampling locations of the soils used in Chapter 3 from the Gower Peninsula (South Wales, UK). Bottom: close up of the locations: Cefn Bryn, referred to as CB (star), and Southgate, referred to as SG (square).	29
Fig. 1.9:	(A) Experimental burnt plots (EBPs) at the Kruger National Park (KNP). Source: Smit et al. (2010); (B) Grass in the PB3 site before the fire; (C) Burnt grass in the MB1 site after the fire.	30
Fig. 2.1:	Example of representative intact core soil surfaces of the two experimental soils before wetting. BwA (left), BnoA (right).	38
Fig. 2.2:	Response of CO ₂ efflux to wetting, with water (water-repellent scenario) and water mixed with wetting agent (wetable scenario), under laboratory conditions of recently	42

	burned soils with ash (BwA) and with ash removed (BnoA).	
Fig. 2.3:	A) Size of the CO ₂ pulse and B) cumulative efflux after wetting under both field and core-scale in burnt soils with ash (BwA) and ash removed (BnoA) under water-repellent (wetted with water) and wettable (wetted with water and wetting agent) conditions.	43
Fig. 2.4:	Relationship between cumulative flux and the change in SWC with wetting under laboratory conditions (n = 5).	44
Fig. 2.5:	CO ₂ efflux response to wetting under field conditions for burnt soils with ash (BwA) and with ash removed (BnoA). Water-repellent scenario (orange shaded circles) represents wetting with water and wettable scenario (blue open circles) represent wetting with water and wetting agent.	45
Fig. 2.6:	Frequency distribution of SWR represented as the percentage of points for each repellency class in recently burned soils with ash layer (BwA) and ash layer removed (BnoA).	48
Fig. 2.7:	SWC after wetting with depth. A) Burnt soil with ash (BwA) before wetting, B) BwA under wettable scenario, C) BwA under water-repellent scenario, D) Burnt soil with ash removed (BnoA) before wetting, E) BnoA under wettable scenario, F) BnoA under water-repellent scenario.	51
Fig. 2.8:	Representative example of SWC distribution after wetting of intact core samples under laboratory conditions: a) Burnt soil with ash (BwA) under wettable conditions (wetted with water and wetting agent), b) BwA under water-repellent conditions (wetted with water), c) Burnt soil with ash removed (BnoA) under wettable conditions (wetted with water and wetting agent), d) BnoA under water-repellent conditions (wetted with water).	52
Fig. 3.1:	Schematic illustration of rewetting and CO ₂ analyser system.	64
Fig. 3.2:	Response of CO ₂ efflux to wetting above and below the sample	67

	for autoclaved wettable (CB-NWR) and water-repellent (CB-WR) soil from CB under the 4 different rewetting rates.	
Fig. 3.3:	Response of CO ₂ efflux to wetting above and below the sample for autoclaved wettable (SG-NWR) and water-repellent (SG-WR) soil from SG under the 4 different rewetting rates.	68
Fig. 3.4:	Cumulative CO ₂ efflux (top and bottom chambers combined) for wettable (CB-NWR and SG-NWR) and water-repellent (CB-WR and SG-WR) soils from CB and SG under the four different rewetting rates.	69
Fig. 3.5:	Relationship between cumulative CO ₂ efflux (top and bottom chambers combined) and water retained in the soil after wetting in wettable (CB-NWR and SG-NWR) and water-repellent (CB-WR and SG-WR) soils from CB and SG.	70
Fig. 3.6:	Conceptual diagram of the development of wetting patterns with increasing rewetting rate in water-repellent and wettable soils and its effect on the displacement of CO ₂ stored in the pore-space prior to wetting both upwards (emitted from soil surface) and downwards (contributing to CO ₂ entrapment).	74
Fig. 4.1:	Experimental plot diagram for PB1 and PB3 plots (and dimensions for the MB1 plot in brackets).	83
Fig. 4.2:	Response of CO ₂ flux to wetting of pre (PreF) and post-fire soils (PostF) and post-fire soils with added ash (PostF_wA).	88
Fig. 4.3:	Cumulative flux for the duration of the observations (28 d) (total columns) and proportion of the cumulative flux released only during the CO ₂ pulse (filled columns) in the pre-fire (PreF) and post-fire soils (PostF) and in the post-fire soils with added ash (PostF_wA).	92
Fig. 4.4:	A) Relationship between cumulative flux and dissolved organic carbon (DOC) ($p < 0.001$) and B) relationship between cumulative flux and total carbon (TC) ($p = 0.016$).	93

Abbreviation

AS:	Aggregate stability
DIC:	Dissolved inorganic carbon
DOC:	Dissolved organic carbon
EFFIS:	European Forest Fire Information System
FAO:	Food and Agriculture Organisation of the United Nations
IPCC:	Intergovernmental Panel on Climate Change
IRGA:	Infrared gas analyser system
KNP:	Kruger National Park
MED:	Molarity of an ethanol droplet
POC:	Pyrogenic organic carbon
PyC:	Pyrogenic carbon
SOC:	Soil organic carbon
SOM:	Soil organic matter
SWC:	Soil water content
SWR:	Soil water repellency
TG-DSC:	Thermogravimetry-Differential Scanning Calorimetry
WDPT:	Water drop penetration test

1

2

3

4

5

6

7

8

9

10

11

12

13

14

15

16

Chapter 1. Introduction

17

18

19

20

21

22

23

24

25

26

1 1.1. Introduction and thesis outline

2 Wetting of dry and fire-affected soil often results in a large pulse of CO₂ from soil to the
3 atmosphere known as “the Birch effect” and these intense periods of CO₂ release can
4 contribute substantially to annual C emissions from soils (Birch, 1958; Leon et al., 2014). Soil
5 water repellency (SWR), a very common property of dry and fire-affected soils, is expected to
6 become more persistent and widespread due to the increase in the frequency and severity of
7 droughts as a consequence of climate change (Doerr, 2000; Goebel et al., 2011; Schimel,
8 2018).

9 At the same time, climate change is altering fire patterns, with projections expecting an
10 increase in the frequency and severity of fires in water-limited ecosystems as well as an
11 increase in the total area burned in many regions of the world (Doerr and Santín, 2016; Rogers
12 et al., 2020). Heating from fires has a direct impact on C dynamics by altering soil C pools
13 (Santín and Doerr, 2018). Globally vegetation fires are estimated to emit 2.2 Pg C yr⁻¹ to the
14 atmosphere (1997-2016) mostly in the form of CO₂ (van der Werf et al., 2017).

15 Understanding CO₂ emissions from soil in response to wetting is essential in order to
16 accurately predict the impacts of climate change on C dynamics. However, little is known
17 about the influence of wetting both water-repellent and fire-affected soils on CO₂ fluxes,
18 especially during the short-term period following the wetting. This thesis addresses some of
19 the key challenges that potentially limit our understanding of C dynamics following a natural
20 disturbance such as a drought or a fire. The overall aim of this thesis is, therefore, to study the
21 effects of SWR and vegetation fires on soil CO₂ flux upon wetting and some of the main factors
22 driving this response. The term “CO₂ flux after/upon/following soil wetting” used throughout
23 this thesis refers to any CO₂ flux response observed from the beginning of the wetting period
24 onwards (i.e. either during the wetting period or after it).

25 Chapter 1 provides the conceptual framework for the effects of vegetation fires and SWR on
26 soil CO₂ fluxes. The material presented in this chapter aims to set the basis for the more in
27 depth discussions in chapters 2, 3 and 4. The specific objectives and a more detailed structure
28 of this thesis are outlined at the end of Chapter 1. Chapters 2 and 3 are versions of peer-
29 reviewed publications (Sánchez-García et al., 2020a; b) and the material from Chapter 4 forms
30 a third publication currently under second revision in a peer-reviewed journal (Sánchez-García
31 et al., *In submission*). Chapters 2, 3 and 4 have been reformatted to incorporate the published
32 articles and to ensure consistency throughout the thesis. The individual reference lists have
33 been combined into one at the end of the thesis.

1

2 1.2. Soil CO₂ flux

3 Soil plays a critical role in the global carbon (C) cycle storing up to 80% of the total terrestrial C
4 (i.e. ~2400 Gt C) (Lal, 2008). This is approximately three to five times higher than the C stored
5 in vegetation, and double the atmospheric C pool (Fig. 1.1; Latjha et al., 2018). Because of the
6 difficulties in quantifying the C fluxes between different reservoirs (e.g. between ocean and
7 land, and the atmosphere), the C budget estimates are expressed with an average uncertainty
8 of 68% (Friedlingstein et al., 2020). The global carbon budget is updated annually along with a
9 detailed discussion of the uncertainties associated with the individual pools and fluxes
10 (<https://www.globalcarbonproject.org/carbonbudget>).

11 The C balance in the soil is primarily controlled by inputs of C from photosynthesis and plant
12 residue, and outputs of C from soil respiration. Through photosynthesis plants convert
13 atmospheric CO₂ into plant tissue and incorporate some of this C into the soil in the form of
14 organic material (e.g. plant residue, exudates and secretions from living roots) (Kuzyakov,
15 2006). In the soil, microorganisms decompose some of the organic C, producing CO₂ during
16 microbial respiration, which in turn contributes to soil respiration (Schlesinger et al., 2000).
17 Another fraction of the organic C is retained in the soil through the formation of soil organic
18 matter (SOM) (Horwath, 2008). The equilibrium between inputs and outputs of soil C is
19 strongly influenced by climate, which affects the ability of soil to act as a sink or as a source of
20 C, and can have profound effects on the concentration of atmospheric CO₂ (Reischstein et al.,
21 2013).

1

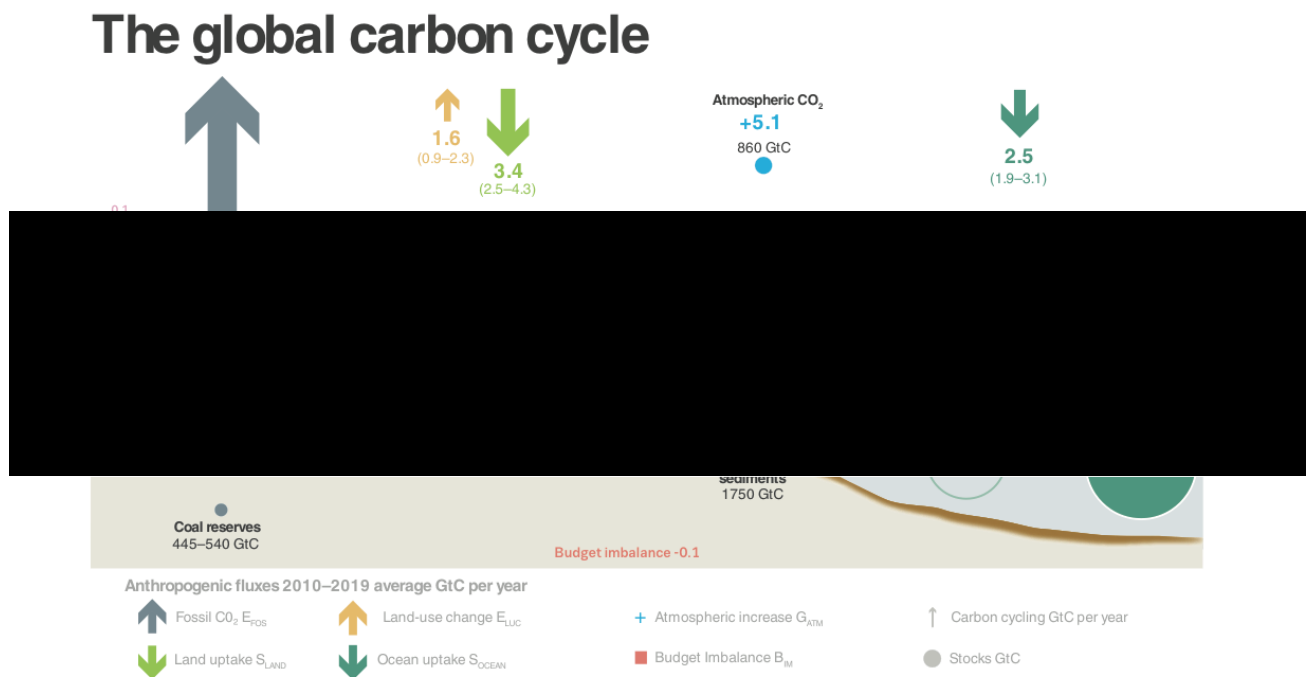


Fig. 1.1. Schematic representation of the perturbation of the global carbon cycle caused by anthropogenic activities (average for 2010-2019) and the active carbon cycle, with fluxes and stocks. Source: Friedlingstein et al. (2020).

2

3 CO₂ emissions from soil (i.e. CO₂ flux) constitute the largest C flux from terrestrial systems. Soil
4 CO₂ flux results from the production and transport of CO₂ from soil to the atmosphere
5 (Longdoz et al., 2000). The estimated global CO₂ flux from soil to the atmosphere is
6 ~300 mg CO₂ m⁻² h⁻¹ (Oertel et al., 2016). However, this figure should be exercised with
7 caution since uncertainty and bias exist when estimating global GHG from soil (Friedlingstein
8 et al., 2020). For example, a standard methodology for measuring and calculating soil CO₂
9 fluxes and C budgets is still to be developed and differences between the tools and scales
10 chosen for the analysis can induce an error of up to 20% (Oertel et al., 2016).

11 In the past decades, soil CO₂ flux has received considerable attention because of the key role it
12 plays in driving feedbacks to climate change (Singh et al., 2011). This growing research has
13 been summarised in several review papers focusing on identifying the sources of soil CO₂
14 (Kuzakov, 2006; Rey, 2015), methods for measuring soil CO₂ (Bruggemann et al., 2011; Subke
15 et al., 2006), estimates of global soil CO₂ fluxes (Bond-Lamberty & Thomson, 2010), effects of
16 climate on soil CO₂ flux (Jarvis et al., 2007; Kim et al., 2012; Vicca et al., 2014) and the main

1 challenges of integrating experimental data with models (Vargas et al., 2010). Increases in soil
2 CO₂ emissions associated with anthropogenic activities (i.e. changes in land-use) have
3 contributed to the increase in atmospheric CO₂ concentration and the subsequent acceleration
4 of climate change (Cox et al., 2000). At the same time, climate change, and global warming in
5 particular, enhances soil respiration, which further accelerates the carbon cycle (Bond-
6 Lamberty & Thomson, 2010).

7

8 1.2.1. Sources of CO₂ in soil

9 CO₂ in soil is produced via biotic sources, like the decomposition of SOM or plant residue, and
10 abiotic sources like photodegradation, carbonate weathering and geogas (Kuzyakov et al.,
11 2006; Rey, 2015). In most cases, the biological sources of CO₂ represent the main source of soil
12 CO₂ flux but in many areas of the planet, especially in dry arid ecosystems, non-biological
13 processes can contribute substantially to the release of CO₂ from soil (Serrano-Ortiz et al.,
14 2011). Disentangling the individual sources of CO₂ is complex because the boundaries between
15 the biological processes of CO₂ production are not clearly delineated (Kuzyakov et al., 2006).
16 However, identifying and quantifying the individual sources of CO₂ is key in order to make
17 accurate predictions of C dynamics.

18 The biological sources of CO₂ can be grouped into: i) microbial respiration (i.e. CO₂ produced
19 from microbial activity during the decomposition of organic materials) and ii) root respiration
20 (Kuzyakov, 2006). At the same time, microbial respiration results from both the decomposition
21 of SOM and plant residue and can occur in either root-free soil (commonly known as ‘basal
22 respiration’) or in soil with direct contact with roots and plant residue (Kuzyakov, 2006).
23 Traditionally, studies have presented soil CO₂ flux as equivalent to soil respiration (i.e. CO₂
24 from biological sources) but, although C losses from abiotic sources comprise a small
25 proportion of global CO₂ fluxes, in many regions they can contribute substantially to soil CO₂
26 flux (Rey, 2015; Serrano-Ortiz et al., 2010). For instance, Rutledge et al. (2010) calculated that
27 abiotic sources were behind 60% of ecosystem C losses in a Mediterranean oak forest in
28 California during the dry season.

29 Photodegradation of SOM is one of the main abiotic sources of CO₂ flux and results from litter
30 decay due to exposure to UV radiation (Rey, 2015). Photodegradation is a key mechanism in
31 arid ecosystems and can result in substantial losses of C to the atmosphere. In drylands, for
32 example, photodegradation has been estimated to accelerate litter decomposition by as much

1 as 23% (King et al., 2012). Another important abiotic source of soil CO₂ is carbonate
2 weathering, which results from the weathering reaction with inorganic C (Eq. 1):



4 The CO₂ contribution from carbonate weathering might be especially relevant under dry
5 conditions where microbial activity is very low (Inglisma et al., 2009) and in ecosystems with a
6 high concentration of carbonates such as salt pans, where inorganic C can comprise up to 95%
7 of total C (Thomas et al., 2014). Geogas is another non-biological source of CO₂ and originates
8 from the movement of CO₂ from the Earth's crust to the soil surface (Rey, 2015). Geogas is
9 typically observed in seismic areas, areas of active volcanic activity and in areas located in
10 geothermal and fault zones (Rey et al., 2012).

11 It is important to note that C fluxes from non-biological sources are often not considered in
12 global C budgets and, although they can be relatively small when compared with soil global
13 CO₂ fluxes, it is important to quantify their contribution to annual budgets properly (Chen et
14 al., 2014). Inaccurate predictions might result in overestimations of the contribution from soil
15 biological sources to global fluxes.

16

17 1.2.2. Transport of soil CO₂ to the atmosphere

18 After production, CO₂ often accumulates in the soil pore-space and is not always released
19 instantly (Maier et al., 2011). Diffusion is assumed to be the main transport mechanism of soil
20 CO₂ and involves the travelling of CO₂ between the soil and the atmosphere, from areas of high
21 concentration towards areas of lower CO₂ concentration (Maier et al., 2012). Current
22 prediction models are based on the general assumption that diffusion is the primary transport
23 mechanism of soil CO₂ and they can fail to reflect other non-diffusive transport mechanisms,
24 which may also play a significant role (Roland et al., 2015). In some biomes such as grasslands
25 and drylands, where wind can easily affect the topsoil layers, non-diffusive transport can
26 greatly influence the movement of CO₂ between the soil surface and the atmosphere (Rey,
27 2015; Roland et al., 2015). One of the important non-diffusive transport processes is
28 atmospheric pumping, which results from the mass movement of CO₂ molecules by changes in
29 atmospheric pressure between soil and the atmosphere, from areas of low pressure to areas
30 of high pressure (Rey, 2015). On a small scale, uneven wind patterns with frequent fluctuations
31 in speed and direction can result in pressure changes and affect soil CO₂ concentration
32 (Redeker et al., 2015). This mechanism, known as the "turbulence effect", might facilitate the

1 exchange of soil CO₂ between soil and the atmosphere (Maier et al., 2012). Thermal
2 convection is another important transport mechanism by which the movement of CO₂ is
3 controlled by fluctuations in temperature. This process is especially relevant in arid regions
4 due to their relatively larger susceptibility to heat fluxes (Ganot et al., 2014; Rey, 2015).

5 Lateral losses of CO₂, mostly in the form of dissolved organic carbon (DOC), dissolved inorganic
6 carbon (DIC) and particulate organic carbon (POC), comprise another relevant form of CO₂
7 movement in soil (Rey, 2015). These mechanisms are mostly controlled by percolation and
8 precipitation and can result in a significant loss of C from the soil to aquatic systems (Janssens
9 et al., 2013; Wan et al., 2014). In certain conditions, like after a wildfire, enhanced soil erosion
10 and the subsequent movement of water-soluble components contained in the ash material,
11 can deteriorate water quality and pose a risk of watershed contamination (Santín et al., 2015;
12 Rhoades et al., 2019).

13 It is important to note that at short timescales, CO₂ flux is not always coupled with the CO₂
14 concentration below ground (Roland et al., 2015). The amount of CO₂ stored in the soil matrix
15 at a given time has been defined as the 'storage flux' (Maier et al., 2011). With wetting, the
16 CO₂ stored in the pore-space can be physically displaced as water refills the air-filled pores and
17 displaces the CO₂-rich air stored in them (Inglima et al, 2009; Liu et al., 2002). This process is
18 particularly relevant after wetting of dry soils, characterised by a large volume of air-filled
19 pores.

20 When measuring soil CO₂ fluxes, most studies apply chamber-based techniques to measure
21 emissions at the soil surface but it should be noted that while CO₂ flux surface chambers are
22 relatively low-priced and suitable to use in different field conditions, they provide limited
23 knowledge about the subsurface CO₂ dynamics (Rochette & Hutchinson, 2005). Recent studies
24 have demonstrated that alternative approaches to measure CO₂ concentration belowground,
25 such as the CO₂ concentration gradient technique, can be successfully used in combination
26 with chamber techniques to provide a more comprehensive image of CO₂ dynamics between
27 soil and the atmosphere (e.g. Riveros-Iregui et al., 2008; Vargas et al., 2010).

28

29 1.2.3. Main environmental controllers of soil CO₂ flux

30 Inputs and outputs of soil C are mainly controlled by climatic factors like soil temperature and
31 moisture (Davidson and Janssens, 2006; Moyano et al., 2013). The effects of soil temperature
32 and moisture on soil CO₂ are closely linked and their interaction (i.e. both temperature and

1 moisture conditions together) shapes CO₂ flux dynamics from soil. However, their individual
2 study is essential to understand and model belowground C dynamics (Qi & Xu, 2001).

3

4 *1.2.3.1. Effect of temperature on soil CO₂ flux*

5 Soil respiration is strongly dependent on soil temperature, with elevated temperatures
6 boosting the decomposition of SOM and, in turn, increasing CO₂ flux (Bradford et al., 2008).
7 Previous research has shown an exponential increase of soil respiration to increasing
8 temperatures of up to 40 °C in most climates where soil moisture is not a limiting factor
9 (Hamdi et al., 2013; Kirschbaum, 2010; Pietikainen et al., 2005). A critical parameter to predict
10 changes in soil respiration due to global warming is the optimum temperature; i.e., the
11 temperature at which maximum soil respiration occurs (Liu et al., 2018). The optimum
12 temperature was traditionally assumed to be around 35 °C in most biomes, however large
13 variations have been reported amongst regions; from optimum temperatures of 30 °C in
14 temperate ecosystems (Blaser and Firestone, 2005) to more than 40 °C in a New Mexican
15 desert (USA) (Parker et al., 1983).

16 The response of microbial respiration to an increase in temperature is temporary and, over
17 time, soil respiration declines to pre-warming values (Eliasson et al., 2005; Luo et al., 2001;
18 Melillo et al., 2002). Two main hypotheses have been proposed to explain this transient effect:
19 i) the depletion of labile pools of SOC with time, also known as the 'substrate-supply
20 hypothesis', and ii) the thermal adaptation of microbial communities to rising temperatures
21 (Bradford et al., 2008). Nonetheless, evidence of both hypotheses is contradictory and, while
22 studies have shown that soil microbial respiration adapts to ambient temperature in both cold
23 climates (Karhu et al., 2014) and also in drylands (Dacal et al., 2019), other studies found no
24 evidence of thermal adaptation in, for example, arctic soils (Hartely et al., 2008). Further
25 research is needed to understand the extent to which both mechanisms facilitate the return of
26 soil respiration to pre-warming values.

27 Regardless of the uncertainties over the effects of thermal adaptation on the decomposition of
28 SOM in different regions of the world, the trend for the soil C response to global warming is
29 consistent and there is a clear consensus that rising temperatures will result in the loss of soil C
30 to the atmosphere (Crowther et al., 2016). A review by Crowther et al. (2016) looked into a
31 substantial number of studies located in North America, Europe and Asia covering 6 different
32 biomes, from arctic permafrost to dry Mediterranean forest. The authors found that the size of
33 the soil C stock and the intensity and duration of the warming are the main factors controlling

1 the response of CO₂ flux to increasing temperatures. As a consequence, substantial C
2 emissions are expected in areas of high-latitude as a result of their large soil C stocks and the
3 predicted fast rates of warming (Benavides et al., 2013; Öztürk et al., 2015).

4

5 *1.2.3.2. Effect of soil moisture on soil CO₂ flux*

6 Soil moisture regulates both the production and transport of CO₂ in soils (Davidson and
7 Janssens, 2006; Vicca et al., 2014). Soil water content influences microbial activity, and hence
8 soil respiration, in various ways. Firstly, water is a resource for microorganisms and controls
9 their functioning and existence (Tecon and Or, 2017). Microorganisms need to exist in
10 equilibrium with the solution surrounding them and, consequently, they lose moisture during
11 dry periods due to the reduction in soil water content (Schimel, 2018). This moisture loss can
12 result in the failure of cellular functions, reductions in microbial respiration and even in
13 microbial death (Jansson and Hofmockel, 2020; Moyano et al., 2013). Secondly, water acts a
14 solvent since the majority of the substrate essential for microbial metabolic functions is water-
15 soluble (Tecon and Or, 2017). Finally, water is the main transport mechanism for the diffusion
16 of substrates and microorganisms (Schimel, 2018). The connection between water-filled pores
17 is vital for effective substrate diffusion to microbes and, as soil moisture decreases, the water
18 films acting as transport paths become thinner and may fracture, constraining the diffusion of
19 substrate (Bailey et al., 2017; Moyano et al., 2013).

20 In general, microbial activity is reduced at both ends of soil moisture content; i.e. at very dry or
21 at saturated conditions (Fig. 1.2, A and C, respectively). Maximum microbial respiration occurs
22 at some point with intermediate water content where the ratio of water to oxygen availability
23 is optimal (Fig. 1.2, B).

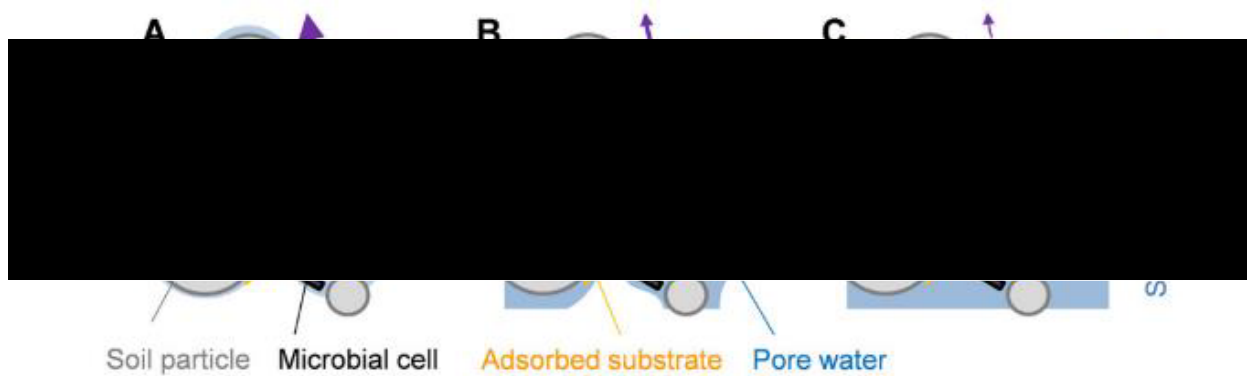


Fig. 1.2. Schematic illustration of the effect of different moisture conditions on microbial respiration. A) Very dry conditions, B) intermediate moisture availability and C) saturated conditions. Source: Moyano et al. (2013).

1

2 1.2.4. CO₂ flux upon wetting: the “Birch effect” and mechanisms underlying the CO₂ 3 pulse following wetting

4 The Birch effect can be defined as the sudden flush of CO₂ to the atmosphere commonly
5 observed after the start of wetting of dry soil. It was first characterized by Birch (1958) who
6 observed a rapid increase in organic matter decomposition following the wetting of dry soils.
7 He also observed a repetition of this pattern with successive drying-wetting events, although
8 the magnitude of the flush decreased with each drying-wetting cycle.

9 This transient increase in CO₂ flux following wetting has been extensively observed in a variety
10 of ecosystems and soil types like drylands (Sponseller, 2007; Thomas & Hoon, 2010; Thomas et
11 al., 2014), savanna soils (Andersson et al., 2004), forest soils (Muhr et al., 2008; Waring &
12 Powers, 2016), Mediterranean soils (Lado-Monserrat et al., 2014; Rey et al., 2016) and also
13 after the wetting of burnt soils (Castaldi et al., 2010; Marañón-Jiménez et al., 2011). The Birch
14 effect has been the subject of several reviews about the effects of drying and rewetting on C
15 mineralization (Canarini et al., 2017; Jarvis et al., 2007; Kim et al., 2012; Muhr and Borken,
16 2009) and on modeling the CO₂ efflux response to changes in moisture (Moyano et al., 2013;
17 Vicca et al., 2014).

18 Despite the growing attention, the processes behind the sudden increase in CO₂ upon the
19 beginning of wetting remain a subject of debate. The sources of the flush of CO₂ have been
20 mainly identified with i) decomposition of microbial biomass killed during the dry period that
21 can accumulate in soil and become a source of easily accessible substrate after the wetting; ii)

1 osmotic stress during the wetting event resulting in cell lysis which provides accessible
2 substrate for surviving microorganisms; iii) microbial access to OM previously protected in soil
3 aggregates disrupted by the drying-wetting event; iv) increase in microbial biomass due to the
4 increase in water availability; v) increase in root exudates from drought-surviving plants; and
5 vi) the physical displacement of CO₂-rich air from air-filled pores with infiltration (Fraser et al.,
6 2016; Jarvis et al., 2007; Schimel, 2018; Kim et al., 2012).

7 The size of the CO₂ pulse following wetting, i.e. the amount of C mineralized, is influenced by
8 several environmental factors. First, the length of the dry period preceding the wetting has
9 been positively linked to the size of the pulse; i.e. longer and more severe droughts result in
10 higher CO₂ pulses upon wetting (de Nijs et al., 2018; Meisner et al., 2017). The intensity of the
11 wetting event (i.e. the amount and rate of water application) has been described as another
12 determining factor of the size of the Birch effect (Borken and Matzner, 2009) but only when
13 soil water content prior to wetting is below a threshold value (Lado-Monserrat et al., 2014).
14 Another factor influencing the size of the CO₂ pulse is the frequency of the drying-wetting
15 events, with CO₂ pulses decreasing with consecutive drying-wetting cycles (Fierer and Schimel,
16 2002; Sponseller, 2007).

17

18 Although the duration of the CO₂ pulses following drying-wetting is short-lived, their
19 magnitude can be relatively large and might represent an important mechanism of C loss to
20 the atmosphere (Castaldi et al., 2013; Leon et al., 2014). We now understand that more CO₂ is
21 released from soil during drying-wetting cycles than at intermediate and constant moisture
22 and that even sporadic drying-wetting events increased the overall CO₂ released from soil
23 compared to those under continuous moist conditions (Miller et al., 2005; Xiang et al., 2008).
24 In savannah soils, for instance, CO₂ pulses occurring after drying-wetting represented 25% of
25 the total C loss to the atmosphere annually (Fan et al., 2015). With climate change already
26 increasing the frequency and intensity of drying-wetting cycles in some parts of the world
27 (Coumou et al., 2012; Trenberth et al., 2013), these quick and large episodes of CO₂ release
28 constitute additional soil C losses to those already occurring as a result of other climatic
29 changes such as increased warming (Smith et al., 2017).

30

1 1.3. Soil water repellency

2 1.3.1. Origins, implications and measurement methods

3 Soil water repellency (SWR), or hydrophobicity, is a transient property found in many dry soils
4 that reduces the soil infiltration capacity (Dekker et al., 2001; Doerr, 2000). SWR is caused by
5 the coating of soil particles with water-repellent compounds from sources like living and
6 decomposing vegetation, SOM and soil fungi (Doerr et al., 2000). Soils under some evergreen
7 vegetation have been traditionally associated with SWR, particularly those with high contents
8 of resins and waxes like conifers, pines or eucalyptus, but SWR has been also observed under a
9 range of other vegetation like some heathland and shrublands species (Doerr et al., 2006).

10 SWR is mainly controlled by soil moisture and, in soils prone to water repellency, it develops
11 under a critical soil water content level (Doerr and Thomas, 2000). This critical soil water
12 content value varies widely depending on the soil from as low as 2% observed in a sandy dune
13 soil in the Netherlands (Dekker et al., 2001) to around 40% observed in a silty loam soil from a
14 grassland site also in the Netherlands (Dekker and Ritsema, 1995). In most soils, water
15 repellency disappears above the moisture threshold (Dekker and Ritsema, 1994).

16 Soil texture also influences the susceptibility of soils to develop water repellency. Coarse-
17 textured soils, like sandy soils, are more prone to developing water repellency; however, under
18 appropriate conditions most soils will show some degree of repellency (Dekker and Ritsema,
19 1994; de Jonge et al., 2009).

20 Another controlling factor of SWR is temperature, with SWR having an affinity for higher
21 temperatures (Doerr et al., 2000). Apart from soil drying, soil heating from high temperatures
22 can result in the polymerisation of organic molecules to form water-repellent ones (Giovannini
23 and Lucchesi, 1983; Savage, 1974). Heating can also melt and release waxes from the OM
24 causing them to attach to soil particles (Franco et al., 2000). These physicochemical changes
25 are also observed during soil heating from vegetation fires, where induced or enhanced SWR
26 repellency has been extensively observed (DeBano, 2000; Doerr, 2000). Most studies on fire-
27 induced water repellency have been conducted in fire-prone ecosystems, often characterised
28 by dry and warm summers, which provide the ideal conditions for development of water
29 repellency. However, recent evidence has shown the development of SWR following fire in less
30 anticipated areas such as peatlands (Kettridge et al., 2017; Moore et al., 2017). Besides
31 inducing SWR, extreme temperatures (~300 °C) reached during vegetation fires can result in
32 the opposite effect and reduce or eliminate SWR through volatilisation and combustion of

1 organic molecules (DeBano et al., 2000; Doerr et al., 2004). A more detailed description of the
2 effects of fire on SWR is given in section 1.4.1 of this chapter.

3 SWR influences key soil processes related with hydrological and geomorphological functions
4 and the intensity of these effects depends mostly on the severity of SWR (Doerr et al., 2000;
5 Shakesby et al., 2000). SWR is commonly classified into categories from wettable to extremely
6 water-repellent. Two common techniques to assess the severity of SWR are the “Water Drop
7 Penetration Test” (WDPT) and the “Molarity of an Ethanol Droplet” (MED) (Doerr, 1998). The
8 WDPT measures the delay in infiltration of droplets placed on the soil surface, which can range
9 from seconds to several hours (Doerr, 1998). The MED test technique measures the soil
10 surface tension by placing drops on the surface from ethanol solutions at different
11 concentrations. Both the WDPT and MED test are low-cost and easy to carry out both *in situ*
12 and in the laboratory. Another laboratory technique often used to assess the severity of SWR is
13 the “Contact Angle Method”, which measures the contact angle between the soil surface and a
14 drop of water (Bachmann et al., 2003).

15

16 *1.3.1.1. Implications for soil hydro-geomorphological processes*

17 SWR affects soil infiltration in various ways and these can have important effects on basic soil
18 hydro-geomorphological functions. First, SWR can delay infiltration from seconds to hours,
19 which during rainfall events can lead to ponding of water in the soil surface until a favourable
20 infiltration path is found or until overland flow develops (Doerr et al., 2000; Shakesby et al.,
21 2000). For example, infiltration was reduced by up to 70% in water-repellent soils under a
22 eucalyptus plantation in north-central Portugal compared with wettable ones (Leighton-Boyce
23 et al., 2007). The resulting run-off not only reduces infiltration but also has the potential to
24 increase soil erosion (Doerr et al., 2009). Although isolating the effects of SWR on soil erosion
25 from other factors such as vegetation and litter cover is complex, the positive relationship
26 between SWR and soil erosion has been extensively reported (e.g. Jordán et al., 2009;
27 Shakesby et al., 2000; Osborn et al., 1964).

28 Infiltration patterns in water-repellent soils tend to differ from those in wettable soils mostly
29 due to preferential infiltration. Preferential infiltration is very common in water-repellent soils
30 with water infiltrating mostly along wettable patches, macropores, cracks, roots and stones
31 (Ritsema and Dekker, 1994; Urbanek et al., 2015). In these cases, most of the water flow
32 moves towards deeper areas along constricted sections of the soil matrix (Dekker et al., 2001).
33 As a consequence, even after apparent infiltration through the water-repellent soil surface,

1 the wetting front might by-pass the top layers and leave large areas of the soil dry, resulting in
2 large moisture variations between close soil areas (Dekker and Ritsema, 1996; Urbanek et al.,
3 2015). As shown in Fig. 1.3, areas of low soil water content usually correspond to areas of
4 severe water repellency, while areas of preferential flow coincide with areas of low degree of
5 repellency (Ritsema and Dekker, 1995).

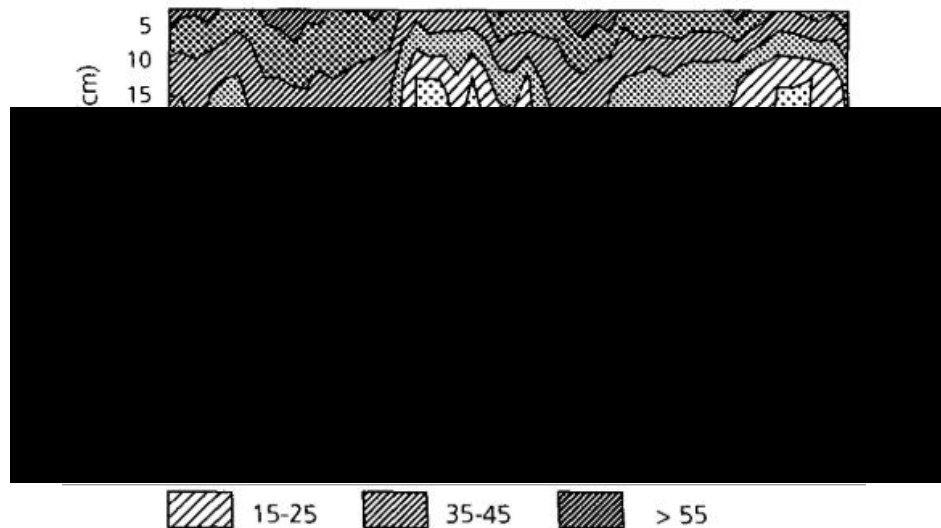


Fig. 1.3. Contour plot showing soil water content distribution and preferential flow in a silt loam water-repellent soil. Source: Ritsema and Dekker (1995).

6

7 1.3.1.2. Implications for organic matter and soil respiration

8 While the effects of SWR on soil hydrology and geomorphology are well documented, the
9 implications of SWR on relevant soil C processes are still not well understood (Goebel et al.,
10 2011). On the one hand, limited infiltration in water-repellent soils favours aggregate stability
11 and protects the OM inside the aggregate from microbial mineralisation (Bachmann et al.,
12 2008; Goebel et al., 2005; Hallet et al., 2001). For instance, Arcenegui et al. (2008) observed
13 increased aggregate stability in burnt Mediterranean soils and attributed this to enhanced
14 water repellency after the fire. On the other hand, enhanced soil erosion in water-repellent
15 soils might result in substantial losses of SOM by, for example, surface runoff and slopewash
16 (Lal, 2003; Shakesby et al., 2000).

17 Evidence of the direct effects of SWR on C mineralization and, hence, soil respiration remains
18 sparse. Increasing degrees of repellency have been positively related to reduced respiration
19 rates (Goebel et al., 2007). Following dry periods, a few studies reported slow recovery of soil

1 moisture, and, in turn, of soil respiration after abundant rainfall and attributed this to water
2 repellency (e.g. Chowdhury et al., 2011; Muhr et al., 2010; Schindlbacher et al., 2012). For
3 instance, Muhr et al. (2008) during an incubation experiment with soil from a Norway spruce
4 site in Bavaria (Germany) reported low soil water content after wetting dry soil for several
5 weeks compared with continuously moist soil. In another study, Muhr et al. (2010) subjected
6 undisturbed soil columns to different drought treatments and soil water content (SWC) did not
7 increase back to pre-drying levels after wetting. In another long-term drought simulation study
8 on heathland soils from NW Wales (UK), central Netherlands and East Jutland (Denmark), soil
9 moisture also failed to return to pre-drying conditions even after sufficient rainfall was applied
10 (Sowerby et al., 2008). The authors suggested that preferential flow, developed as a result of
11 drought-induced water repellency, prevented soil moisture from reaching values similar to
12 those before drying.

13 The typical heterogeneous distribution of moisture, common in water-repellent soils, results in
14 the discontinuity of water films, limiting substrate and oxygen diffusion and affecting soil C
15 mineralization (Dekker et al., 2001; Goebel et al., 2011). During a field experiment in forest and
16 a grassland sites in eastern England, Urbanek and Doerr (2017) observed higher CO₂ fluxes in
17 soil with patchy water repellency, and hence uneven moisture distribution, than in severely
18 repellent soils. The authors suggested that dry water-repellent areas, characterised by air-filled
19 pores and low microbial respiration, might favour gas diffusion and the exchange of CO₂ with
20 the atmosphere, enhancing microbial respiration in the surrounding wet areas (Or et al., 2007).

21

22 1.3.2. Soil water repellency and climate change

23 SWR is particularly sensitive to changes in climate given its dependency on soil moisture and
24 temperature and its development might be enhanced by the increase in the frequency and
25 severity of droughts due to climate change (Goebel et al., 2011). In general, SWR can be
26 anticipated in those areas where rising temperatures, along with an increase in the frequency
27 of dry periods, are expected (Goebel et al., 2011). Often, SWR does not easily revert with
28 wetting and this might compromise the infiltration capacity of soils beyond the end of the dry
29 period (e.g. Muhr et al., 2010; Sowerby et al., 2008). Robinson et al. (2016) presented evidence
30 of irreversible wetting after drought simulation experiments, which prevented the soil from
31 wetting even during the winter months. The theory of Alternative Stable States (ASS), which
32 supports the idea that ecosystems can exist in many stable states and after a natural
33 disturbance they may appear in a different state than prior to the disturbance, has been used

1 as an explanation for the long-term changes induced by drought (Beisner et al., 2003;
2 Robinson et al., 2016). Therefore, there is a risk that climate-induced SWR might lead to semi-
3 permanent shifts in soil even after the addition of water, with important implications for
4 aspects like microbial community structure, plant productivity and even induce changes in
5 vegetation (Goebel et al., 2011).

6

7 1.4. Fire effect on soil

8 Vegetation fires are a natural ecosystem process that affects 340 million ha of land every year
9 (EFFIS, 2021). Fire induces changes to soil by, for example, altering vegetation patterns and
10 enhancing soil erosion, both by wind and water (Shakesby and Doerr, 2006). This section
11 focuses mainly on the effects of 'natural' fires (i.e. wildfires) on soil as opposed to 'human-
12 induced' fires, which are mainly used as a land management tool. It is important to note that
13 wildfires often begin with a human ignition, unintentional or deliberate, but they mostly share
14 the characteristics of those wildfires originated naturally by, for example, lightning (Santín and
15 Doerr, 2016).

16

17 1.4.1. Fire effects on relevant soil properties

18 Fire affects important physical, chemical and biological soil properties and the magnitude of
19 these changes is mostly controlled by fire severity and soil type (DeBano, 1991; González-Pérez
20 et al., 2004; Matáix-Solera et al., 2011). The transfer of heat to soil during a fire is largely
21 responsible for most of the direct effects on soil properties; however, thermal conductivity in
22 soil is poor so these changes are usually located in the top centimetres of the soil (Certini,
23 2005). Studies looking at the immediate effects of fire on soil often focus on the maximum
24 temperature reached in the topsoil layers during the fire (Santín and Doerr, 2016; Fig. 1.4).

25

26

27

28

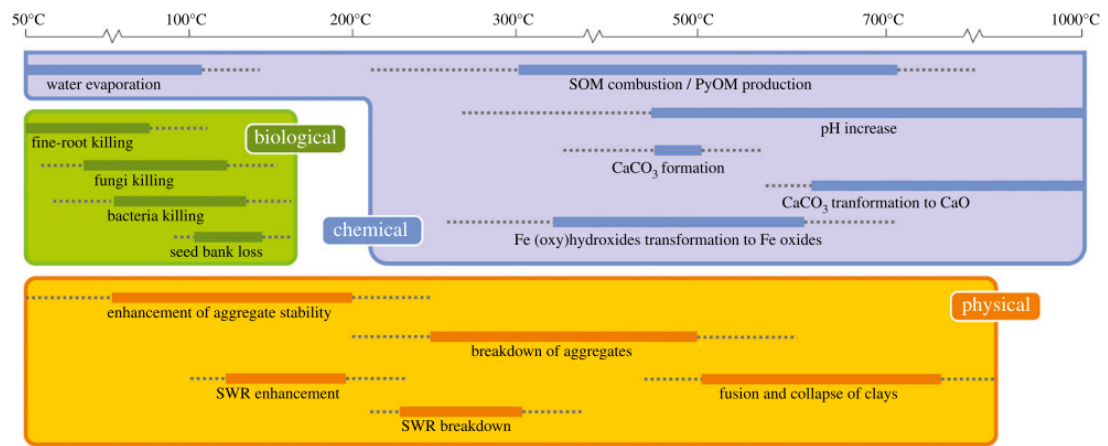


Fig. 1.4. Fire effects on biological, chemical and physical soil properties and the estimated temperature ranges at which the changes occur. Modified from Santín and Doerr (2016).

1

2 1.4.1.1. Physical properties

3 Aggregate stability (AS) is one of the main physical properties that can be affected by fire. The
 4 magnitude of this effect depends mainly on fire severity and on soil characteristics like SOM,
 5 water repellency and texture (Matáix-Solera et al., 2011). Contrasting results are reported
 6 when studying the relationship between fire and AS. While most studies report a decrease in
 7 AS after fire (e.g. Giovannini et al., 1987; Matáix-Solera et al., 2002; Úbeda et al., 1999), others
 8 have observed an increase in structural ability due to fire (e.g. Arcenegui et al., 2008; Fox et al.,
 9 2007) and even no direct effect of fire on AS (e.g. García-Oliva et al., 1999; Jordán et al., 2011;
 10 Valzano et al., 1997). In high severity fires the combustion of OM, which in most cases is the
 11 main binding agent between soil particles, generally explains the decrease in AS (Soto et al.,
 12 1991). In some cases, for example when fires spread mostly through the crown of the tress,
 13 soil properties are not directly affected and hence no changes in AS are observed following the
 14 fire (Matáix-Solera et al., 2011). Opposite to this, when adequate temperatures are reached as
 15 to produce thermal alterations in the clay fraction, more resistant aggregates can be created
 16 with the consequent increase in AS (Giovannini and Lucchesi, 1997).

17 Another important physical property that can be substantially affected by fire is soil water
 18 repellency (SWR). As seen in section 2, SWR reduces the affinity of soil to wetting (Doerr,
 19 2000). Changes in soil wettability after a fire are very common, being mainly attributed to the
 20 thermal degradation of SOM due to heating (DeBano, 2000). Fire can affect soil wettability in
 21 various ways depending on the initial soil wettability and the temperature reached in the soil.

1 Heating at around 200 °C has been shown to enhance SWR, whereas a breakdown in SWR
2 typically occurs at temperatures above 300 °C (DeBano, 1981). For example, Doerr et al. (2004)
3 in naturally water-repellent soil from a long-unburnt eucalyptus stand in south-eastern
4 Australia observed both a substantial increase in SWR with heating and an elimination of SWR
5 with temperatures above 260 °C. The authors noticed that the duration of heating was a
6 controlling factor in the elimination of SWR, which occurred at lower temperatures (260 –
7 300 °C) in soils undergoing longer heating duration (40 min) and vice versa. While several
8 studies have reported the development or enhancement of SWR following a fire in wettable or
9 slightly water-repellent soils (e.g. Arcenegui et al., 2008; Huffman et al., 2001; Matáix-Solera
10 and Doerr, 2004), others observed a reduction in SWR in previously water-repellent soils
11 (Doerr et al., 2006; García-Corona et al., 2004). In some other cases, fire might not largely
12 affect SWR if the soils were already extremely water-repellent before the fire and
13 temperatures did not exceed the SWR breakdown threshold (Doerr et al., 1998; 2006). For
14 instance, fire had little effect on the persistence of SWR in extensive areas of a burnt water-
15 repellent soil under dry eucalyptus woodland near Sydney (Australia) (Doerr et al., 2006).

16

17 *1.4.1.2. Chemical properties*

18 The evaporation of soil moisture in the topsoil as a consequence of heating is perhaps one of
19 the most intuitive direct effects of fire on soil. Although SWC increases the soil thermal
20 conductivity, it also prevents soil temperature increasing drastically during heating, often not
21 exceeding 100 °C until total soil moisture evaporation (Campbell et al., 1994; Santín and Doerr,
22 2016). Burning of the aboveground vegetation during severe fires further affects soil moisture
23 dynamics. First, the unprotected bare soil is more susceptible to heating from solar radiation
24 and will likely dry faster than soils with vegetative cover (Moody et al., 2007; Shakesby and
25 Doerr, 2006). In addition, the elimination of the vegetative cover reduces the water storage
26 capacity of soil, facilitating runoff and soil erosion (Malvar et al., 2001; Moody et al., 2013).

27 Another chemical property altered by fire is soil pH. Increases in pH are normally reported
28 immediately after the fire and are mainly attributed to the degradation of OM and ash
29 deposition (Bodí et al., 2014). The changes in pH are usually transient and the recovery time is
30 associated with the removal and redistribution of ash in the landscape; ranging from only
31 three months, as a result of the removal of ash by wind in a Mediterranean heathland in
32 south-western Spain (Jordán et al., 2010), to up to five years in semi-arid ecosystems in north-
33 western Australia (Muñoz-Rojas et al., 2016). In the short-term, the increase in soil pH along

1 with the usual increase in nutrient availability immediately after a fire might induce changes in
2 microbial community structure and abundance (Matáix-Solera et al., 2009; Perkiomaki et al.,
3 2003).

4 Fire can also affect soil nutrient levels, distribution and processes. During a fire, nutrients
5 might be volatilized or dispersed in smoke in the form of particulate compounds (Neary et al.,
6 1999), whereas the remaining nutrients can be located in the ash produced during the burning
7 (Bodí et al., 2014). Ash deposition results in a large input of nutrients to soil traditionally
8 known as the “fertilizing effect” (González-Perez et al., 2014). Increases in phosphorus (P) and
9 inorganic N, both in ammonium (NH_4^+) and nitrate (NO_3^-) forms, are frequently observed after
10 fire (e.g. Feig, 2004; Hamman et al., 2008; Muñoz-Rojas et al., 2016). For instance, Andersson
11 et al. (2004) in a field experiment observed increases in soil NO_3^- immediately after the fire in
12 African savannah woodland in Ethiopia. Increases in the content of other elements such as
13 calcium (Ca), magnesium (Mg) and potassium (K) are also commonly reported (Zimmerman
14 and Frey, 2002).

15 The impact of fire on soil C stocks has received substantial attention in recent years because of
16 its relevance to the global C cycle. SOC is the primary component of soil C and accounts for up
17 to 58% of SOM (Heaton et al., 2016; Scharlemann et al., 2014). Fire can affect soil C directly, as
18 a result of soil heating, and indirectly by modifying factors controlling the concentration and
19 characteristics of SOC (Santín and Doerr, 2018). One of the immediate effects of fire on SOC is
20 the change in concentration. Contrasting results have been reported previously when studying
21 the direction of these changes, which only evidences the broad range of soil and fire types
22 (Santín and Doerr, 2018). In general, the effect on SOC in organic soils has been more uniform
23 than in mineral soils. Most studies report a reduction in the amount of SOC as a result of the
24 combustion of the top organic layer (e.g. Czimczik et al., 2005; De Baets et al., 2016). For
25 example, Startsev et al. (2017) observed a reduction in dissolved organic C (DOC) in organic
26 soils from Central Siberia after a fire followed by an increase in DOC during the post-fire
27 recovery period. In mineral soils, decreases in SOC are often observed after substantial soil
28 heating (Badía et al., 2014; Miesel et al., 2015; Vega et al., 2013). For instance, both Lozano et
29 al. (2016) and Vega et al. (2013) sampled shrubs and pine forest soils after fires and reported
30 losses in SOC only at high burn severities, while no losses were observed at lower fire
31 severities. In some occasions, particularly when soils experience low-intensity fires, fire might
32 not alter the SOC concentration substantially (Alcañiz et al., 2018; Alexis et al., 2007; Novara et
33 al., 2013). Increases in SOC after fire are also common in mineral soils mostly due to the input

1 of ash or from charred or dead remains of vegetation (González-Pérez et al., 2004; Novara et
2 al., 2011).

3 Besides changes in the concentration of SOC, fire can induce profound changes to the
4 characteristics of SOC when soil temperatures reach 200 - 300 °C (Santín and Doerr, 2018).
5 Perhaps the most relevant change in SOC is the production of recalcitrant compounds, known
6 as pyrogenic C (PyC), which results from heating of SOM and/or the incomplete combustion of
7 biomass (González-Pérez et al., 2004; Santín et al., 2015). PyC represent a C sink and buffer
8 CO₂ emissions from soil during fires (Jones et al., 2019). Immediately after the fire, most of the
9 PyC is found on the soil surface as part of charred materials and in the ash layer (Santín et al.,
10 2012). Although PyC is highly resistant to biodegradation, a fraction of it can also be water
11 soluble and easily mineralized (Jones et al., 2019; Santín et al., 2016).

12 The indirect effects of fire on SOC are mostly related to post-fire changes in hydro-
13 geomorphological processes; i.e. changes in vegetation cover and erosion processes that, in
14 turn, affect the accumulation and characteristics of SOC (Shakesby and Doerr, 2006; Santín and
15 Doerr, 2016). Given that vegetation contributes substantially to SOC concentration, alterations
16 in the vegetative cover can result in large changes in SOC stocks (Santín and Doerr, 2018). Fire
17 has been traditionally used to managed land-use, for example to convert woodlands and
18 pasturelands into farmland, however it is estimated that up to 50% of the SOC in the first 1 m
19 of soil can be lost after converting native vegetation to cropland (Houghton et al., 2012; Santín
20 and Doerr, 2016). Considering that SOC at the surface layer is particularly susceptible to soil
21 erosion during the post-fire period, enhanced erosion in burnt soil might contribute to local
22 losses of SOC (Lal, 2005; Shakesby and Doerr, 2016). However not all the SOC lost by erosion
23 constitutes a net loss since some of this C is reallocated and redeposited elsewhere in the
24 landscape (Santín and Doerr, 2018; Shakesby et al., 2015).

25

26 *1.4.1.3. Biological properties*

27 Fire affects soil biological processes through, for example, killing of fine-roots, reductions in
28 microbial biomass and by causing losses in the seed bank (Fig. 1.4). For the purpose of this
29 thesis, this section focuses on the effect of fire on soil microbiology since it directly regulates
30 soil C mineralization and, in turn, soil respiration. Fire can have substantial effects on soil
31 microbial activity directly, by heating, or indirectly by altering processes essential for microbial
32 functioning like nutrient and moisture availability (Mataix-Solera et al., 2009). The changes to
33 soil properties induced by fire linked to soil microbial processes, particularly those related to

1 vegetation dynamics, soil temperature and moisture dynamics and the typical increase in soil
2 erosion, are closely linked (González-Perez et al., 2014; Hart et al., 2005; Neary et al., 1999).

3 The amount and duration of heating in the soil surface are the main controlling factors of soil
4 microbiology (Holden et al., 2016; Prieto-Fernández et al., 1998). Negative impacts of fire on
5 soil microbes have been widely observed, as shown in a recent meta-analysis by Pressler et al.
6 (2018). In general, many microbes will be killed when temperatures exceed 70 -80 °C and most
7 organisms will disappear completely above 115 - 150 °C (Matáix-Solera et al., 2009). The range
8 of maximum temperatures reached during fires is wide, typically ranging from 200 - 300 °C in
9 forest fires (up to 500 - 700 °C when heavy fuels are burnt) to 300 – 700 °C in shrublands and
10 200 - 300 °C in grasslands (Matáix-Solera et al., 2009; Neary et al., 1999). Soil microbes can be
11 highly sensitive to increasing temperature (threshold temperature of 40 - 121 °C) and often the
12 temperature reached in the topsoil during a fire is enough to cause disturbances in
13 microbiology (Pressler et al., 2018). Soil moisture also controls the impact of fire on microbes
14 because the presence of soil water prevents temperature from going over 95 °C during the fire
15 until the soil is dry (Matáix-Solera et al., 2009). Nonetheless, it is important to note that water
16 enhances thermal conductivity in the soil when compared to the poor conductivity observed in
17 dry soils, and that moist heat is more lethal for microorganisms than dry heat (Dunn et al.,
18 1985).

19

20 1.4.2. Effect of ash on fire-affected soils

21 Ash is a product of vegetation fires and, after a fire, it is found partially or completely covering
22 the soil (Bodí et al., 2014). As mentioned earlier ash deposition can have important effects on
23 key soil processes by, for example, inducing changes in soil pH and adding easily accessible
24 nutrients. Further changes to physical properties after ash deposition include, for instance,
25 modifications of the soil color (Ulery and Graham, 1993). Inputs of ash and charred material
26 often darken the soil surface, decreasing its albedo (Massman et al., 2008). Water retention is
27 another property that is commonly modified by ash deposition. This is because the highly
28 porous and swelling characteristics of the ash have the ability to intercept and store rainfall
29 (Bodí et al., 2014; Stoof et al., 2010). In a rainfall simulation study on a severely burnt forest in
30 Montana (USA), Woods and Balfour (2008) reported an increase in infiltration of
31 approximately 2 cm in soils covered with a layer of ash (1 – 3.5 cm) compared with burn soil in
32 which the ash layer had been removed.

1 Ash might also modify soil water repellency. On the one hand, reductions in SWR have been
2 observed when a layer of wettable ash, with high water storing capacity, covers a water-
3 repellent soil and prolongs the contact time between the moist and the dry water-repellent
4 layers (Nyman et al., 2014). On the other hand, increases in SWR might occur when water-
5 repellent ash is incorporated into the soil by wind or bioturbation (Bodí et al., 2014).

6 Ash deposition can also affect important post-fire soil hydrological processes like overland flow
7 and erosion (Cerdá and Doerr, 2008). The direction of these effects is mainly a function of the
8 characteristics of the ash layer (e.g. depth, composition and particle size), the type of soil (e.g.
9 particle size, texture) and the type of wetting event (e.g. duration, magnitude and intensity)
10 (Bodí et al., 2014). In many cases, a layer of ash has reduced overland flow and runoff
11 generation as a result of its high water storing capacity (Martin and Moody, 2001; Girona-
12 García et al., 2007; Woods and Balfour, 2008). Opposite to this, reductions in infiltration, and
13 the concomitant increase in overland flow and runoff, have been attributed to clogging of the
14 soil pores with ash particles after ash deposition (Nyman et al., 2013). Wood and Balfour
15 (2010) observed that clogging of the soil pores in a sandy soil depended fundamentally on the
16 thickness of the ash layer, with thinner layers (1 cm) resulting in pore clogging when compared
17 with thicker (2 and 5 cm) ash layers.

18 With regards to the effect of ash input on soil microbiology, it is traditionally assumed that the
19 input of water-soluble nutrients, along with the increase in pH, stimulates soil microbial
20 activity and, hence, soil respiration (Raison, 1979; Mataix-Solera et al., 2009). However the
21 literature shows contrasting results. While some studies have observed an increase in
22 microbial activity following ash input (Andersson et al., 2004; Badía and Martí, 2003; Raison
23 and McGarity, 1980), others have found opposite results (García-Oliva et al., 1999; Hogg et al.,
24 1992) or even detected no changes following the addition of ash to post-fire soils (Raison and
25 McGarity, 1980). These varying results are evidence of the wide range of interacting variables
26 that have an effect on soil microbes such as the type and amount of fuel burnt, fire
27 characteristics, soil type and post-fire climatic conditions. Isolating the effects of ash on soil
28 microbial activity is complex and most available studies have been done under controlled
29 conditions using laboratory-produced ash. The effect of ash produced *in situ* during a fire on
30 microbial activity is a subject that requires further attention.

31

1 1.4.3. Fire effects on soil CO₂ flux

2 Climate change is altering wildfire patterns and current projections expect an increase in fire
3 frequency and severity in water-limited ecosystems, while the opposite is expected in fuel-
4 limited ecosystems with already increasing aridity (Andela et al., 2017; IPCC, 2000; Rogers et
5 al., 2020). Vegetation fires are estimated to emit 2.2 Pg C yr⁻¹ to the atmosphere globally
6 (1997-2016) mostly from biomass burning in the form of greenhouse gases (GHG) like CO₂ and
7 CH₄ (van der Werf et al., 2017). The changes exerted in the soil during fires strongly influence
8 the CO₂ flux from soil to the atmosphere in fire-affected soils (González-Pérez et al. 2004;
9 Meiggs et al., 2009; Pellegrini et al., 2018). In the short-term, the high temperatures reached
10 during the fire can kill large numbers of microorganisms, which along with a lack of water
11 availability due to evaporation results in low soil CO₂ flux immediately after the fire (Matáix-
12 Solera et al., 2009; Song et al., 2019). For example, substantial reductions in CO₂ fluxes of up to
13 70% have been reported from both a recently burnt African savannah (Castaldi et al., 2010)
14 and a recently burnt arid grassland in New Mexico (USA) (Vargas et al.; 2012).

15 Wildfires usually coincide with severe dry periods so, in the absence of rain following the fire,
16 it is likely that soil CO₂ fluxes will remain low until the next wetting event. In severe cases in
17 which the vegetative cover has been consumed exposing the bare soil surface, the direct
18 effects of fire on CO₂ fluxes can be aggravated by the subsequent increase in radiation in the
19 topsoil and potentially enhanced wind erosion. The first rain after the fire is key as wetting of
20 the fire-affected soil will trigger a succession of events, starting with the mobilization of
21 nutrients vital for microbial functioning and resulting in the recovery of microbial activity
22 (Matáix-Solera et al., 2009). This increase in microbial respiration along with other physical
23 sources of CO₂ flux, such as the degassing of CO₂ stored in the air-filled pores or a potential
24 reaction of water with carbonates, often results in a large flush of CO₂ from burnt soil (i.e. the
25 Birch effect, as seen in section 1). The Birch effect, although mostly studied in dry unburnt soil,
26 has also been observed in fire-affected soils (e.g. Castaldi et al., 2010; Marañón-Jiménez et al.,
27 2011; Pinto et al., 2002). For instance, Pinto et al. (2002) observed CO₂ fluxes trebled after
28 artificial wetting in a burnt savanna in Central Brazil during the same day of wetting and
29 returned to pre-wetting levels two days after wetting. It is important to mention that wide
30 differences are commonly observed amongst studies in the time elapsed between the fire and
31 the beginning of the field investigations, which might have a substantial effect on the
32 magnitude of the CO₂ flux response to wetting.

33

1 1.5. Synthesis of research gaps, thesis objectives and structure

2 This chapter has focused on the concepts of soil CO₂ flux, soil water repellency and fire effects
3 on soil. Following this comprehensive revision of the relevant literature the following key
4 research gaps are identified:

- 5 • Research gap 1: The effect of soil water repellency on soil CO₂ flux during the short-
6 period following wetting (i.e. the Birch effect).

7 Understanding the short-lived but large episodes of CO₂ release in response to large rainfall
8 events is important because they can constitute substantial fractions of the total C loss to the
9 atmosphere (Castaldi et al., 2013; Leon et al., 2014). In general very little is known about the
10 effects of SWR on C dynamics. Some work has been done to study how SWR affects the
11 mineralization of organic matter and soil respiration but these laboratory-based studies focus
12 on overall C emissions from soil rather than CO₂ emissions in response to large rainfall events
13 (e.g. Goebel et al., 2007; Goebel et al., 2005). To our knowledge, only the study by Urbanek
14 and Doerr (2017) focused on *in situ* CO₂ flux from water-repellent soils under natural
15 conditions. Although a few authors (e.g. Muhr et al., 2008; 2010; Sowerby et al., 2008) had
16 suggested SWR as an explanation for surprisingly low soil CO₂ flux after rewetting of dry soils,
17 to the author's knowledge, the hypothesis that SWR directly reduces the Birch effect had
18 never been tested before this research.

- 19 • Research gap 2: The main factors controlling the production and transport of CO₂ in
20 response to wetting in water-repellent soils.

21 Climate change is modifying rainfall regimes and, in some regions of the world, severe dry
22 spells followed by heavy rainfall events are becoming more frequent (Coumou and Rahmstorf,
23 2012; Trenberth et al., 2013). It is common for studies looking at the Birch effect to identify the
24 wetting amount as a controlling factor of the magnitude of the Birch effect (Lado-Monserrat et
25 al., 2014; Muhr et al., 2008) but these studies mostly assume unrestricted wetting of the soil
26 matrix and a proportional increase in soil moisture with the increase in rewetting rate. This
27 hydrological pattern is rarely observed in water-repellent soils, where limited infiltration and
28 highly heterogeneous wetting are dominant factors (Doerr et al., 2000; Ritsema and Dekker,
29 1994). It is, therefore, anticipated that the CO₂ flux in response to wetting from water-
30 repellent soils differs from that typically observed in wettable ones but, to the author's
31 knowledge, no previous studies have looked into the main factors controlling the CO₂ flux
32 response to wetting. To address this research gap the following hypotheses have been

1 formulated: i) the amount of released CO₂ is proportional to the rewetting rate of the soil and
2 ii) the initial CO₂ pulse can be mainly caused by the physical release of gas present in soil pores
3 by infiltrating water rather than a spike in microbial activity.

- 4 • Research gap 3: The effects of heating from wildland fire and ash deposition on CO₂
5 flux during the early post-fire recovery period.

6 Wildland fires (or vegetation fires) induce changes in the soil C pool, which can substantially
7 influence CO₂ emissions from soil to the atmosphere (González-Pérez et al. 2004; Meiggs et al.,
8 2009; Pellegrini et al., 2018). However, little is known about soil CO₂ fluxes from fire-affected
9 soils during the immediate period following the first post-fire rainfall. Understanding C
10 dynamics during the post-fire recovery time is particularly relevant in fire-prone ecosystems
11 like savannahs, where their high fire frequency and the large area burnt each year results in
12 savannahs emitting ~62% of the total global CO₂ from vegetation fires (van der Werf et al.,
13 2017).

14 In addition, because of the difficulty of studying the effect of wildland fire ash on soil C
15 dynamics while ash is still intact on the soil surface, most studies used laboratory-produced
16 ash instead (e.g. Andersson et al., 2004; Badía and Martí, 2003; Raison and McGarity, 1980).
17 However physico-chemical properties differ substantially between ash produced naturally
18 during vegetation fires and laboratory-produced ash, due to differences in the production,
19 thus affecting C mineralization and, in turn, soil CO₂ flux (Santín et al., 2017). Although it is
20 largely assumed that ash deposition enhances soil CO₂ flux due to the input of easily-accessible
21 C, water-soluble nutrients and the increase in pH (Raison, 1979; Matáix-Solera et al., 2009), to
22 the author's knowledge, only two studies look at wildland fire ash and report largely
23 contradictory results (e.g. Andersson et al., 2004; García-Oliva et al., 1999). Therefore, the role
24 of wildland-fire ash on CO₂ emissions during the early post-fire recovery period remains poorly
25 understood. To address this research gap, the following hypotheses are tested in this thesis: i)
26 the input of wildland fire ash to post-fire savannah soil will stimulate CO₂ fluxes, and ii) the
27 effect of fire will lead to enhanced CO₂ fluxes when soils are wetted.

28

29 This thesis aims to answer the following research questions:

- 30 1) Does SWR affect the CO₂ pulse in response to wetting (i.e. the Birch effect) and what are
31 the main factors affecting the magnitude of the response?
- 32 2) What are the main sources of C underpinning the quick release of CO₂ upon wetting?

- 1 3) How does soil CO₂ flux respond to vegetation fire during the early post-fire period and
- 2 following the first wetting event after the fire?
- 3 4) What is the role of wildfire-produced ash in post-fire soil CO₂ flux?
- 4 5) Does wildfire-produced ash have an effect on the magnitude and timing of the Birch
- 5 effect?

7 1.5.1. Research design

8

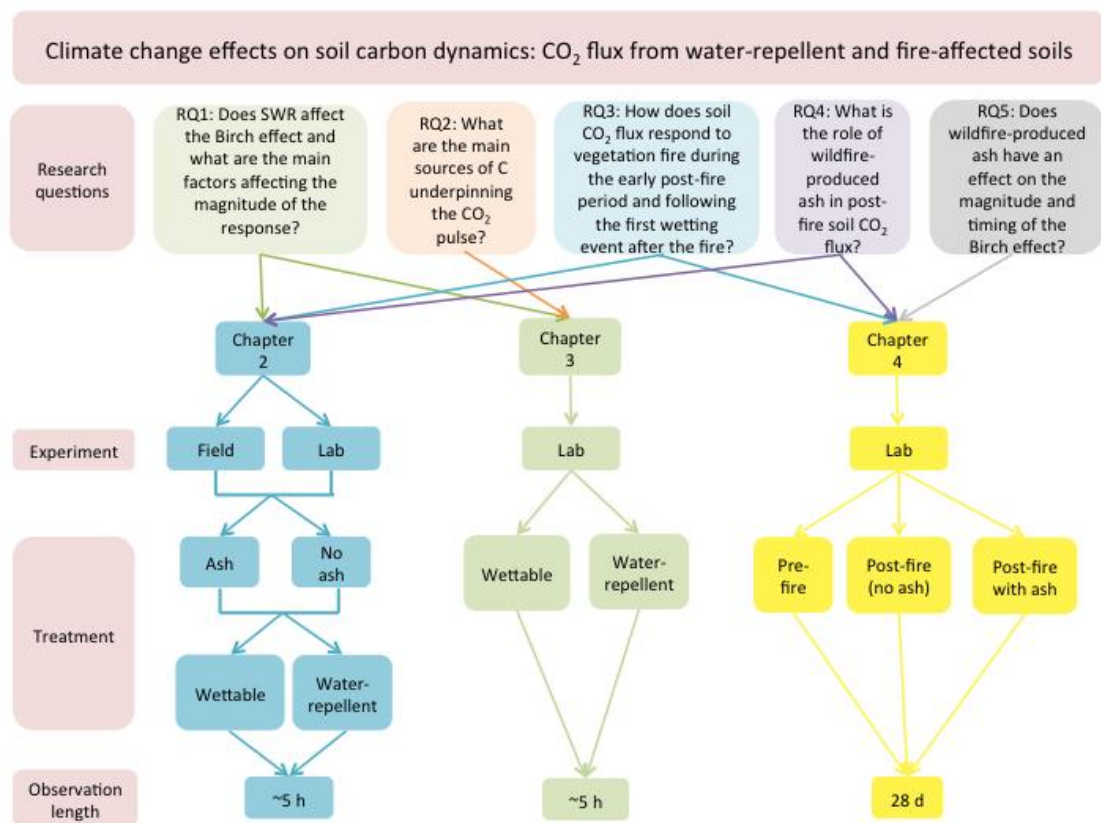


Fig. 1.5. Diagram of research design.

9

10 1.5.2. Research structure

11 This thesis comprises five chapters. Chapter 1 and 5 provide a general introduction and
 12 discussion respectively. The remaining three chapters comprise individual studies, two of
 13 which have been published in scientific journals (Sánchez-García et al., 2020a; b) and a third
 14 one is currently under second revision after receiving a positive review from the journal
 15 (Sánchez-García et al., *In Submission*).

1 Chapter 2 examines the CO₂ response to wetting in relation to SWR and changes in soil
2 moisture in water-repellent soil and compares this response to that of wettable soils. Two
3 study sites with naturally water-repellent soils were selected in a recently burnt eucalyptus
4 and pine stand in Central Portugal (Fig. 1.7). The predominant soil type was an arenic skeletal
5 Regosol (IUSS Working Group WRB, 2015). A wettable scenario was simulated by adding a
6 wetting agent to the water. To help understand the influence of an ash layer on wetting and
7 CO₂ flux the ash layer was brushed off the surface in one of the sites, exposing the bare soil.
8 Artificial wetting experiments in the laboratory, on intact core samples, and *in situ* were
9 conducted. (Manuscript published).

10



Fig. 1.6. (a) CO₂ analyser system measuring in the site in which the ash layer was left untouched (burnt with ash, BwA), and (b) Burnt site in which the ash layer was removed before the experiments (burnt without ash, BnoA).

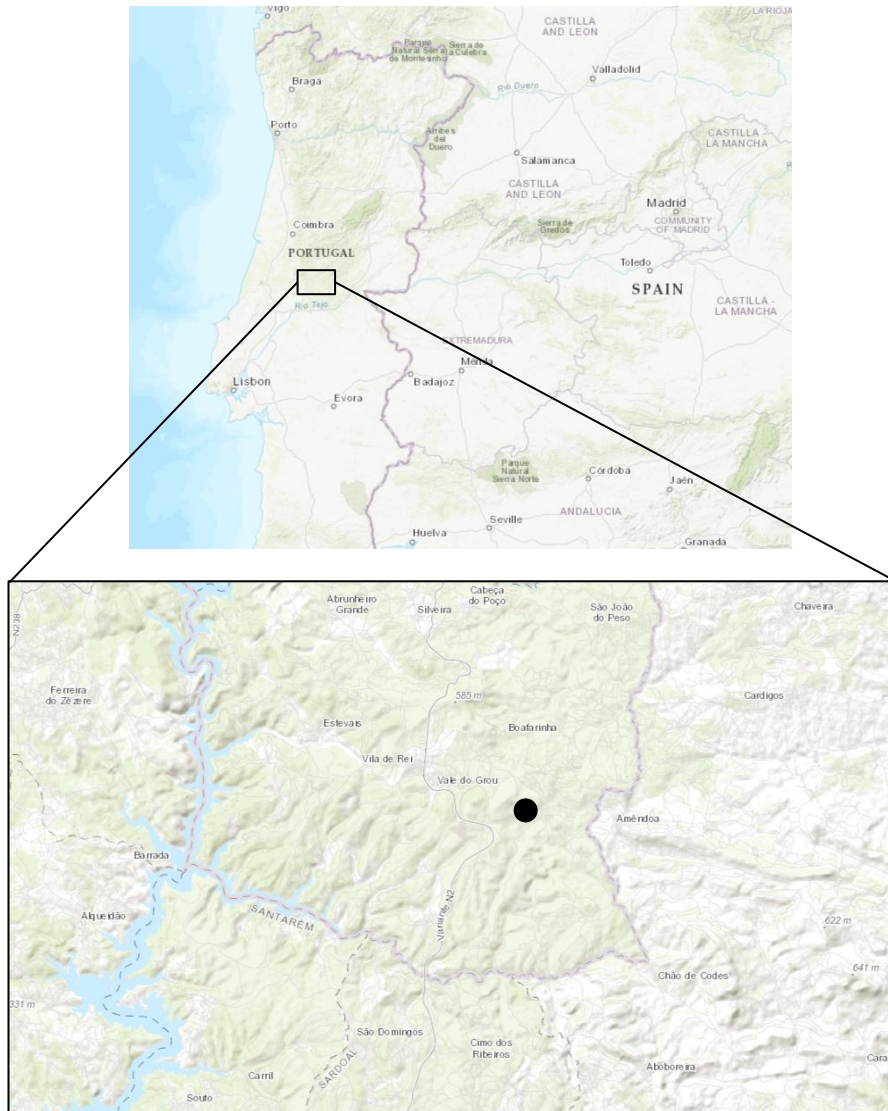


Fig. 1.7. Location of the study area from Chapter 2 in Portugal (dot).

1

2 Chapter 3 improves understanding of the mechanisms influencing the spike of CO₂ after
 3 wetting in water-repellent soils by studying the effect of differing rewetting amounts on CO₂
 4 flux release from water-repellent soils. The chapter also helps to identify the sources behind
 5 the short-term release of CO₂ upon wetting. A series of wetting experiments were conducted
 6 in the laboratory on soils under both wettable and extremely water-repellent conditions. Two
 7 soils were selected for the study both collected from the Gower peninsula (South Wales), an
 8 Endoleptic Podzol (Anglezarke Classification of England and Wales), referred to as Cefn Bryn
 9 (CB), and a Calcaric Stagnic Vertic Cambisol (Evesham Classification of England and Wales),
 10 referred to as Southgate (SG) (Fig. 1.8) (Manuscript published).

1

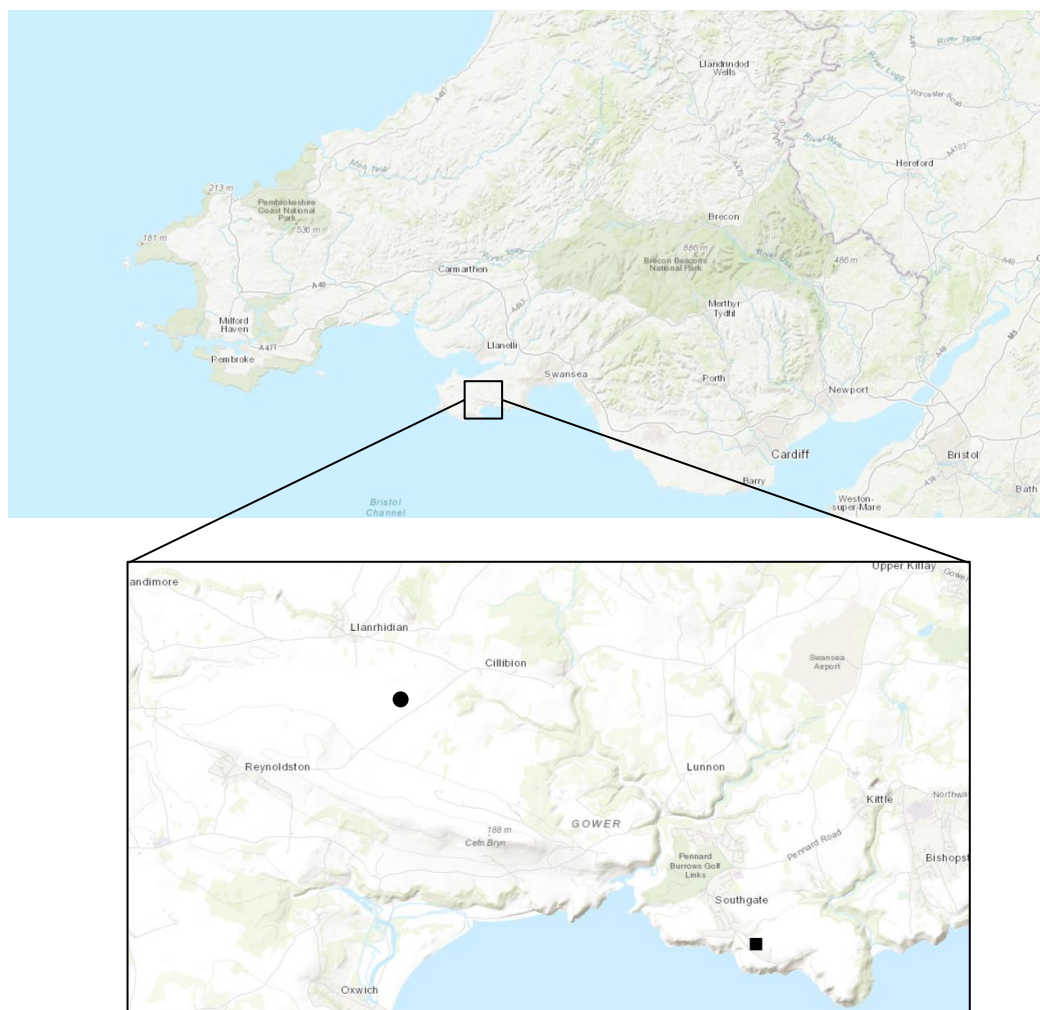


Fig. 1.8. Sampling locations of the soils used in Chapter 3 in the Gower Peninsula (South Wales, UK). Bottom: close up of the locations: Cefn Bryn, referred to as CB (dot), and Southgate, referred to as SG (square).

2

3 The main aim of chapter 4 is to study the effect of heating from fire and the role of ash on soil
4 CO₂ fluxes during the early post-fire period on savannah soils. Savannah fires are the largest
5 contributor to global fire carbon (C) emissions as a result of their high fire frequency and the
6 large area burnt each year. A series of incubation experiments were performed on soil and ash
7 samples collected from an African savannah in the Kruger National Park (KNP, South Africa)
8 before and immediately after experimental fires (Fig. 1.9). Three locations were selected for
9 the study: two in the Pretoriuskop area, one burnt annually and the other burnt triennially,
10 and one in the Mopani area, which was burnt annually (Fig. 1.9) (Manuscript under second
11 review). The soils in the Pretoriuskop sites (PB1 and PB3) can be classified as Oxisols, while in

1 Mopani (MB1) they can be classified as Vertisols (IUSS, Working Group WRB, 2006; Venter and
2 Govender, 2012).

3
4
5
6
7
8
9
10
11
12
13
14
15
16
17
18
19
20
21
22
23
24

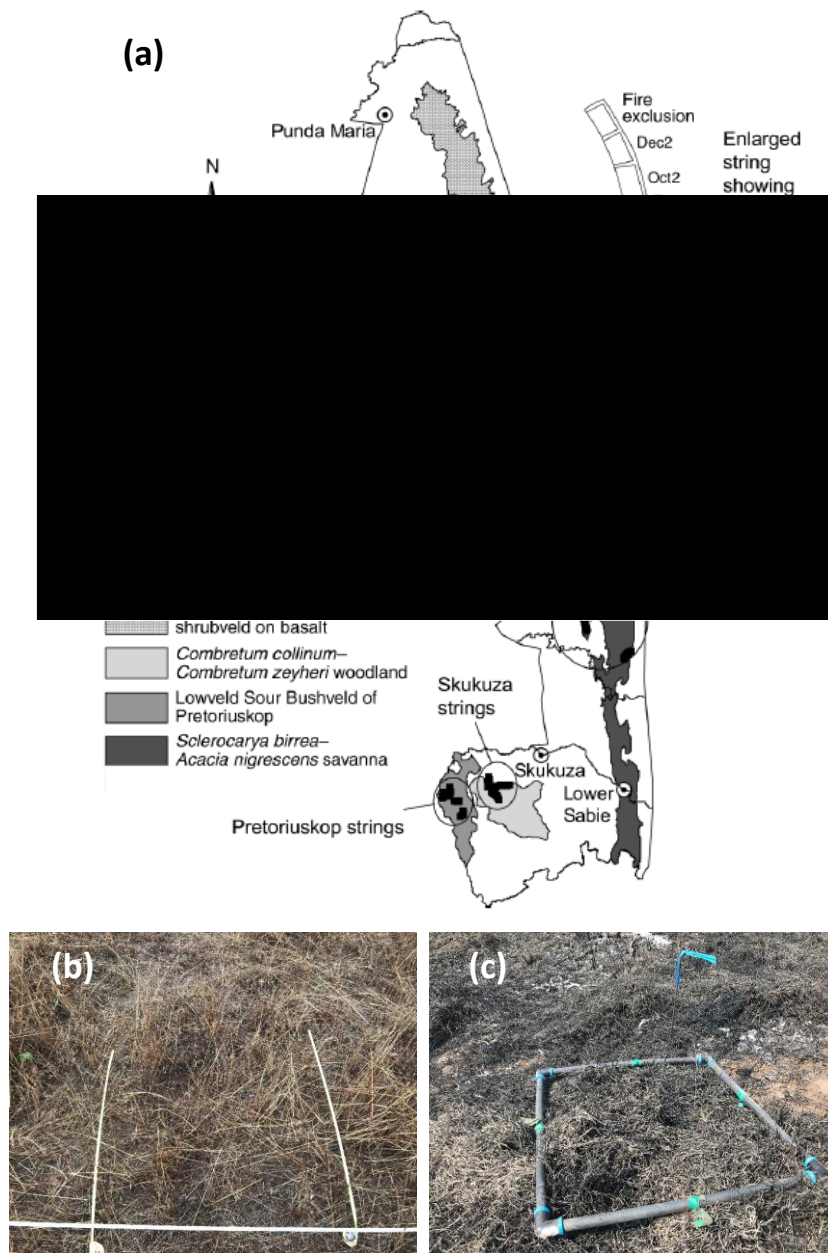


Fig. 1.9. (a) Experimental burnt plots (EBPs) at the Kruger National Park (KNP). Source: Smit et al. (2010); (b) Grass in the PB3 site before the fire; (c) Burnt grass in the MB1 site after the fire.

1
2
3
4
5
6
7
8
9
10
11

12 Chapter 2. Water repellency reduces CO₂ efflux upon rewetting

13

14 Carmen Sánchez-García, Bruna R. F. Oliveira, Jan Jacob Keizer, Stefan H. Doerr, Emilia Urbanek

15

16 **Published in:** Science of the Total Environment (2020) 708, 135014.

17 (DOI: <https://doi.org/10.1016/J.SCITOTENV.2019.135014>)

18

19

1 2.1. Introduction

2 Carbon dioxide (CO₂) emissions from soils represent the largest terrestrial carbon (C) flux to
3 the atmosphere (Longdoz et al., 2000). Given that soil moisture is one of the main controllers
4 of the soil C efflux (Davidson and Janssens, 2006; Moyano et al., 2013), there is great concern
5 that alteration of precipitation patterns due to climate change could result in a reduction of
6 soil C storage and an increase in emissions (Falloon et al., 2011). Drought periods followed by
7 heavy rainfall events have already become more frequent and extreme in many regions
8 (Coumou and Rahmstorf, 2012; Trenberth et al., 2014). Extended dry periods result in severe
9 reduction of soil moisture vital to sustain many aspects of soil functioning (IPCC, 2018). Lack of
10 available water in soil pores reduces microbial activity and root respiration rates (Moyano et
11 al., 2013; Or et al., 2007), resulting in overall low soil CO₂ efflux to the atmosphere.

12 Rewetting of dry soils has been associated with a sudden, large pulse of CO₂ to the atmosphere
13 known as the 'Birch effect' (Birch, 1958), recognised as a key contributor to soil C losses and
14 representing a large fraction of the overall C flux (Leon et al., 2014; Smith et al., 2017). This
15 CO₂ pulse is believed to originate predominantly from a rapid restoration of microbial
16 respiration caused by microbial biomass growth (Waring and Powers, 2016) and activation of
17 extracellular enzymes (Fraser et al., 2016; Smith et al., 2017) as water availability increases
18 pore connectivity and mobilizes previously unavailable C (Kim et al., 2012; Marañón-Jiménez et
19 al., 2011; Schimel, 2018). Part of the rewetting CO₂ pulse is assigned to degassing of air-filled
20 pores as CO₂ is often stored in the available pore-space and not always released instantly
21 (Maier et al., 2011). Several factors influence the size of this wetting pulse. Low soil moisture
22 prior to wetting as a result of longer and more intense drying periods has been linked to an
23 increase in the size of the CO₂ pulse (Meisner et al., 2017), while the rewetting of soil at
24 optimum moisture levels results in smaller pulses (Muhr and Borken, 2009). The size of the CO₂
25 pulse is expected to increase with larger wetting intensities, i.e., rate and amount of water
26 added (Lado-Monserrat et al., 2014; Muhr and Borken, 2009; Sponseller, 2007) as well as with
27 lower frequencies of the drying-wetting cycles (Christensen and Prieme, 2001; Fierer and
28 Schimel, 2002). Several reviews have specifically focused on the Birch effect, addressing the
29 effects of drying and rewetting on CO₂ fluxes and C mineralization (Jarvis et al., 2007; Muhr
30 and Borken, 2009), rewetting effects on CO₂ fluxes (Kim et al., 2012) and modelling the CO₂
31 efflux from responses to moisture changes (Moyano et al., 2013; Vicca et al., 2014).

32 A few studies have reported unexpectedly low CO₂ fluxes upon rewetting of very dry soil,
33 speculating that the lack of CO₂ flush upon rewetting could be due to soil water repellency

1 (SWR) (Lado-Monserrat et al., 2014; Muhr and Borken, 2009) reducing water infiltration into
2 the soil. This explanation may seem reasonable given that SWR is a common feature of dry soil
3 under permanent vegetation and many drought-affected soils undergo temporal physical
4 transformation to prevent further moisture loss, which does not readily revert with addition of
5 water (Schimel, 2018). However, none of the aforementioned studies suggesting that the lack
6 of CO₂ flush upon rewetting is due to SWR actually performed any SWR measurements, so this
7 explanation remains speculative. Therefore, a clear research gap exists regarding the effect of
8 SWR on CO₂ efflux upon rewetting, especially given that future climate scenarios, predicting
9 greater drought and more wildfires, are likely to enhance the development of SWR (Goebel et
10 al., 2011; Muhr and Borken, 2009).

11 Very little is known about the effect of SWR on CO₂ efflux and how inhibited infiltration will
12 affect the release of CO₂ to the atmosphere. In a field-based study in the UK, Urbanek and
13 Doerr (2017) focused specifically on the effect of water repellency on CO₂ effluxes. They
14 observed lower CO₂ effluxes under severe and uniformly distributed SWR than under patchy
15 SWR and moisture distribution. Soil respiration in water-repellent soils has also been
16 addressed under laboratory conditions (Goebel et al., 2007; Goebel et al., 2005), but the few
17 prior studies focused on overall CO₂ emission rates, rather than CO₂ emissions rates occurring
18 during rewetting events. Furthermore, relatively little is known about the effect of the first
19 rainfall on CO₂ emissions from fire-affected soils. Fire is known to enhance SWR at or below
20 the soil surface (Mataix-Solera et al., 2011; Moody et al., 2013; Shakesby and Doerr, 2006) and,
21 simultaneously, it has a direct effect on carbon pools (Amiro et al., 2003; Bond-Lamberty et al.,
22 2007; Meigs et al., 2009) and reduces microbial activity due to sterilization (Mataix-Solera et
23 al., 2009). The first post-fire rainfall event will play a major role in activating the recovery of
24 soil respiration. Similar to unburnt soil, the wetting of recently burned soil has been shown to
25 induce a short-lived CO₂ pulse (Castaldi et al., 2010; Marañón-Jiménez et al., 2011; Pinto et al.,
26 2002; Vargas et al., 2012), which is possibly enhanced by the input of nutrients from scorched
27 plant material and/or ash (Concilio et al., 2006; Marañón-Jiménez et al., 2011).

28 Although water repellency is a common feature of fire-affected soils (Shakesby and Doerr,
29 2006), there is a clear lack of understanding of how SWR may affect soil CO₂ effluxes from
30 burnt soils. Areas affected by recent fire are likely to exhibit water repellency and combined
31 with their lack of surface vegetation during the initial post-fire period, provide ideal conditions
32 for isolating the effects of SWR on the Birch effect. Therefore, the aim of our study was to test
33 the hypothesis that SWR suppresses CO₂ effluxes upon wetting of burnt soils. The objectives
34 were to: 1) compare the CO₂ response to wetting under wettable and water-repellent scenarios

1 at the core (cm) scale under controlled laboratory conditions; II) examine the CO₂ responses to
2 wetting in relation to SWR and changes in soil moisture and III) validate the CO₂ response to
3 wetting under field conditions.

4

5 2.2. Research design and methods

6 This study comprises a series of wetting experiments and CO₂ efflux measurements on water-
7 repellent soils in fire-affected areas: *i*) under laboratory conditions on intact core soil samples
8 and *ii*) *in situ* under field conditions. Soil sampling and *in situ* measurements were carried out
9 at two sites within a recently burned forest in October 2017, two months after a wildfire and
10 before the first major rainfall in the area. Fire severity at the study site was classified by the
11 European Forest Fire Information System (EFFIS, 2017) as moderate to high. Field observations
12 during the first month after the fire revealed that consumption of the tree crowns as well as of
13 the litter layer were generally complete, and that the ash layer was predominantly black. Both
14 sites are located in Central Portugal in Vale das Casas, 7 km South East of the municipality of
15 Vila de Rei and were affected by the same wildfire event in August 2017. A field survey and soil
16 profile description revealed that the predominant soil type of the study site was an arenic
17 skeletal Regosol (FAO, 2014), derived from sedimentary sandstone. The climate in the area is
18 classified as hot-summer Mediterranean, with annual precipitation of 900 mm y⁻¹, average air
19 temperature of 14 °C (with maximum and minimum air temperatures of 42 °C and -1 °C,
20 respectively) and wind direction predominantly NW. To be able to assess the hydrological
21 effect of differing topographies on the CO₂ pulse after wetting, site 1 is located in a burnt pine
22 forest (*Pinus pinaster*) on flat terrain, while site 2 is located in a pine-dominated (*Pinus*
23 *pinaster*) forest with some eucalyptus (*E. globulus*) on a slope (approx. 30°, facing ESE) (Table
24 2.1). At site 1, the ~2 cm layer of black ash was retained untouched with only the pine needles
25 removed from the surface; hence this site is called burnt with ash (BwA). At site 2, both the
26 pine needles and the layer of black ash (~2 cm thick) were brushed off the surface, exposing
27 the bare soil to simulate the removal of the ash layer by wind erosion. Including a bare soil
28 (BnoA) in the experimental design helps to understand the influence of an ash layer on wetting
29 and CO₂ efflux. Air temperature during sampling and field measurements ranged between 23
30 and 31 °C with the exception of the 15th October, which coincided with measurements in the
31 BwA site plot 4, when temperatures reached up to 37 °C.

32

1 Individual intact cores and field plots were subjected to one of two rewetting treatments:
2 water only, to observe the response of water-repellent soils, and water mixed with a wetting
3 agent (Revolution[®], Aquatrols, 1:42) to alleviate water repellency, thus simulating wettable
4 soil. Preliminary tests confirmed that the addition of the wetting agent itself did not affect
5 microbial activity in the soil (Lewis, 2019). All samples were rewetted from above to simulate a
6 rainfall event. In the laboratory, effluxes were monitored from above and below the soil
7 sample in order to capture movement of CO₂ in both directions.

8

9

Table 2.1. General characteristics of the topsoil (0-5 cm depth) at the two recently burned soils with ash (BwA) and with ash removed (BnoA). Values are the mean with SD in brackets. The ash layer in the top 0 – 2 cm of the BwA soil was left untouched for all characterisation analysis.

	BwA	BnoA
Bulk density (n=10)	1.13 (0.11)	1.01 (0.11)
Stone content (% of total weight)	10.70 (3.85)	23.34 (8.57)
Texture (n=10)	Sandy loam	Sandy loam
% Sand	58.45 (7.49)	55.96 (5.21)
% Silt	36.28 (6.77)	37.50 (3.83)
% Clay	5.23 (1.27)	6.54 (1.55)
% Soil organic matter (SOM) with depth (< 2 mm fraction) (n=20)		
Overall % SOM (0 -5 cm)	8.50 (8.28)	11.34 (7.49)
0 - 1 cm	23.35 (9.30)	19.45 (1.30)
1 - 2 cm	10.35 (3.60)	15.44 (0.97)
2- 3 cm	4.85 (1.79)	8.53 (1.36)
3 - 4 cm	4.03 (1.33)	9.75 (1.05)
4 - 5 cm	3.99 (1.61)	7.88 (0.51)
% Soil water content (at time of sampling)	2.76 (2.22)	7.63 (3.75)
Surface water drop penetration test (s) (n=5)	2404 (3162)	9509 (5843)
Surface water repellency classification*	Severely repellent	Extremely repellent

* According to Doerr (1998).

2.2.1. Laboratory methods

Intact cores (8 cm diameter, 5 cm height) were collected from both study sites near the *in situ* measurement plots. Fifteen soil cores were collected from each site along a 12 m transect (3 cores × 5 sampling points) from 0 - 5 cm depth in metal cylinders. Pine needles were removed from the surface before sampling in the BwA site, leaving the ash layer (~2 cm) on the surface. Pine needles together with the ash layer were removed from the surface in the BnoA site, exposing the mineral soil before sampling (Fig. 2.1). After sampling, plastic caps were immediately fitted to the cylinders to preserve soil moisture which were then thereafter stored at 4 °C. Prior to the wetting experiments, the samples were equilibrated at 20 °C for 24 h.

The cores were rewetted from above using a custom-made rainfall simulator fitted between the soil collar and the CO₂ flux chamber. The rainfall simulator comprised one spiral tube with uniformly distributed drips, to ensure spatially uniform wetting, suspended 1 cm above the soil surface and connected via a tube to a large syringe to supply water. All cores received one single and uniform wetting event of 25 mm with an intensity of 100 mm h⁻¹. The amount of water applied to soil cores was equivalent to 80 % of water-filled pore-space (WFPS) and the duration of wetting was approximately 15 min. WFPS was calculated individually for each core by dividing volumetric water content by pore space. Pore space (PS) was obtained from soil bulk density (dB) as follows: $PS = (1 - dB d_p^{-1}) \times 100$; assuming a particle density (d_p) = 2.65 g cm⁻³ (Blake, 2008). Water retention was measured as the weight difference in the soil before and after wetting. Percolation time was determined, and drained water was collected and quantified.

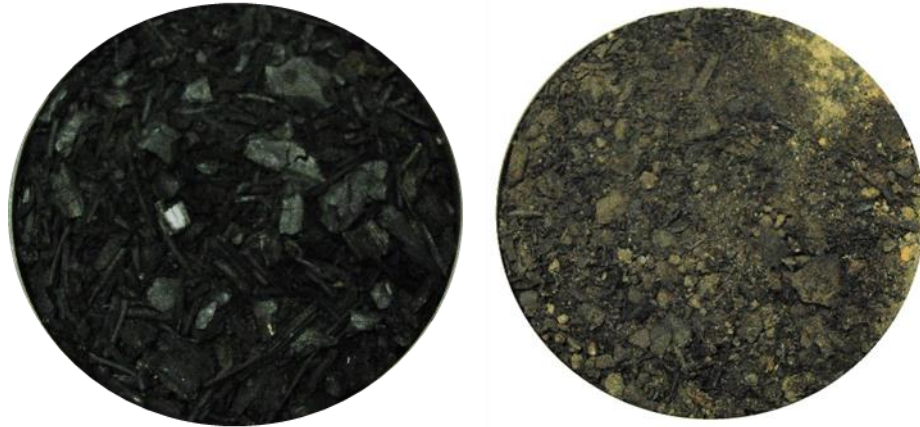


Fig. 2.1. Example of representative intact core soil surfaces of the two experimental soils before wetting. BwA (left), BnoA (right).

Each core was suspended on a set of collars allowing monitoring of the CO₂ concentration in the chamber above and below the sample during the rainfall simulation, and collection of the drained water (supplementary Fig. S1). The CO₂ concentration was monitored via a 10 cm survey chamber connected to an infrared CO₂ analyser system (IRGA, Li-8100A) from above (LI-COR Inc.) and a plastic container with a similar headspace connected to a separate IRGA CO₂ analyser system below the sample. A fine mesh was placed under the cores to allow any drainage of water while holding the core inside the cylinder. The entire system (chambers, rainfall simulator and soil sample) was sealed to avoid gas leakage. The chamber's inbuilt pressure vent helped maintain ambient pressure inside the chamber (supplementary Fig. S1). CO₂ effluxes were monitored in 30 min intervals with 1 min for pre and post-purge, over a total of 340 min. Initial CO₂ effluxes were measured before wetting, during the simulated rainfall, which lasted approximately 15 min, and for 270 min after the rainfall.

Of the three intact cores obtained at each sampling point, two were randomly allocated to one of the rewetting treatments. The third core was used to determine soil water content (SWC) and SWR distribution at different depths prior to wetting, following the subsampling method of Liu et al. (2019) which involved sampling the core in 5 locations at 5 different depths using a small ring of 1 cm height by 2 cm diameter (supplementary Fig. S2). A custom-made Plexiglas disk (1 cm height, 7.9 cm diameter) was placed under the soil core to bring the soil upwards. After subsampling, the remaining soil was removed from the surface with a knife. This process was repeated for each cm of the 5 cm depth of the soil cores.

SWR prior to wetting was determined for each of the core's subsamples following the water drop penetration test (WDPT) (Doerr, 1998) by applying 3 drops of water to the surface of each subsample and measuring the infiltration time of each drop. 15 drops in total were applied to each layer of the core (3 drops × 5 subsampling points per layer). Drops were applied using a pipette to equalise drop size. Infiltration times were categorised into the following classes (Doerr, 1998): wettable (< 5 s), slightly repellent (5-60 s), moderately repellent (60-600 s), severely repellent (600-3600) and extremely repellent (> 3600 s).

SWC of the subsamples was determined by calculating the weight loss of the sample after drying at 105 °C for 24 h (van Reeuwijk, 2002). The five oven-dried subsamples per layer were combined into one sample per layer to determine soil organic matter (loss of ignition, Nelson and Sommers (1996)) and particle size distribution (laser diffraction, Beckman Coulter, Inc.). The remaining sample was pooled into a single sample and hand sieved through a 25 mm mesh size to determine stone content (Urbanek & Shakesby, 2009).

2.2.2. Field methods

At each study site, four 1 m² plots were selected along a 12 m transect. At each plot four PVC collars (12 cm height, 20 cm diameter) were installed, two for measuring soil CO₂ efflux and two others for measuring SWC and soil temperature. Although not ideal, it was necessary to install SWC and temperature sensors in separate collars than those designated for CO₂ monitoring to avoid soil disturbance and potential changes to the CO₂ efflux response. Two SWC and temperature sensors (ECH₂O 5-TM, Meter-Group, USA) were installed horizontally, opposite to each other at 3 cm below the surface of the mineral soil (supplementary Fig. S3) and monitored continuously for the duration of the observations. PVC collars were inserted into the soil at least 24 h before the beginning of the experiments, approximately 8 cm into the soil, leaving an offset of 3 to 4 cm to place the CO₂ analyser chamber and provide a strong seal.

The rainfall simulations were performed using a watering can with the distributor applying one single and uniform rainfall event of 25 mm at an intensity of 100 mm h⁻¹ during 15 min to simulate a heavy rainfall event. CO₂ efflux was measured using a Li-8100A infrared gas analyser system with a 20 cm survey chamber (LI-COR, Inc.) before, immediately after wetting and at 15, 30, 60, 90 and 120 minutes after the end of wetting. At each observation time, three 2 min measurements were taken.

2.2.3. Data analysis

The CO₂ concentration data obtained was fitted exponentially excluding the first 30 s of measurements, which is the typical time required to achieve steady mixing inside the chamber (LICOR, 2010). The following equation (Eq. 2) was applied to calculate CO₂ efflux as the rate of change in CO₂ concentration released from soil (LICOR, 2010):

$$\text{Eq. 2} \quad Fc = \frac{10VPo\left(1-\frac{Wo}{1000}\right)}{RS(To+273.15)} * \frac{dC'}{dT}$$

Fc = soil CO₂ efflux (μmol m⁻² s⁻¹), V = volume (cm³), Po = initial pressure (kPa), Wo = initial water vapour mole fraction (mmol mol⁻¹), S = soil surface area (cm²), To = initial air temperature (°C) and dC'/dT = initial rate of change in water-corrected CO₂ mole fraction (μmol mol⁻¹). CO₂ efflux data below R² ≥ 0.95 were rejected with a total of 1.3 % of total rejected measurements. CO₂ flux graphs were created by calculating the mean flux for each treatment at each measurement time, along with 95% confidence intervals and standard deviation for laboratory and field graphs respectively. The estimated CO₂ flux pulses under field conditions were calculated proportionally to the size of the pulse observed under laboratory conditions for the same soil and wetting scenario. The Mann-Whitney U-test was applied to test for statistical differences between wetting scenarios. Statistical differences were accepted at p < 0.05.

Spatial frequency graphs of SWR were obtained by calculating the percentage of WDPT measurement points per soil depth falling into each WDPT category (Doerr, 1998). The Kolmogorov-Smirnov two-sample test was applied to determine statistically significant differences (p < 0.05) in water repellency between the five different depths analysed. A linear regression analysis was performed between cumulative flux and the change in SWC with wetting in all soils under field and laboratory conditions.

2.3. Results

2.3.1. CO₂ efflux prior to and after wetting

2.3.1.1. Laboratory measurements

CO₂ efflux prior to wetting was very low in all soils under laboratory conditions ranging between 0 and 1 μmol m⁻² s⁻¹ (Fig. 2.2). CO₂ effluxes increased immediately in response to the simulated rainfall. The CO₂ pulse under water-repellent conditions (orange line in Fig. 2.2) was significantly lower in both soils (p = 0.024, p = 0.005 in the BwA and BnoA respectively)

compared to wettable conditions, but the duration of the peak was relatively similar. The effluxes decreased rapidly with the end of wetting and stabilized at approximately 10 to 15 min after wetting, remaining at a constant value until the end of the observation (4.5 h after wetting). The CO₂ effluxes were slightly above pre-wetting values by the end of the observation period, but <1 μmol m⁻² s⁻¹ in all cases. The CO₂ efflux observed below the sample was very close to the pre-wetting values and no significant CO₂ response to the wetting event was observed.

The mean size of the CO₂ pulse, under water-repellent conditions, was <1.5 μmol m⁻² s⁻¹, whereas peaks nearly 4 times higher were observed under wettable conditions (4.4 and 5 μmol m⁻² s⁻¹ in the BnoA and BwA soil respectively). Similarly, the cumulative efflux from soil under water-repellent conditions was half (9 and 10 μmol m⁻² s⁻¹ in the BnoA and BwA) of that measured under wettable conditions (20 and 22 μmol m⁻² s⁻¹ in the BnoA and BwA; p = 0.005, p = 0.024 respectively) (Fig. 2.3). The overall cumulative CO₂ efflux upon wetting was proportional to the change in SWC, as shown in Fig. 2.4.

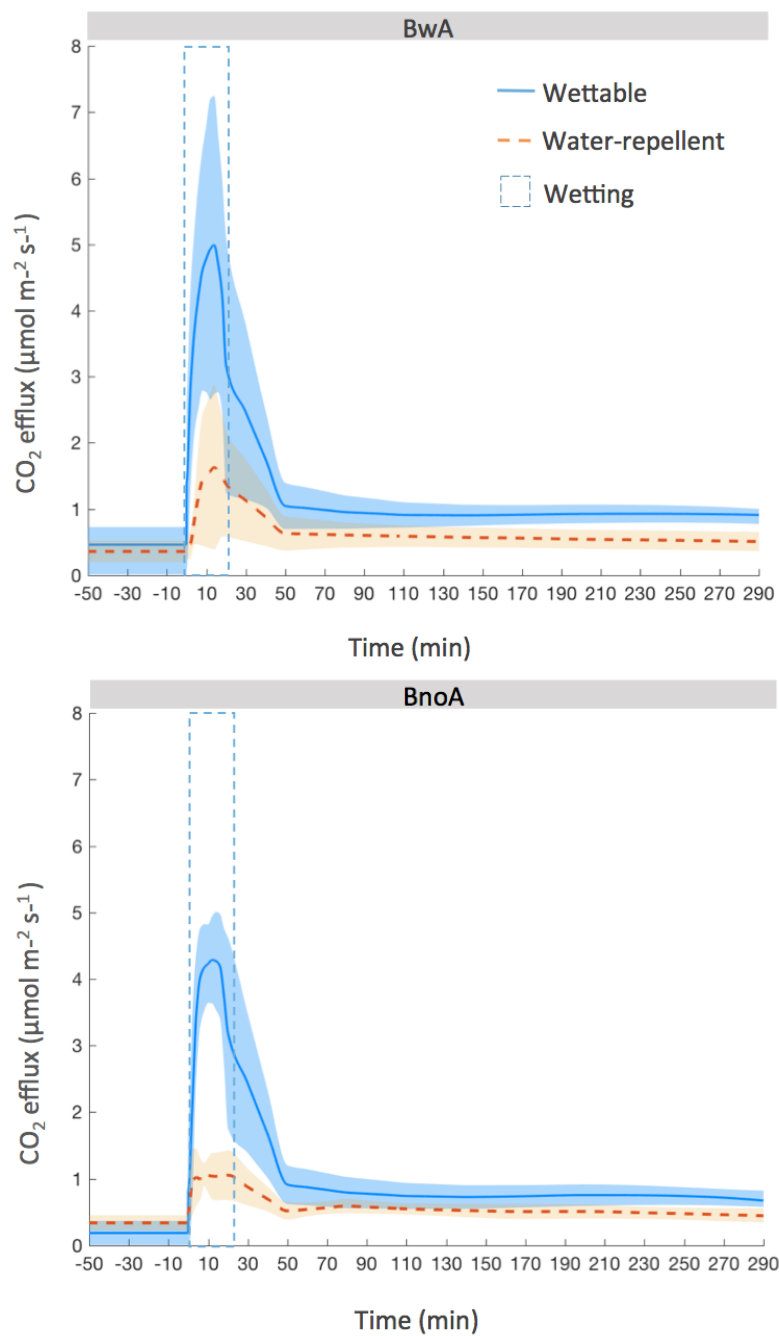


Fig. 2.2. Response of CO₂ efflux to wetting, with water (water-repellent scenario) and water mixed with wetting agent (wetable scenario), under laboratory conditions of recently burned soils with ash (BwA) and with ash removed (BnoA). The orange dashed line and shaded area represent the mean response ($n = 5$) with 95% confidence interval to wetting under the water-repellent scenario and the blue solid line with shaded area represents the mean response ($n = 5$) with 95 % confidence intervals to wetting under the wettable scenario.

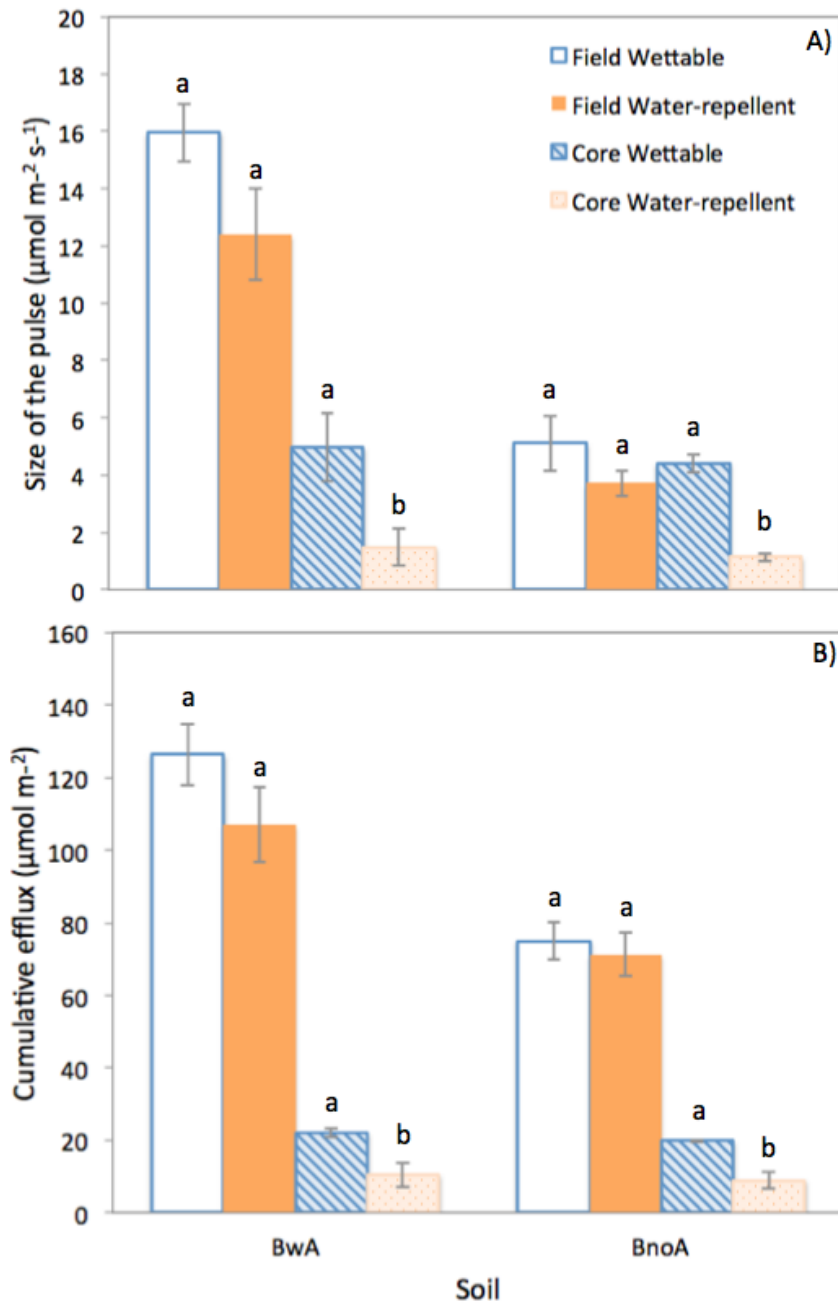


Fig. 2.3. A) Size of the CO₂ pulse and **B)** cumulative efflux after wetting under both field and core-scale in burnt soils with ash (BwA) and ash removed (BnoA) under water-repellent (wetted with water) and wettable (wetted with water and wetting agent) conditions. Values represent the mean (n = 4 for field results, n = 5 for core results) with standard error bars. Different lowercase letters (a-b) within the same site and scale (field vs. core-scale) indicate significant differences between wettable and water-repellent conditions at p < 0.05.

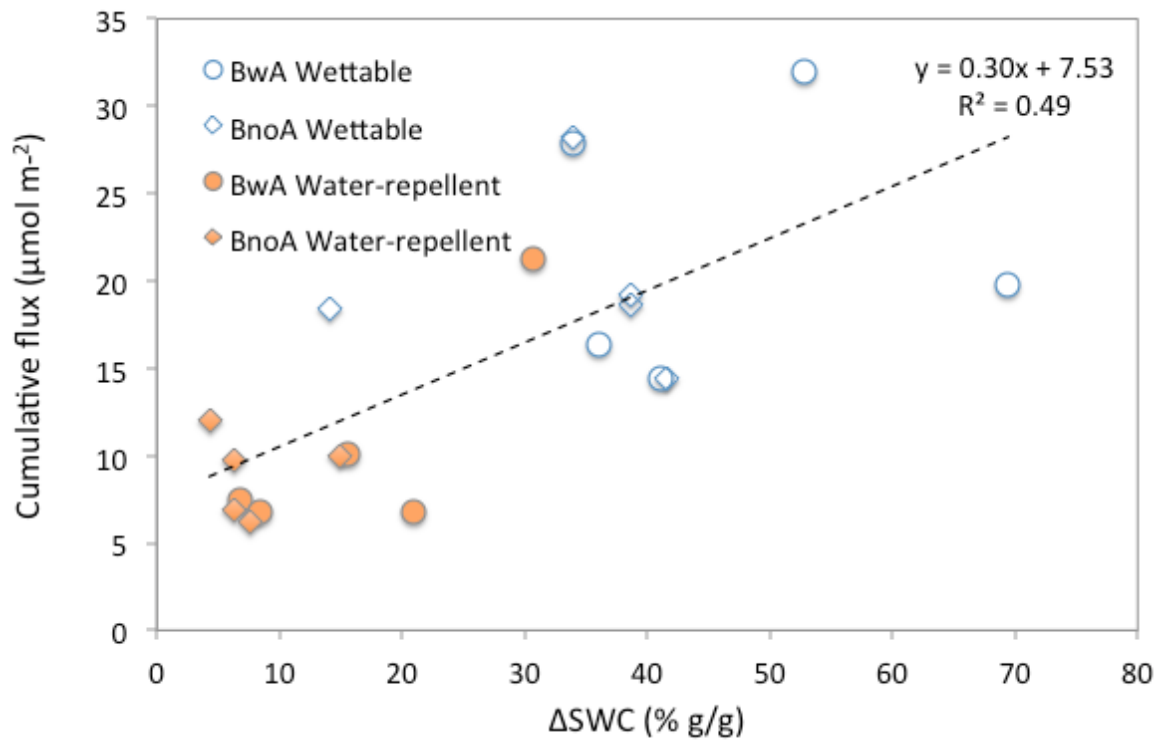


Fig. 2.4. Relationship between cumulative flux and the change in SWC with wetting under laboratory conditions (n = 5).

2.3.1.2. Field measurements

Under field conditions, the CO₂ efflux prior to wetting was low, ranging from 0.98 to 2.1 µmol m⁻² s⁻¹ in the BwA and BnoA soil respectively. An increase in the CO₂ efflux was observed in response to wetting, but the CO₂ efflux decreased steadily after the wetting stopped. At both sites and for both water-repellent and wettable scenarios, the CO₂ efflux remained above pre-wetting values by the end of the observations (120 min after the start of wetting) and no significant differences were observed between wetting scenarios at the end of the observations.

The observed CO₂ efflux peak was especially high in the BwA plots, reaching values of 12 μmol m⁻² s⁻¹ for the water-repellent scenario and 17 μmol m⁻² s⁻¹ for the wettable scenario. The CO₂ efflux in response to wetting observed in the BnoA soil was lower than in the BwA soil, reaching values of 5 and 4 μmol m⁻² s⁻¹ under wettable and water-repellent scenarios respectively. The duration of the pulse was shorter in the BnoA soil, lasting only up to 30 min after the start of wetting (Fig. 2.5).

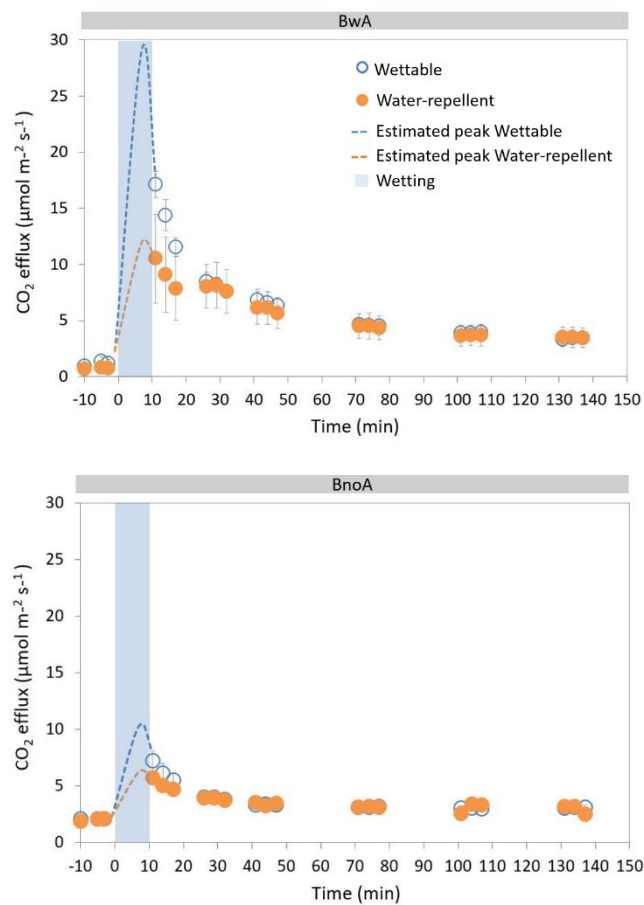


Fig. 2.5. CO₂ efflux response to wetting under field conditions for burnt soils with ash (BwA) and with ash removed (BnoA). Water-repellent scenario (orange shaded circles) represents wetting with water and wettable scenario (blue open circles) represent wetting with water and wetting agent. Missing CO₂ peaks under wettable and under water-repellent conditions are represented by the blue and orange dashed lines respectively. Values are the mean flux (n = 4) with 95 % CI.

Field *in situ* experiments allowed CO₂ efflux measurements only after the rainfall simulations. The estimated CO₂ pulse reached lower values under water-repellent (12 and 6 $\mu\text{mol m}^{-2} \text{s}^{-1}$ in the BwA and BnoA respectively) than under wettable conditions (29 and 10 in the BwA and BnoA respectively).

The size of the CO₂ pulse, calculated as the difference between the peak efflux and the average efflux prior to wetting, was higher, although not significantly, under wettable (5 and 16 $\mu\text{mol m}^{-2} \text{s}^{-1}$ in the BnoA and BwA site respectively) compared to water-repellent conditions (4 and 12 $\mu\text{mol m}^{-2} \text{s}^{-1}$ in the BnoA and BwA site respectively) ($p = 0.074$, $p = 0.124$ in the BwA and BnoA, respectively, between wettable and water-repellent conditions) (Fig. 2.3). Overall, the field-scale cumulative efflux (Fig. 2.3), which included the height and the duration of the peak, was lower, but not significantly, under water-repellent conditions, with average values ranging between 107 and 71 $\mu\text{mol m}^{-2} \text{s}^{-1}$ in the BwA and BnoA respectively ($p = 0.074$, $p = 0.282$); while the cumulative efflux under wettable conditions oscillated between 126 and 75 $\mu\text{mol m}^{-2} \text{s}^{-1}$ in the BwA and BnoA respectively.

2.3.2. Water repellency distribution prior to wetting

All soils exhibited SWR prior to wetting, but its distribution varied strongly with soil depth and the presence of ash (Fig. 2.6). At the surface layer (0 - 1 cm depth) in the BwA soil, 64 % of measured points, directly on the ash layer, were water-repellent (WDPT > 5 s); while for BnoA, water repellency was significantly higher than in the BwA soil ($p < 0.001$) with 100 % of sample points classified as water-repellent of which 80 % were in the extreme SWR class (WDPT > 3600 s) (Fig. 2.6).

In the BwA soil, similar SWR distribution to the surface layer was observed in the 1 - 2 cm depth layer (62 % of points water-repellent), but further down, at 2 - 3 cm depth, SWR increased significantly ($p = 0.01$) with up to 88 % of points classified as water-repellent. The percentage of SWR decreased with depth, reaching 60 % of points classified as water-repellent at the 4 - 5 cm depth. It is worth noting that although the overall percentage of water-repellent soil was the highest at 2-3 cm depth, the percentage of soil in the extreme water-repellent class was the highest (47 %) at 4 - 5 cm depth in comparison with the lowest percentage (19 %) at 1 - 2 cm depth. Slightly different patterns of SWR distribution with depth were observed in the BnoA soil, where the percentage of SWR decreased steadily and significantly with depth (from 95 % at 1 - 2 cm to 45 % at 4 - 5 cm depth; $p < 0.001$ in all cases),

with a proportional decrease in the percentage of extreme water-repellent points (from 50 % at 1 – 2 cm to 28 % at 4 - 5 cm depth).

An exception was found between 3 - 4 and 4 -5 cm depth where the difference in SWR distribution was not significant ($p = 0.68$).

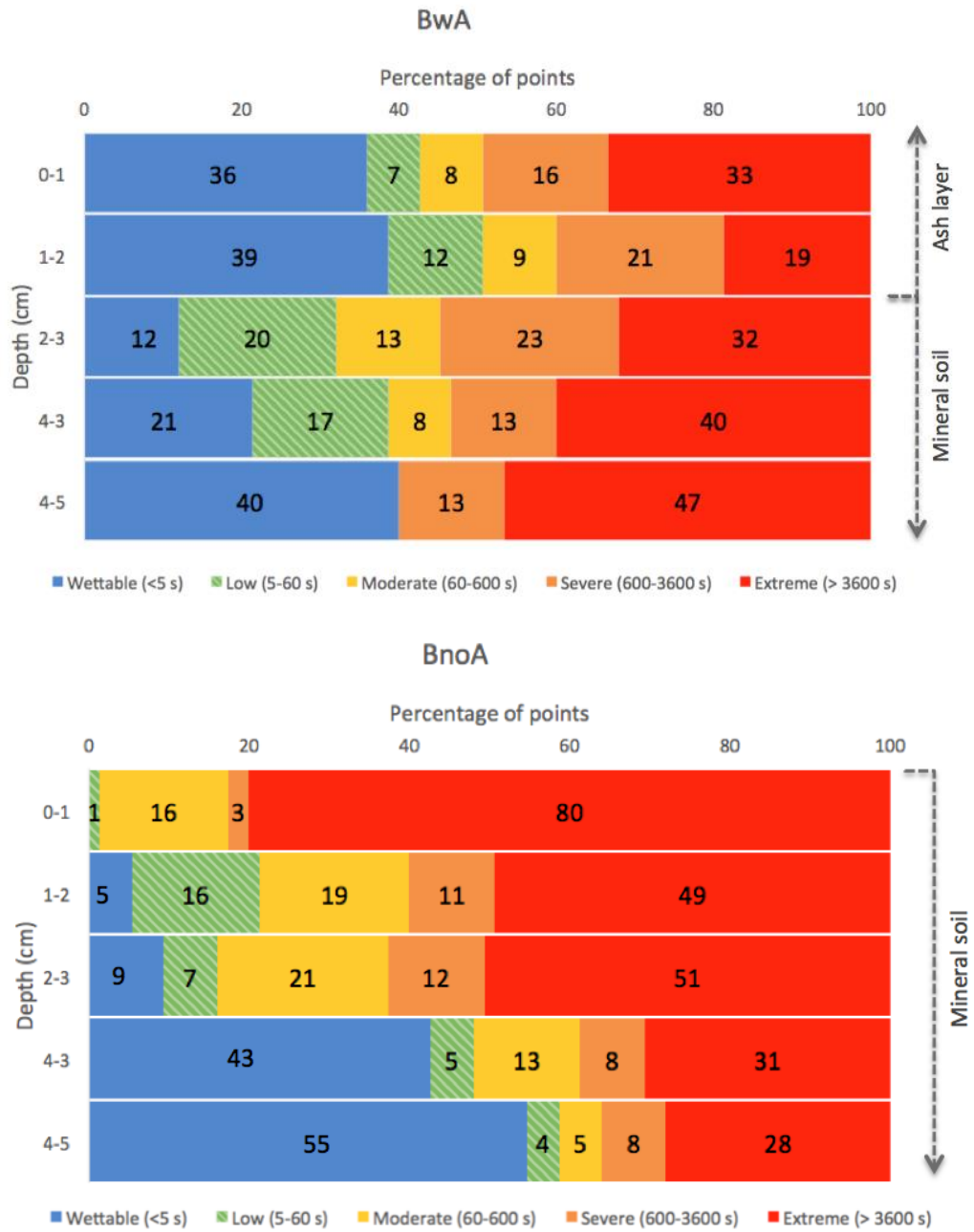


Fig. 2.6. Frequency distribution of SWR represented as the percentage of points for each repellency class in recently burned soils with ash layer (BwA) and ash layer removed (BnoA) ($n = 75$ per soil depth: 15 points per each core's depth \times 5 cores per soil).

2.3.3. Soil moisture prior to and after wetting

2.3.3.1. Laboratory measurements

Prior to wetting, all soils under wettable and water-repellent conditions (0 - 5 cm) were very dry, with mean SWC (vol.) values below 2 % and 4 % for BwA and BnoA respectively (Table 2.2). Upon wetting, SWC increased by 16 % and 8 % for BwA and BnoA soils respectively in the water-repellent scenario, while in the wettable scenario, the observed SWC change was significantly higher ($p < 0.001$) increasing by 47 % in BwA soil and 33 % in BnoA soil (Table 2.2). In this laboratory set up, water was able to drain out of the soil samples, resulting in 76 and 82 % (BwA and BnoA respectively) drainage in the water-repellent scenario, starting within 3 minutes of the start of wetting. Drainage was significantly lower under wettable conditions with only 14 % and 36 % (BwA and BnoA, respectively) beginning at approximately 9 min after the start of wetting (Table 2.3).

Table 2.2. Average SWC (measured volumetrically (% v v⁻¹) in the field and gravimetrically (% g g⁻¹) in the intact cores) before and after wetting with water (water-repellent scenario) and wetting with water and wetting agent (wetable scenario). Values are the mean with SD in brackets.

	Soil	Water-repellent scenario					Wetable scenario				
		Before wetting		After wetting		Δ SWC (%)	Before wetting		After wetting		Δ SWC (%)
Intact cores (n = 10)	BwA	2.8	(2.2)	19.3	(22.2)	16.5	2.8	(2.2)	49.4	(35.5)	46.7
	BnoA	7.6	(3.8)	15.5	(8.0)	7.9	7.6	(3.8)	41.0	(14.7)	33.4
In situ (n = 8)	BwA	1.6	(0.5)	15.8	(2.6)	14.3	1.9	(1.7)	18.5	(5.8)	16.6
	BnoA	4.4	(2.5)	20.3	(11.9)	15.9	4.2	(1.6)	26.7	(5.5)	22.5

SWC within the intact cores before wetting was low and rather uniformly distributed, falling within the 0 - 10 % SWC class. Wetting resulted in a significant increase in SWC at all soil depths under both water-repellent and wettable scenarios ($p < 0.001$) (6), except at 2 - 3 cm depth in the BnoA soil. The difference in SWC after wetting was especially pronounced in the BwA soil, where surface SWC (0 - 1 cm depth) under water-repellent conditions was nearly half that under wettable conditions for the same depth (Fig. 2.7). The difference in SWC in the BwA site is more pronounced with depth, with SWC approximately 3 times lower under water-

repellent conditions. The distribution of SWC after wetting was highly variable (Fig. 2.8) and larger variation was observed under water-repellent conditions (coefficient of variation, $CV = SD \text{ Mean}^{-1}$, ranging from 67 to 84 % and 39 and 73 % in the BwA and BnoA soil respectively).

Table 2.3. Time to drainage (min after the start of wetting) and drainage as a percentage of total water added under laboratory conditions in burnt soils with ash (BwA) and ash removed (BnoA) under water-repellent (wetted with water) and wettable (wetted with water and wetting agent) conditions. Values are the mean with SD in brackets.

Soil	Time to drainage (min)				Drainage (%)			
	Water-repellent		Wettable		Water-repellent		Wettable	
BwA (n=5)	3.4	(1.3)	12.3	(3.3)	76.3	(19.1)	14.0	(7.5)
BnoA (n=5)	3.5	(1.9)	8.8	(6.1)	82.8	(12.6)	36.6	(29.0)

2.3.3.2. *Field measurements*

The wetting experiments in the field resulted in infiltration into all soils under both water-repellent and wettable scenarios, with an increase in SWC observed in all plots. However, depending on the wetting treatment, the change in SWC was very variable. SWC in the soil wetted with water increased significantly by 14 and 16% in the BwA and BnoA with respect to pre-wetting values ($p < 0.001$). The soil wetted with the wetting agent reached significantly higher SWC values ($p = 0.035$) than in the water-repellent scenario, resulting in a significant increase in SWC of 17 % and 23 % in BwA and BnoA with respect to pre-wetting values ($p < 0.001$) (Table 2.2). Infiltration differed between the sites. In the BwA, on flat terrain, 100 % infiltration was observed in both collars, those wetted with water and those with water and a wetting agent. While at the BnoA site, situated on a 30° slope, 100 % infiltration was also observed under wettable conditions whilst under water-repellent conditions, 65 % of the total water added infiltrated into the soil with the remaining 35 % transformed into overland flow and leaving the respiration collar without infiltrating.

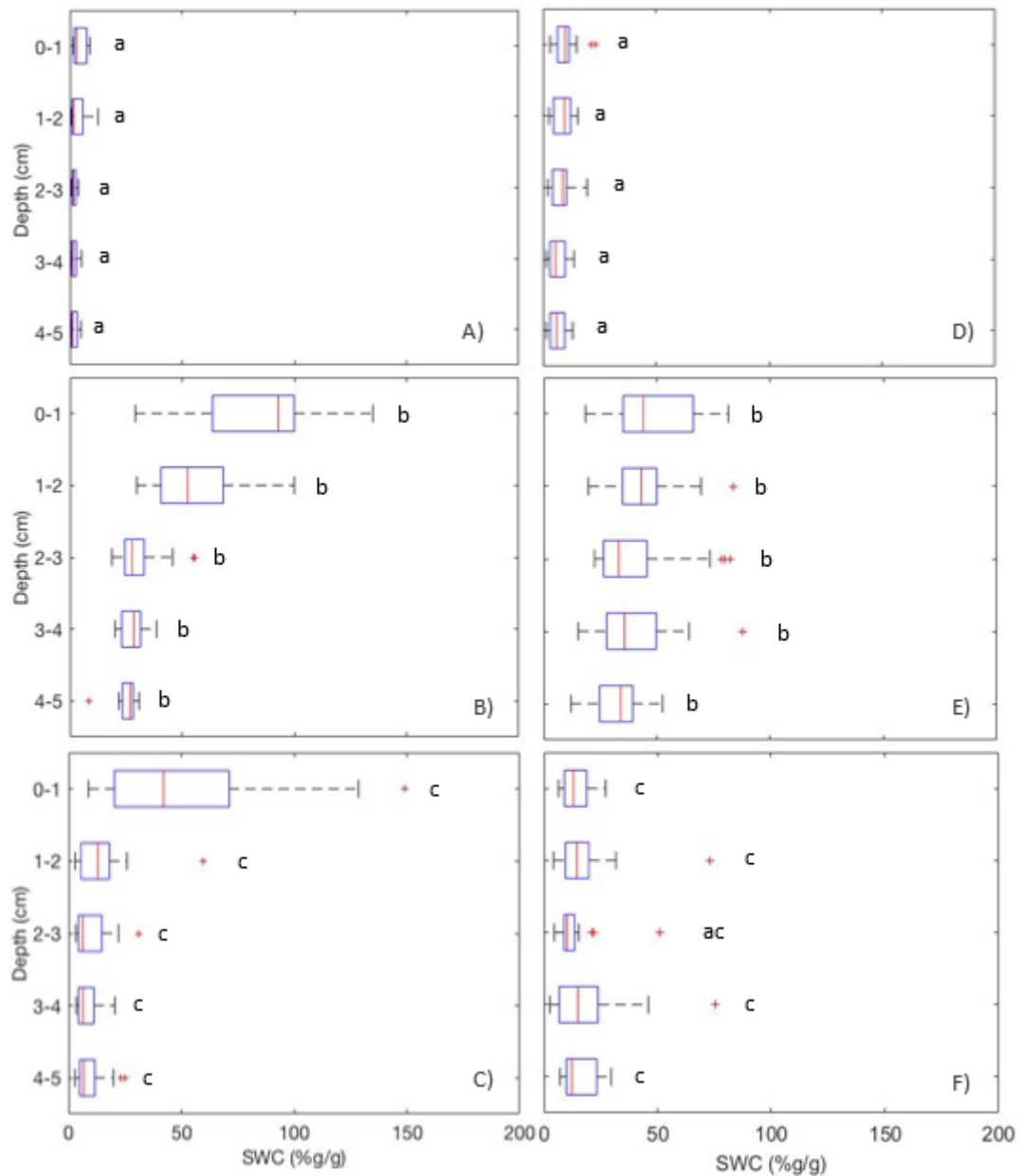


Fig. 2.7. SWC after wetting with depth. **A)** Burnt soil with ash (BwA) before wetting, **B)** BwA under wettable scenario, **C)** BwA under water-repellent scenario, **D)** Burnt soil with ash removed (BnoA) before wetting, **E)** BnoA under wettable scenario, **F)** BnoA under water-repellent scenario. Central mark indicates the median, bottom and top edges indicate 25th and 75th percentiles. Whiskers represent maximum and minimum data points. Outliers are plotted as '+' and represent points that are 1.5 times less or greater than the 25th and 75th percentiles respectively. Different lowercase letters (a-c) within the same layer and site indicate significant differences between SWC before wetting and after wetting under wettable and water-repellent conditions at a $p < 0.05$.

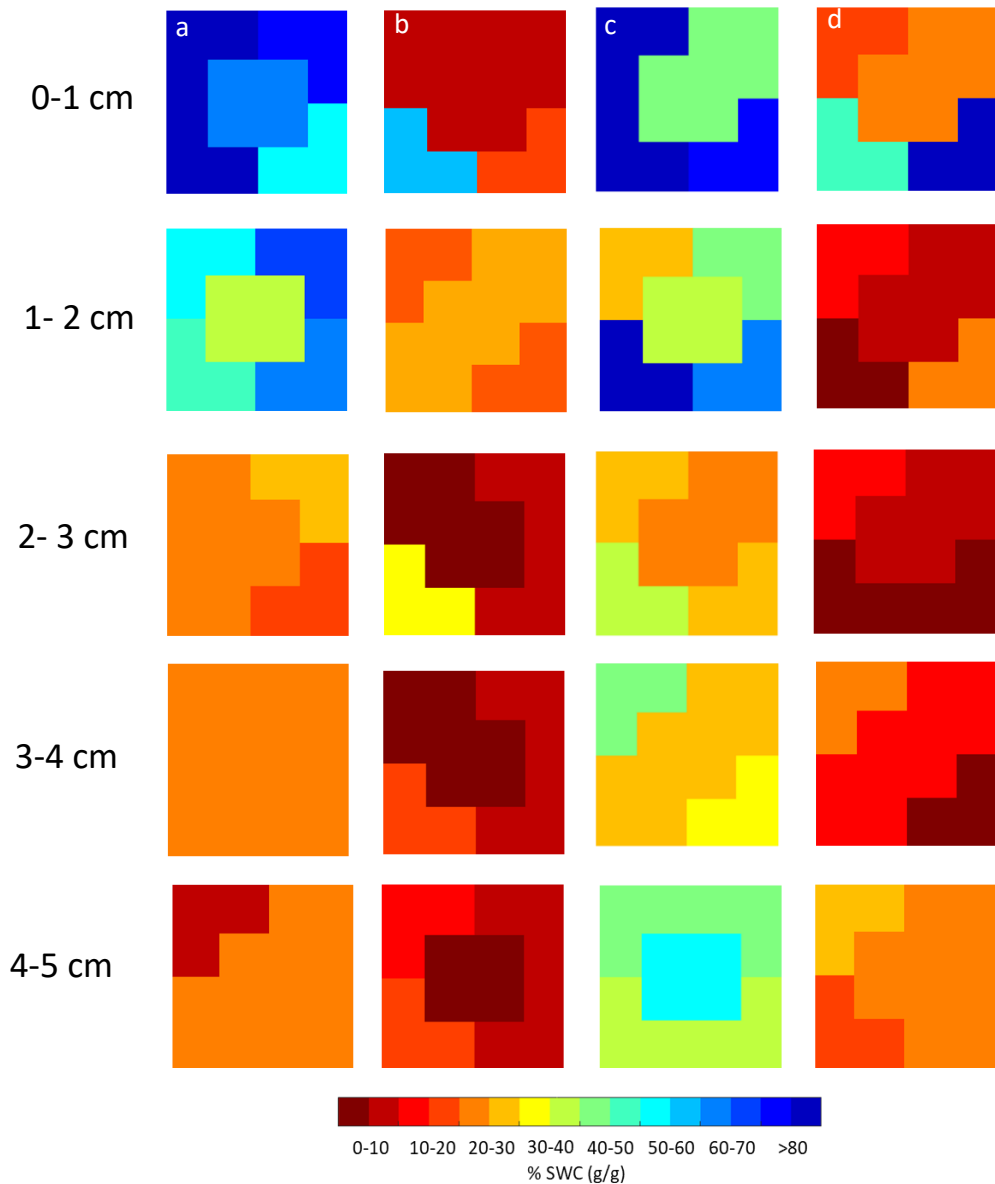


Fig. 2.8. Representative example of SWC distribution after wetting of intact core samples under laboratory conditions: a) Burnt soil with ash (BWA) under wettable conditions (wetted with water and wetting agent), b) BWA under water-repellent conditions (wetted with water), c) Burnt soil with ash removed (BnoA) under wettable conditions (wetted with water and wetting agent), d) BnoA under water-repellent conditions (wetted with water).

2.4. Discussion

The first significant wetting after the fire, simulated in the experiment, resulted in a distinct CO₂ pulse under both field and laboratory conditions, but the magnitude of the peak strongly depended on the type of wetting scenario and the presence of ash on the soil surface.

The CO₂ pulse was observed during and immediately after wetting under the wettable scenario, whereas wetting of water-repellent soils showed significantly lower peaks, especially in the laboratory experiment (Fig. 2.3). Under water-repellent conditions, the applied water initially ponded on the surface due to extreme water repellency inhibiting uniform infiltration, but then percolated quickly through the sample, within 3 min after the start of wetting, with up to 70 % of applied water draining out of the soil (Table 2.3). Such behaviour is very typical for water-repellent soil and has been commonly observed by others under field (e.g. Leighton-Boyce et al., 2007) or laboratory conditions (e.g. Urbanek and Shakesby, 2009; Urbanek et al., 2015) in fire-affected as well as unburnt water-repellent soils. This quick percolation resulted in a limited replacement of air in air-filled pores by water in the soil matrix and hence a low CO₂ pulse. The very low SWC in many areas of the soil samples after wetting (Fig. 2.7 and 2.8) supports this interpretation. We expect that movement of water via preferential flow paths resulted in a fractured distribution of SWC, and areas of water-filled pores were adjacent to areas of air-filled pores. It is likely that preferential infiltration increased the pore pressure along the wetting path and facilitated gas movement to air-filled pores of lower pore pressure. These aeration channels within the soil matrix would facilitate gas exchange between the soil matrix and the atmosphere. Smith et al. (2017) argued that hydraulic connectivity at the pore-scale is an important factor affecting CO₂ dynamics after wetting, based on the observation that cumulative CO₂ efflux was higher when larger pores were connected first, during a rainfall event, as opposed to smaller pores filling first, for example, during capillary rise wetting.

Under a wettable scenario, the even increase in SWC throughout the samples suggests that the wetting front moved relatively evenly downwards, refilling most soil pores with water, resulting in the much higher CO₂ pulse observed.

The wetting experiment under field conditions confirmed the observations from the laboratory. The CO₂ pulses were much higher here, but the differences between the wettable and water-repellent scenarios were slightly less distinct. Furthermore, the differences between

the CO₂ pulses from soil in flat terrain with the ash remaining (BwA) and the site on the slope with the ash removed (BnoA) were very significant.

The observed overall larger CO₂ fluxes in the field experiment would be expected because of the larger pore volume of the whole soil profile in comparison to the shorter soil sample cores used in the laboratory. Other studies observed similar (Castaldi et al., 2010; Marañón-Jiménez et al., 2011; Vargas et al., 2012), or even higher (Marañón-Jiménez et al., 2011) CO₂ peaks from field rainfall simulations, presumably because of the deeper soil profiles, compared to the shallow soils present at our study sites.

The actual CO₂ pulses in the field were likely to have been even higher than what we measured as it was not possible to measure the CO₂ flux during the wetting and hence measurements started only after the addition of water was completed. Indeed, the laboratory experiments showed the largest peak to occur during the wetting, suggesting that the actual peak in the field experiment might have been twice as high (as shown in the Fig. 2.5). We expect that this large peak during the rewetting is also often not captured in other field studies because of limitations in the frequency of measurements when using automated soil CO₂ flux monitoring systems or due to other methodological challenges during rainfall events when measuring with the long-term eddy covariance techniques.

In the field wetting experiment, very distinct differences in CO₂ flux responses were observed between the study sites. BwA exhibited much higher CO₂ peaks with a distinct difference between wetting scenarios, while BnoA had much lower CO₂ peaks and no significant differences between wettable and water-repellent scenarios.

We expect that the presence of ash contributed to the magnitude of the pulse for a range of reasons. The ash layer remaining on the surface was able to absorb and retain substantially more water (Table 2.2) than the mineral soil underneath. A higher volume of refilled pores would have resulted in larger CO₂ pulses. The presence of an ash layer also affected the SWR distribution (Fig. 2.6) and consequently the infiltration and the water distribution pattern (Fig. 2.7 and 2.8). In BwA, the first 2 cm of the soil only 60 % of points exhibited water repellency as opposed to the top mineral layer, which showed up to 100 % of water-repellent points (Fig. 2.6). Water-repellent ash has been observed after low severity fires and is mainly related to the organic C content of the samples but, in most cases, wildfire ash has been observed to be wettable (see review by Bodí et al., 2014). Depending on its initial wettability, the incorporation of ash into the soil matrix can enhance or reduce SWR (Bodí et al., 2011). Such patchy distribution of SWR suggests that water infiltration was irregular, possibly even

favouring a rapid gas exchange between the soil and the atmosphere. Urbanek and Doerr (2017), who investigated the effect of water repellency on CO₂ efflux, suggested that patchy SWR can provide very favourable conditions for soil respiration and gas diffusion, because water-repellent zones can create aeration channels adjacent to infiltration paths, in which gas exchange is stimulated.

Another potentially important contribution to the CO₂ pulse might result from abiotic processes such as the chemical reaction of carbonates with wetting. Calcium carbonate produced from the burning of organic matter at high temperatures is commonly observed in wildfire ash (Bodí et al., 2014; Dlapa et al., 2013; Pereira et al., 2012). Carbonates are known to contribute substantially to CO₂ fluxes in calcareous soils (Bertrand et al., 2007; Serrano-Ortiz et al., 2010) or to the rapid flush of CO₂ with wetting observed during the incubation of biochar in soil (Bruun et al., 2014). However, in this case, the addition of acid to the ash suggested low to no presence of carbonates. We therefore expect that the contribution to CO₂ flux from carbonates in the ash layer was negligible. Further studies would be beneficial to understand the role of ash on CO₂ emissions from soil, with a special focus on the specific contribution of ash to CO₂ fluxes after the fire.

It was surprising to find very low CO₂ pulses after wetting of soils at BnoA, and much lower ($p = 0.172$) differences between the wettable and water-repellent scenarios. We expect that the removal of ash was the main reason for the low CO₂ pulses, but we anticipate that the slope of the study site also contributed to it. Increased overland flow is commonly recognized in post-fire environments on slopes where SWR inhibits infiltration, sometimes causing mass movement of the remaining ash down the slopes (Bodí et al., 2012). It was observed (although not shown in the results) that simulated wetting directly on completely water-repellent mineral soil resulted in overland flow, but this was partially blocked by the soil collar and caused ponding of water at the lower part of the collar. We expect some concentrated infiltration occurred at the lower part of the collar resulting in the infiltration and the main gas exchange occurring outside of the collar, which was not captured in the measuring chamber.

The duration of the peak we have observed is relatively short, but it is in line with other studies (Marañón-Jiménez et al., 2011; Munson et al., 2010; Rey et al., 2017; Sponseller, 2007; Wang et al., 2016). For example, Rey et al. (2017), during a field study observed CO₂ effluxes peaking only 15 minutes after wetting during *in situ* rain manipulation experiments. The short duration of the peak could suggest that the flush of CO₂ is mainly caused by degassing (Inglima et al., 2009; Liu et al., 2002), with water refilling the air-filled pores and displacing the CO₂-rich air

previously stored in the pore space (Maier et al., 2011; Schymanski et al. 2017). Although the input of sudden increase in microbial respiration cannot be fully excluded, we suspect that it had a rather low contribution to this initial CO₂ pulse, as fire suppresses microbial activity due to sterilization (Mataix-Solera et al., 2009), along with low microbial respiration caused by lack of available water (Göransson et al., 2013). We expect that the wetting patterns caused by water repellency will have long lasting implications for the overall recovery of soil respiration, an area that warrants attention in future studies.

Although this study focused mainly on the short-term and immediate effects of rewetting of post-burn soils on CO₂ efflux, we anticipate that the overall impact of fire on physical changes to soil conditions are rather long lasting. Fire is known to change the overall C flux system from a sink to a source of CO₂ (Irvine et al., 2007). These so-called 'hot moments', with sudden short-lived but high-magnitude spikes in C release from soil, can have a cumulative effect after rainfall events and make up a substantial fraction of the annual C balance (Leon et al., 2014; Smith et al., 2017). In our study, the CO₂ peak accounted for 78% of the total CO₂ released during the observation in both BwA and BnoA soil under wettable conditions. Schymanski et al. (2017) reported a CO₂ flush of similar magnitude when rewetting a sterilised soil, as a result of physical replacement of CO₂ by water, as when rewetting natural soils under field conditions. In a longer observation, Castaldi et al. (2013) quantified that the pulse of CO₂ in burnt soils, which peaked during the first day after water addition, accounted for about 50% of the total CO₂ emissions over a 15-day observation period. Marañón-Jiménez et al. (2011) observed during an *in situ* rewetting study of recently burned soil that up to 64% of the total CO₂ released during the first 2 hours after wetting was related to degasification of CO₂-rich air in soil pores. Similarly, Maier et al. (2010) showed that during extreme rainfall events, up to 20% of the total flux originated from CO₂ stored in the pore-space prior to the wetting event. While the degassing effect with wetting is short-lived, on the scale of minutes to hours after wetting, overlooking the release of previously stored CO₂ might result in overestimations of the contribution of microbial mineralization to the Birch effect.

The longer-term effects of preferential infiltration on microbial respiration are still not fully understood and future studies should aim at incorporating the dynamic alterations in soil hydraulic functions as a result of SWR (Robinson et al., 2019). Most soils show some degree of repellency, however, models are still limited in their ability to include spatial variability of water content and, when calculating C fluxes, represent only average changes in soil moisture.

It is also important to keep in mind that SWR is not only a feature of burnt soils; extreme water repellency is also commonly observed in dry, unburnt soils (Doerr et al., 2000). Under our changing climate, a higher frequency and intensity of droughts followed by large rainfall events is expected. Water repellency is, therefore, likely to become more common and severe (Goebel et al., 2011). Although the current study was carried out on fire-affected soils, we anticipate that a similar CO₂ efflux behaviour of dry soils in response to rainfall can be expected in any soils affected by water repellency. How common and distinct this behaviour is, however, remains to be confirmed by further studies.

2.5. Conclusions

This study, which focused on investigating the effect of water repellency on CO₂ efflux upon rewetting of recently burned soils, has confirmed that SWR does reduce the Birch effect. Both laboratory and field-based experiments showed that infiltration and percolation patterns in water-repellent soils were concentrated along preferential flow paths, resulting in substantial drainage of applied water and very low rewetting rates of the soil matrix. The smaller the overall changes were in SWC, the lower the cumulative efflux from the soil was, suggesting that concentrated flow in water-repellent soils results in smaller volumes of CO₂-filled pores replaced by water and a lower Birch effect. The study has also shown that the ash layer remaining on the surface of burnt soils contributed substantially to the overall CO₂ flush upon rewetting, most likely due to its higher absorption and retention rates than the mineral soil.

Although this study focused mainly on the short-term and immediate effect of rewetting of burnt soils on CO₂ efflux, which is predominantly caused by soil degassing, the overall implications of fire with regards to physical changes in soil conditions can be expected to be long lasting. Given that fire overturns the overall C flux system from a sink to a source of CO₂, the short-lived but high-magnitude spikes in C release from soil after rainfall are likely to make up a substantial fraction of the annual C balance. It is therefore important to consider SWR as an important factor affecting the rewetting patterns of soil and reducing the CO₂ efflux when calculating and predicting overall C fluxes between soil and the atmosphere. It is also important to remember that SWR is not only a feature of burnt soils but also that extreme water repellency is also commonly observed in dry, unburnt soils. Therefore, we expect similar behaviour in any soil affected by water repellency.

Chapter 3. The effect of water repellency on the short-term
release of CO₂ upon soil wetting

Carmen Sánchez-García, Stefan H. Doerr, Emilia Urbanek

Published in: Geoderma (2020) 375, 114481.

(DOI: <https://doi.org/10.1016/j.geoderma.2020.114481>)

3.1. Introduction

Rewetting of dry soils is associated with a large pulse of carbon dioxide (CO₂) commonly known as the 'Birch effect' (Birch, 1958). The overall contribution of these short-lived but high magnitude spikes of CO₂ to the total soil carbon (C) flux could be large (Leon et al., 2014; Smith et al., 2017), especially with increased frequency and duration of dry spells, which are becoming more common with the climatic change (Coumou and Rahmstorf, 2012; Trenberth et al., 2013). Although the 'Birch effect' has been studied for over 50 years, there is still a lack of consensus about the exact causes and factors affecting the size and duration of the CO₂ pulse (Fraser et al., 2016; Waring & Powers, 2016) which are still not included in the global terrestrial C emissions models (Moyano et al., 2013).

Many studies suggest that the 'Birch effect' originates mainly from a quick restoration of microbial respiration, which is very low in dry soils due to restricted water availability for microorganisms and the disconnection of soil pores (Borken and Matzner, 2009). After rainfall, the sudden input of water reconnects the pore system and mobilizes previously unavailable C (Kim et al., 2012; Schimel, 2018) resulting in a boost of microbial activity and a spike in soil CO₂ efflux. The size of the CO₂ pulse is expected to increase with the amount of water added (Lado-Monserrat et al., 2014; Muhr and Borken, 2009; Sponseller, 2007). Although the boost in microbial respiration is probably the largest contributor of CO₂ to the 'Birch effect', some studies argue that the lag period between the wetting and the reactivation of microbial activity can last several hours (Meisner et al., 2017). It has, therefore, been suggested that the degassing of soil might be the main contributor of the CO₂ pulse during the early post-wetting phase (Kim et al., 2012; Norman et al., 1992). Soil gas is not always emitted immediately. Degassing of CO₂ stored in the pore-space can make up a substantial fraction of the total CO₂ response to wetting during extreme rainfall events (Maier et al., 2010; 2011; Huxman et al., 2004; Inglima et al., 2009; Liu et al., 2002).

'Birch effect' studies have focussed mainly on the duration and intensity of the drought (de Nijs, 2018; Göransson et al., 2013; Meisner et al., 2015), precipitation rates (Lado-Monserrat et al., 2014; Muhr et al., 2008) or the type of wetting (Smith et al., 2017) as the main factors affecting the size of the pulse. In a recent study (Sánchez-García et al., 2020b) we have shown that restricted infiltration, caused by soil water repellency (SWR), can also alter the CO₂ efflux response to wetting substantially. SWR is a transient property of many soils, especially those under permanent (Doerr et al., 2000) and stress-tolerant vegetation at low soil water content (SWC) (Seaton et al., 2019). SWR is primarily caused by the coating of soil particles by hydrophobic organic compounds and can become especially severe after dry periods or fires

(DeBano, 2000; Doerr & Thomas, 2000). Current changing climate conditions resulting in higher incidence and intensity of droughts will likely enhance the occurrence and severity of SWR (Goebel et al., 2011). By inducing changes in soil microbial properties and community structure in response to environmental stressors like drought, soils with stress-tolerant vegetation can develop hydrophobic layers in order to adapt to low water availability (Seaton et al., 2019). Thus many soils subjected to dry spells change their hydrological properties by developing this lack of wettability. Robinson et al. (2019) highlighted the need to incorporate the dynamics of hydraulic properties in response to such biological feedbacks.

Water-repellent soils do not allow free infiltration of water; instead, water runs off the terrain's surface (Doerr et al., 2003) or beads up and percolates quickly into the subsoil through preferential flow paths, leaving much of the topsoil dry (Doerr et al., 2000; Ritsema and Dekker, 1994). The infiltration patterns of water-repellent soils are thus substantially different to wettable ones, and therefore, the CO₂ efflux in response to wetting of such soils is unlikely to be the same.

Despite this, evidence of water repellency-induced changes in soil C dynamics remains sparse. A few studies have focused on respiration rates in water-repellent soils (Goebel et al., 2007; Lamparter et al., 2009) or the overall effects of SWR on CO₂ fluxes (Urbanek and Doerr, 2017) rather than on short-term spikes of CO₂ after rainfall events. In a previous study (Sánchez-García et al., 2020b) evidence was presented that SWR reduces the CO₂ pulse after wetting of soil; however, the effect of the rewetting rate on the magnitude and the duration of the CO₂ pulse in water-repellent soils have remained unclear.

In this study we address this research gap and aim to improve understanding of the effect of SWR on the CO₂ efflux upon rewetting. We hypothesise that i) the amount of released CO₂ is proportional to the rewetting rate of the soil and ii) the initial CO₂ pulse can be mainly caused by the physical release of gas present in soil pores by infiltrating water rather than a spike in microbial activity.

3.2. Research design and methods

This study involves a series of wetting experiments on homogenised soil under laboratory conditions. Soil material used for the experiments was autoclaved to remove the contribution from microbial respiration to CO₂ fluxes and to isolate the physical release of CO₂, but also to obtain soils with contrasting wettability that otherwise have similar physico-chemical properties (Urbanek et al., 2010). Autoclaving of dry or very wet soils keeps the soils wettable, while at intermediate water content prior to autoclaving the soil turns water-repellent. All soil

samples were subjected to one single wetting treatment applied from above to simulate a rainfall event. CO₂ fluxes were monitored above and below the soil sample in order to capture CO₂ movement upwards and downwards.

3.2.1. Soil sampling and preparations

Soil was collected from two locations in the Gower peninsula in South Wales (UK): a sandy loam referred to as Cefn Bryn (CB) (51° 35'N, 4° 10'W) and a loamy sand referred to as Southgate (SG) (51° 33'N, 4° 5'W) (Table 3.1). Soils at both locations are under natural grasslands with occasional animal grazing. The selected soils were used in previous studies (Gazze et al., 2017; Urbanek et al., 2010) and were known to develop SWR under natural conditions. The use of two types of soil material of different texture and SOM content allowed us to examine to what degree similar behaviour is observed in water-repellent soils despite differences in their physico-chemical properties.

Table 3.1. General characteristics of the soil from the two study sites (CB: Cefn Bryn, SG: Southgate) before autoclaving.

	CB		SG	
% Soil organic matter (SOM)	11.1	(0.4)	32.1	(0.5)
Particle density (g cm ⁻³)	2.31	(0.1)	2	(0.1)
% Porosity	56	(1.1)	59	(2.4)
pH (H ₂ O)	4.8	(0.06)	6.4	(0.02)
pH (CaCl ₂)	3.7	(0.04)	5.6	(0.02)
Particle size distribution				
% Sand	64.4	(0.03)	86.6	(1.86)
% Silt	33.6	(2.77)	12.3	(2.72)
% Clay	2.1	(0.18)	0.7	(0.17)
Texture	Sandy loam		Loamy sand	

Values represent the mean (n = 3) with standard deviation in brackets.

Soil material was collected from approximately the top 2 to 10 cm over an area of 2 m², after careful removal of the grass root layer, brought to the laboratory, and air-dried and sieved to

2 mm. In order to prepare soil material of the same physico-chemical properties, but contrasting wettability, soil was pre-treated using a technique developed by Urbanek et al. (2010), which involved autoclaving the soil material at different SWC to obtain wettable and water-repellent soil. In order to determine an optimal SWC that results in the most contrasting wettability, a small sample of each soil at air dry, 10, 15, 40 and 50% SWC (grav.) was autoclaved (121 °C for 1 h) followed by oven-drying at 25 °C for 24 h to achieve similar SWC across all the samples (see Table 3.2 for a full range of results). Soil wettability was measured before and after autoclaving using the water drop penetration time (WDPT) test by placing 5 drops of water on the smoothed surface of a sample and categorised into the following classes (Doerr, 1998): wettable (< 5 s), slightly repellent (5–60 s), moderately repellent (60–600 s), strongly repellent (600–3600 s) and extremely repellent (> 3600 s). Based on these tests, SWC for autoclaving was chosen to be 15% for both CB and SG soils to obtain extreme SWR (thereafter called CB-WR and SG-WR), and for the wettable soil 40% and 50% SWC was used for CB and SG respectively (thereafter called CB-NWR and SG-NWR). Although WDPT does not detect small variations in subcritical water repellency (Goebel et al., 2012; Urbanek et al., 2007), in this case WDPT was suitable given the contrasting wettability between our samples.

Other basic soil properties of the two soil materials were determined using standard methods; pH using a pH electrode in 1:5 dilutions of distilled water and CaCl₂, soil organic matter (SOM) using the loss of ignition method (Nelson and Sommers, 1996), particle size distribution using the laser diffraction method (LS230 laser particle size analyser, Beckman Coulter, Brea, CA) and particle density (ρ) following the Gay-Lussac Specific-Gravity Bottles method (Wofford and Vidrio, 2015 adapted). SWC was determined gravimetrically by moisture loss (105 °C, 24 h).

Table 3.2. Soil water repellency tests results (s) (Doerr, 1998) before and after autoclaving both soils CB and SG at air dry, intermediate and high SWC (% g g⁻¹). Tests were done to assess optimal SWC for autoclaving to obtain wettable and water-repellent samples. Highlighted blue and orange values represent SWC values chosen for the experiment in order to obtain wettable and water-repellent samples respectively.

Soil	Before Autoclaving			After autoclaving			After autoclaving and oven drying (25 °C)		
	SWC	WDPT	SWR rating	SWC	WDPT	SWR rating	SWC	WDPT	SWR rating
CB	2.9	< 5	Wettable	6.1	256	Moderate	1.35	180	Moderate
	10.6	2120	Strong	8	> 3600	Extreme	1.28	4421	Extreme
	15.2	> 3600	Extreme	14	> 3600	Extreme	1.38	7312	Extreme
	38	< 5	Wettable	44.3	< 5	Wettable	1.57	< 5	Wettable
	49	< 5	Wettable	53.3	< 5	Wettable	1.45	< 5	Wettable
SG	4.7	< 5	Wettable	7.2	376	Moderate	3.09	423	Moderate
	11	44	Slight	14	> 3600	Extreme	3.35	8637	Extreme
	15.4	237	Moderate	19.8	> 3600	Extreme	3.42	10368	Extreme
	40.7	< 5	Wettable	40.1	11	Slight	7.1	128	Strong
	53	< 5	Wettable	52.2	< 5	Wettable	1.27	< 5	Wettable

Values represent the mean (n = 3).

3.2.2. Soil wetting and CO₂ efflux measurements

Dry sterile soil at respective wettability (wetable and water-repellent) was packed into cylinders (8 cm diameter, 5 cm height) at bulk densities representative of field conditions: 1.16 and 0.82 g cm⁻³ for CB and SG respectively. The repacked cylinders were rewetted from above using a custom-made rainfall simulator fitted between the soil sample collar and the CO₂ flux chamber (Fig. 3.1). The rainfall simulator comprised one spiral tube with uniformly distributed drips, to ensure spatially uniform wetting, suspended 1 cm above the soil surface and connected via a tube to a large syringe to supply water. All cylinders received one single and uniform wetting application with water at an intensity of 100 mm h⁻¹ to simulate a heavy rainfall event. The applied water was equivalent to 25, 50, 75 and 100% of water-filled pore-

space (WFPS). WFPS for each soil was calculated by dividing volumetric water content by pore-space (PS) and pore-space was obtained from bulk density (dB) as follows: $PS = (1 - \frac{dB}{d_p}) \times 100$; assuming a particle density (d_p) = 2.65 g cm⁻³ (Blake, 2008). After wetting, water retained in the soil sample was quantified via the weight difference in the soil before and after wetting.

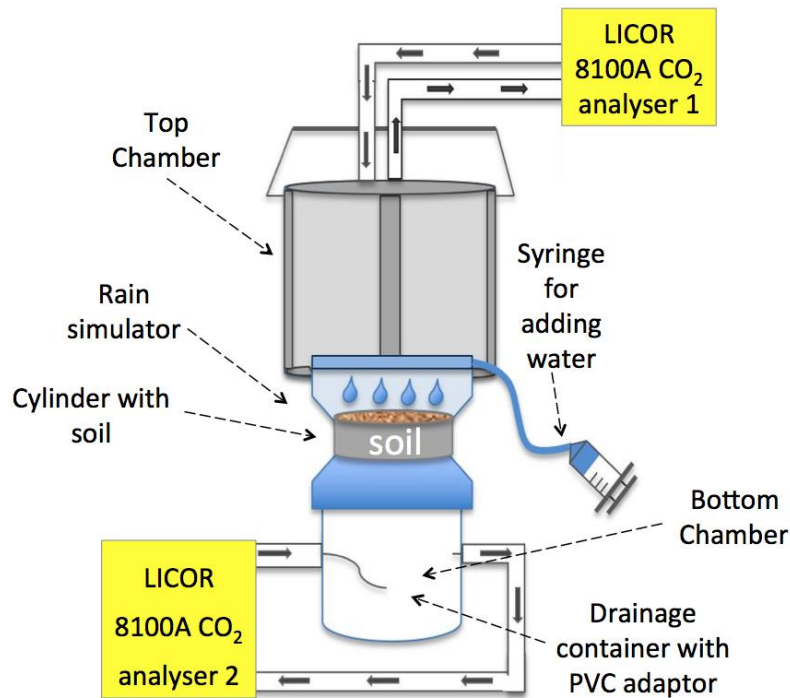


Fig. 3.1. Schematic illustration of rewetting and CO₂ analyser system.

Each cylinder was suspended on a set of collars allowing monitoring of CO₂ concentration in the chamber above and below the sample simultaneously during the wetting and collection of drained water in the container below (Fig. 3.1). CO₂ concentration was monitored via a 10 cm survey chamber connected to an infrared CO₂ gas analyser system (IRGA) from above (Li-8100A, Li-COR Inc., Lincoln, NE) and a plastic container of a similar headspace connected to a separate IRGA CO₂ analyser system below the sample referred to as ‘bottom chamber’ (Li-8100A, Li-COR Inc., Lincoln, NE). A fine mesh was placed under the cylinders to allow any drainage of water while holding the soil inside the cylinder. The entire system (chambers, rainfall simulator and soil sample) was sealed to avoid gas leakage. The chamber’s inbuilt pressure vent maintained ambient pressure inside the chamber (Fig. 3.1). The total time of

post-wetting CO₂ fluxes monitoring was 150 min, the gas chamber remained closed for 30 min and vented for 1 min prior to the next closure.

The CO₂ concentration data obtained were fitted to a single-term exponential model, excluding the first 30 s of measurements, which is the typical time required to achieve steady mixing inside the chamber (LICOR, 2010). The following equation (Eq. 3) was applied to calculate CO₂ flux as the rate of change in CO₂ concentration released from soil (LICOR, 2010):

$$\text{Eq. 3} \quad Fc = \frac{10VPo}{RS(To+273.15)} * \frac{dC'}{dT}$$

Fc = soil CO₂ efflux (μmol m⁻² s⁻¹), V = volume (cm³), Po = initial pressure (kPa), S = soil surface area (cm²), To = initial air temperature (°C) and dC'/dT = initial rate of change in water-corrected CO₂ mole fraction (μmol mol⁻¹). The CO₂ flux data below R² ≥ 0.95 was rejected with a total of 10 and 15% of total rejected measurements above and below the sample respectively. The CO₂ flux graphs were created by calculating the mean flux (n = 3) for each treatment at each measurement time along with 95% confidence intervals. The Mann-Whitney U-Test was applied to test for statistical differences (accepted at p < 0.05) between wettable and water-repellent soils.

3.3. Results

3.3.1. CO₂ efflux before and after wetting

The CO₂ efflux from dry soils prior to wetting was very low. In all soils, the efflux measured in the top chamber was below 1 μmol m⁻² s⁻¹ and negligible in the bottom chamber (Fig. 3.2 and 3.3). The CO₂ efflux increased immediately in response to the wetting, which began exactly 20 min after the initial start of the observation. A clear increase in CO₂ efflux occurred in all wettable soils, with the maximum value observed during the wetting period for most samples, or immediately after the wetting period for SG-NWR with 25 and 50% rewetting rates. Fluxes in the wettable soils peaked 1 and 5 min after the start of wetting for CB and SG respectively. Under wettable conditions, large differences in the size of the pulse were observed between CB and SG soils with similar amounts of water added. In the CB-NWR soil the efflux peaks ranged between 5–7 μmol m⁻² s⁻¹; whereas for SG-NWR soil, peak values were lower, ranging between 2.5–3.5 μmol m⁻² s⁻¹. The larger amount of water added to the soil resulted in a longer duration of the peak, but did not affect the peak size. Overall, the size of the peak was higher

but consistently shorter in CB soil, lasting between 11 and 20 min depending on the rewetting rate. For instance, doubling the rewetting rate from 25 to 50% increased the duration of the pulse by 4 min in both CB and SG soils, but no differences in the duration of the pulse were observed in SG soils with rewetting rates above 50%. In CB soils, the duration of the pulse increased by 4 min with a 75% rewetting rate but remained similar with a 100% rewetting rate.

The differences in the CO₂ efflux between wettable and water-repellent soils were very distinct. In both CB-WR and SG-WR, the size of the CO₂ pulse in the top chamber was up to ten times lower than in the corresponding wettable soils ($p < 0.001$ for both CB and SG soils). Peak sizes in water-repellent soils ranged from 1 to 3 $\mu\text{mol m}^{-2} \text{s}^{-1}$ in the CB-WR, but in the SG-WR the CO₂ efflux hardly changed as a result of wetting (peak size 0.3 to 0.6 $\mu\text{mol m}^{-2} \text{s}^{-1}$). During the wetting of CB-WR, a distinct double peak was observed with rewetting rates above 50%. By the end of the observation period, at 145 min after the start of wetting, the CO₂ fluxes returned to pre-wetting values and no significant differences were observed between soils of contrasting wettability ($p = 0.229$).

Prior to wetting, the CO₂ flux in the bottom chamber, which represented the amount of CO₂ diffused downwards the soil profile, was low in both wettable and water-repellent soils. In CB-WR, CO₂ fluxes did not increase with the start of the wetting in the bottom chamber; instead, a pulse was observed towards the end of the wetting period. Similar to the top chamber, no CO₂ flux response was observed in SG-WR; whereas, in the SG-NWR soil, CO₂ fluxes increased with the beginning of wetting and a significantly higher pulse than in the water-repellent soil was observed ($p < 0.001$). No significant differences were observed between the pulses in the top and bottom chambers in both CB-WR and SG-WR ($p = 0.525$ and $p = 0.184$ respectively); however, the CO₂ pulses were higher in the top than in the bottom chamber for both CB-NWR and SG-NWR ($p = 0.001$ and $p < 0.001$ respectively).

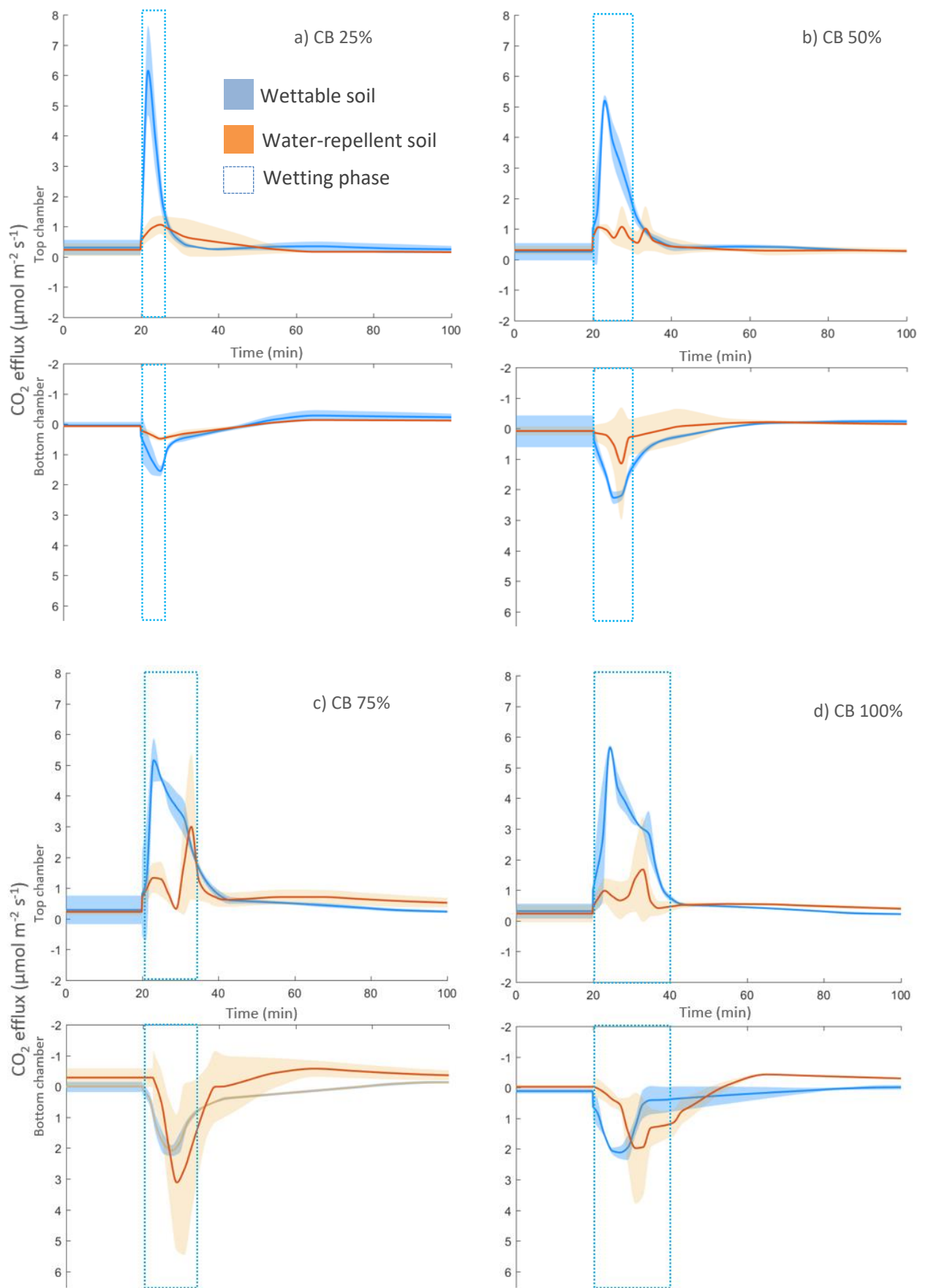


Fig. 3.2. Response of CO₂ efflux to wetting above and below the sample for autoclaved wettable (CB-NWR) and water-repellent (CB-WR) soil from CB under the 4 different rewetting rates (% of the water-filled pore-space). The orange line and shaded area represent the mean response (n = 3) with 95% confidence interval to the wetting of water-repellent soil and the blue line and shaded area represent the mean response (n = 3) with 95% confidence interval to the wetting of wettable soil.

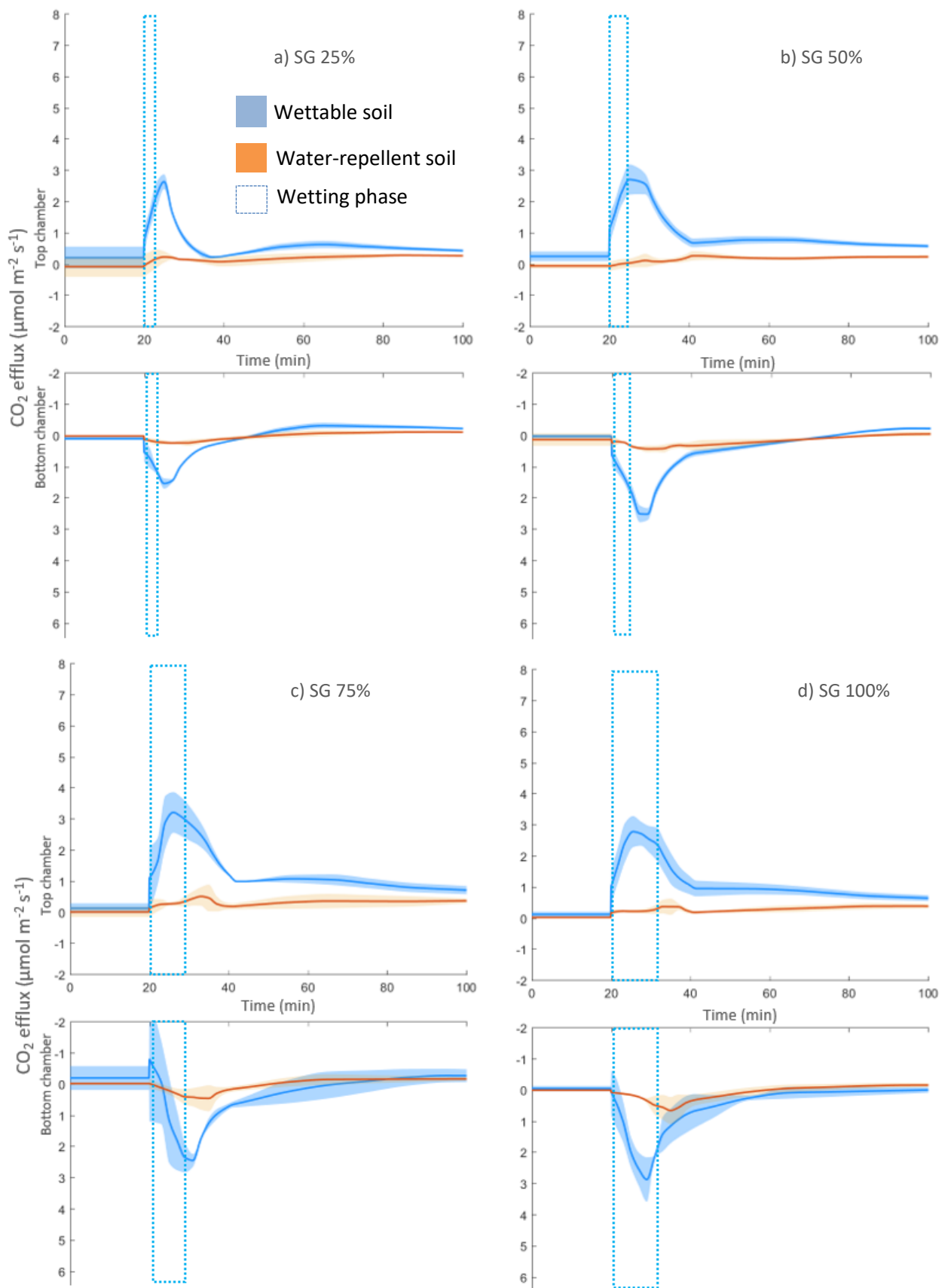


Fig. 3.3. Response of CO₂ efflux to wetting above and below the sample for autoclaved wettable (SG-NWR) and water-repellent (SG-WR) soil from SG under the 4 different rewetting rates. The orange line and shaded area represent the mean response ($n = 3$) with 95 % confidence interval to the wetting of water-repellent soil and the blue line and shaded area represent the mean response ($n = 3$) with 95 % confidence interval to the wetting of wettable soil.

3.3.2. Cumulative CO₂ efflux

The cumulative CO₂ efflux, calculated as the total CO₂ flux from both the top and bottom chambers combined, increased with the rewetting rate in wettable soils. The more water that was added to the soil, the higher the cumulative efflux was in the CB-NWR soil. In the SG-NWR, the cumulative efflux with the higher rewetting rates ($\geq 50\%$) was very similar, but in contrast, the cumulative efflux at the lowest rewetting rate (25% WFPS) was significantly lower. In water-repellent soils, the cumulative efflux from both CB and SG soils was significantly lower ($p < 0.01$ for both CB and SG) than in the corresponding wettable soils, except in the CB soil with 25% rewetting rate (Fig. 3.3). The cumulative CO₂ efflux increased only slightly, but not significantly, with rewetting rates above 50% in CB-WR. In SG-WR, the cumulative efflux was similar independently of the rewetting rate; only at 25% rewetting rate was the cumulative efflux lower, but not significantly, than for the rest of rewetting rates.

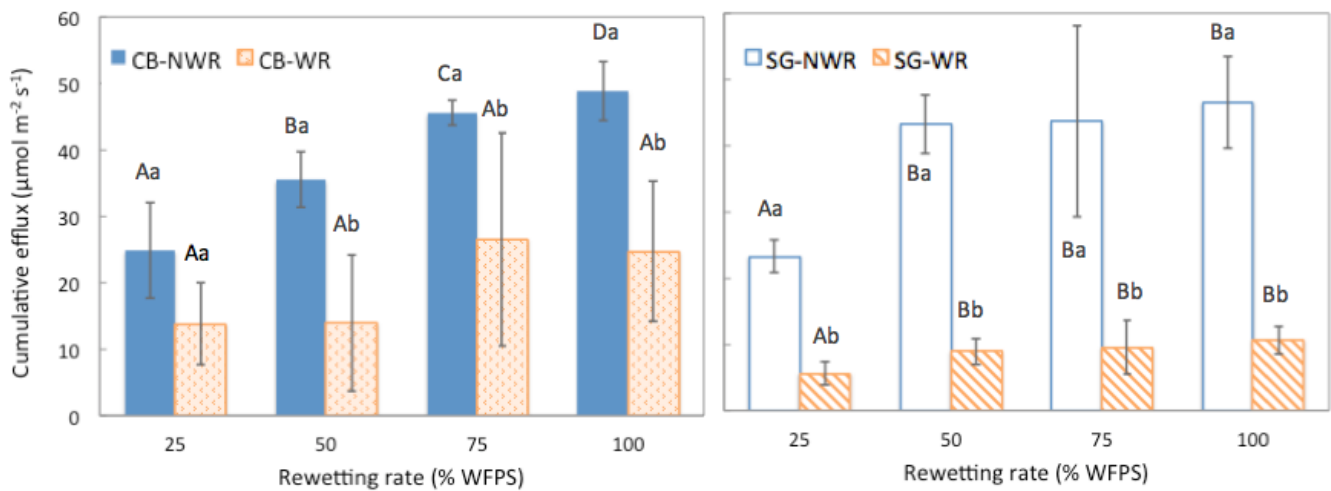


Fig. 3.4. Cumulative CO₂ efflux (top and bottom chambers combined) for wettable (CB-NWR and SG-NWR) and water-repellent (CB-WR and SG-WR) soils from CB and SG under the four different rewetting rates. Values are the mean ($n = 3$) with standard deviation bars. Different lowercase letters (a – b) within the same site and rewetting rate indicate significant differences between wettable and water-repellent soils at $p < 0.05$. Different uppercase letters (A – D) within the same site and soil wettability (wettable and water-repellent soil) indicate significant differences between rewetting rates at $p < 0.05$.

In wettable soils, the cumulative CO₂ efflux was positively correlated to the water retained in the soil after wetting (Fig. 3.4). In the CB-NWR soil, a positive relationship between the

cumulative CO₂ efflux and the amount of water retained in the soil after wetting was observed, but a surprisingly large efflux was observed in CB-WR with only a small amount of water retaining in the soil. For example, 8 cm³ of retained water resulted in cumulative efflux of 5.8 mmol m⁻², a value similar to those observed in the wettable soils where more than 90% of water was retained in the soil after the wetting.

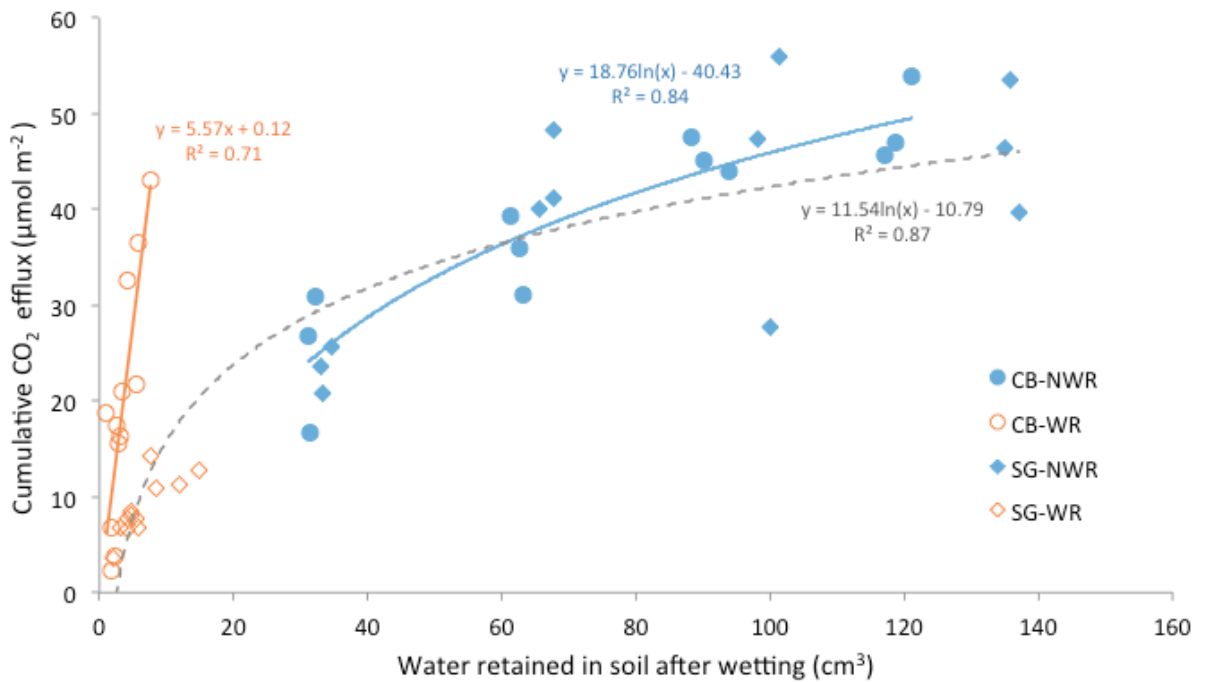


Fig. 3.5. Relationship between cumulative CO₂ efflux (top and bottom chambers combined) and water retained in the soil after wetting in wettable (CB-NWR and SG-NWR) and water-repellent (CB-WR and SG-WR) soils from CB and SG. Blue and orange solid lines represent the trendlines for CB-NWR and CB-WR respectively. The dashed line represents the trendline for the combined SG-NWR and SG-WR.

3.3.3. Effect of SWR on wetting, drainage and retained water

Soils of contrasting wettability (wetable WDPT < 5 s; extremely water-repellent WDPT > 3600 s) showed a very different response to wetting. All the water applied during the rainfall simulations infiltrated eventually into the soil, but for the wettable soils the infiltration was instant (WDPT < 5 s), while for the water-repellent soils, the average WDPT infiltration times were 7312 s and 10368 s for CB-WR and SG-WR respectively (Table 3.2). For the wettable soils, over 90% of the water added was retained in the soil, with only a small fraction of it draining to the container below the soil sample. In contrast, for the water-repellent soils,

a significantly lower fraction of the total water applied (up to 6 and 10 % in the CB-WR and SG-WR respectively) was retained in the soils ($p < 0.001$ for both soils), with the remaining 94 to 90%, respectively, draining out of the soils (Table 3.3). Following wetting, SWC significantly increased accordingly with the rewetting rate in wettable soils, but in water-repellent soils, only small and non-significant differences were observed between different rewetting rates in CB and SG soils. An exception was SG-WR with 25% rewetting rate where SWC was significantly smaller than with the rest of rewetting rates.

Table 3.3. Average water retained in soil (expressed as volume in cm³ and as % of total water applied) and SWC after wetting (% g g⁻¹) for autoclaved wettable and water-repellent soils from CB and SG.

Soil	Rewetting rate (%)	Water added (ml)	Wettable				Water-repellent							
			Water retained in soil (cm ³)		Water retained in soil (%)		SWC (%)		Water retained in soil (cm ³)		Water retained in soil (%)		SWC (%)	
CB	25	33	31.23	(0.05)	94.7	(0.07)	13.89	(0.02)	1.93	(0.85)	5.9	(0.85)	2.17	(0.34)
	50	65.5	62.33	(0.93)	95.2	(0.93)	26.33	(0.37)	3.23	(1.91)	4.9	(1.91)	2.69	(0.76)
	75	98	90.73	(2.84)	92.6	(2.84)	37.69	(1.14)	4.77	(2.63)	4.9	(2.63)	3.31	(1.05)
	100	131	118.97	(1.98)	90.8	(1.98)	48.99	(0.79)	4.1	(1.49)	3.1	(1.49)	3.04	(0.60)
SG	25	35	33.2	(0.30)	94.9	(0.3)	20	(0.15)	3.07	(1.00)	8.8	(1.0)	2.83	(0.50)
	50	70	67.27	(1.53)	96.1	(1.5)	37.03	(0.76)	6.9	(4.42)	9.9	(4.4)	4.75	(2.21)
	75	105	100.63	(2.18)	95.8	(2.2)	53.72	(1.09)	6.3	(1.23)	6	(1.2)	4.45	(0.61)
	100	140	136.53	(0.70)	97.5	(0.7)	71.67	(0.35)	9.33	(5.20)	6.7	(5.2)	5.97	(2.60)

Values represent the mean (n = 3) with standard deviation in brackets.

3.4. Discussion

A distinctively lower CO₂ efflux response to the simulated rainfall was observed in the water-repellent soils compared to the typical 'Birch effect' seen in the wettable soils. Limited water infiltration and percolation patterns, characteristic of water-repellent soils, affected not only soil hydrology, but also led to reduced CO₂ efflux. SWR delays and limits infiltration of water to specific pathways of higher wettability or macropores created by roots, cracks, stones (Urbanek and Shakesby, 2009; Urbanek et al., 2015) and can result in rapid percolation of water downward to the subsoil via preferential flow paths (Ritsema and Dekker, 2000; Müller et al., 2014). Water typically travels in water-repellent soils through a narrow cross-section of soil pores, which results in the majority of the soil matrix remaining dry after rainfall (Hendrickx and Flury, 2001). Such rapid percolation through the water-repellent soil was also observed in this study. The water travelled only through a small fraction of the soil pores and within a short period of time (2 min of the start of wetting), up to 95% of the water applied drained into the container below the sample. The amount of water retained in the soil after wetting was minimal, with SWC ranging between 2–6% (Table 3.3). Only slight increases in the SWC were observed when higher amounts of water were applied, suggesting that the water moved through similar cross-sections of the pore-space regardless of the amount added to the surface. We expect that, in the water-repellent soils, infiltrating water released the soil CO₂ only from the affected sections of the soil matrix, resulting in the low CO₂ efflux observed in the headspace of the top and bottom chambers (Fig. 3.2 and 3.3). In contrast, in wettable soils, the large CO₂ pulse observed is likely to have resulted from the relatively uniform infiltration of water, which released the CO₂ out of the whole cross-section of the soil matrix (Fig. 3.5). Over 95% of the applied water was retained in the wettable soils. The more water that was applied, the higher the SWC was after wetting, resulting in higher CO₂ release from the soil.

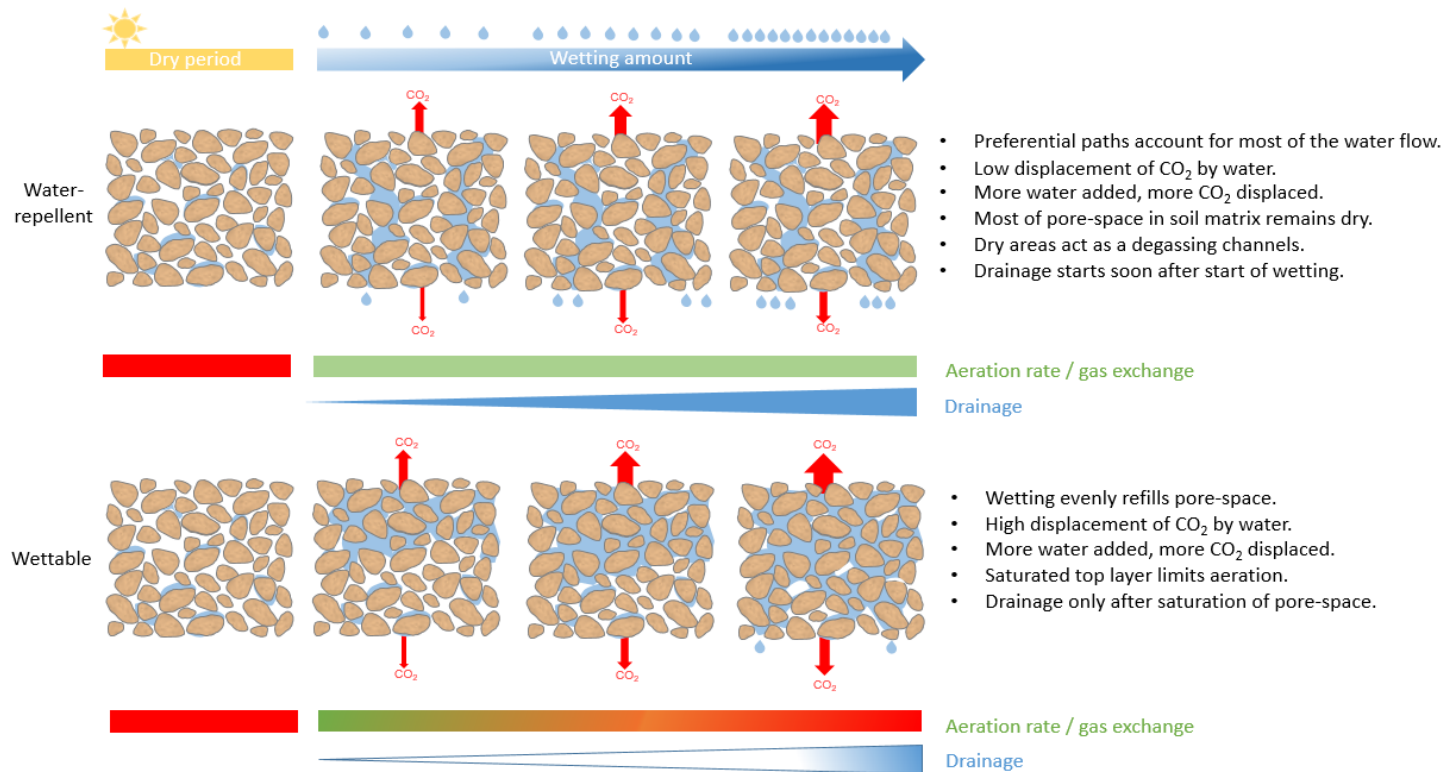


Fig. 3.6. Conceptual diagram of the development of wetting patterns with increasing rewetting rate in water-repellent and wettable soils and its effect on the displacement of CO₂ stored in the pore-space prior to wetting both upwards (emitted from soil surface) and downwards (contributing to CO₂ entrapment). Red arrows represent cumulative CO₂ efflux.

The total CO₂ released from soils (also referred to as cumulative CO₂ efflux) was proportional to the water retained in the soil after the wetting in both wettable and water-repellent soils (Fig. 3.4). The almost immediate increase in CO₂ efflux with wetting of sterilised soil and its return to pre-wetting values after the wetting period suggests that this efflux increase has very unlikely been due to a rapid increase in microbial respiration, triggered by the reactivation of microbial activity after the sudden availability of water (Moyano et al., 2013). Several previous studies showed that the timescale for the reactivation of soil microbial activity under water-limiting conditions is a few hours (rather than seconds) after the input of water (Barnard et al., 2015; Salazar et al., 2018; Placella et al., 2012). The contribution of CO₂ from the chemical reaction with inorganic C (Rey, 2015) is also likely to be negligible as no inorganic C was detected in the soil. We expect that displacement of gas from soil pores by infiltrating water could be one of the sources, as suggested by Inglima et al. (2009) and Liu et al. (2002), but the amount of the cumulative efflux measured in the experiment was at least ten times higher than expected from the gas replacement. One possible mechanism responsible for the immediate CO₂ release after wetting may originate from the desorption of CO₂ molecules adsorbed to the surface of soil particles which are replaced by water molecules, as observed by Kemper et al. (1985). De Jonge & Mittelmeijer-Hazeleger (1996) estimated the adsorption capacity of highly organic soils and concluded that the surface of SOM has the capacity to adsorb CO₂. Based on their findings we estimated an adsorption capacity in the range of 0 – 25 mmol for the soils used in this study. Given that the adsorption capacity increases with soil organic carbon (Ravikovitch et al., 2005), we expect that the adsorption capacity will be at the lower end of that estimate. Higher cumulative CO₂ effluxes measured from the soil with higher SOM content (SG soil) could thus be the result of increased adsorption capacity in comparison to CB soil. Other biochemical processes related to enzyme activity, as suggested by Fraser et al. (2015), could also have contributed to the overall CO₂ release.

Regardless of the source of the CO₂ it was very clear that the more water retained in the soil the higher was the cumulative CO₂ efflux. Unexpectedly high cumulative CO₂ efflux was observed with 75 and 100% rewetting rates in CB-WR and, to a lesser extent, in SG-WR despite the very low retention of water upon wetting. The cumulative efflux from the water-repellent soil was significantly lower than in CB-NWR ($p < 0.001$), but disproportionately high compared to the amount of retained water (Fig. 3.4). One possible explanation for such behaviour could be the localised increase in air pressure below the uneven wetting front (Wang et al., 2000) and

along the preferential flow paths (Delahaye and Alonso, 2002), which could have facilitated gas movement out of the soil.

While the CO₂ release with wetting observed in this study is short-lived, its high magnitude is in line with previous studies (Marañón-Jiménez et al., 2011; Rey et al., 2017; Sánchez-García et al., 2020b). In a recent laboratory study using intact core samples, Sánchez-García et al. (2020b) estimated that the CO₂ peak during a wetting period accounted for nearly 80% of the total CO₂ released over the 5 h observation period. Similarly, Marañón-Jiménez et al. (2011) estimated that the degassing of soil pores was responsible for up to 64% of the total CO₂ released over the 2 h following wetting. It is common that studies investigating soil surface CO₂ emissions inherently identify the CO₂ effluxes with soil respiration (Maier et al., 2011) and do not account for the storage of gas in the soil matrix. According to Maier et al. (2010) up to 20% of the soil-produced CO₂ is not simultaneously emitted to the atmosphere, but it is instead stored in the pore-space and released during precipitation. As it has been shown in studies by White et al. (1977) and Wang et al. (2000), air entrapment is common in dry soils and could lead to fingered flow of rainwater, but SWR could further enhance air entrapment especially during high-intensity rainfall events. Our results, which show that some of the CO₂ is transported downwards upon wetting, support the idea of CO₂ storage (air entrapment) in the soil matrix and its release at a later stage. Whereas in the bottom chamber, a significantly lower peak than in the top chamber was observed in wettable soils ($p < 0.001$, $p = 0.001$ for CB-NWR and SG-NWR respectively), in water-repellent soils, the peak in both the top and bottom chambers showed similar magnitudes ($p = 0.525$, $p = 0.184$ for CB-WR and SG-WR respectively). This downward movement of gas suggests that under natural conditions, part of the stored CO₂ stored might be transported downwards upon wetting towards deeper areas of the soil profile until a favourable degassing route is found.

Another characteristic behaviour for the release of CO₂ from water-repellent soils was the second CO₂ pulse observed with higher rewetting rates in CB-WR, but not present during the rewetting of SG-WR (Fig. 3.2 and 3.3). We expect that dual porosity of soil could have led to the second peak. The first peak likely originated from the release of CO₂ from macropores followed by the release of gas from inside the small aggregates, which could have had different wettability characteristics compared to the bulk soil (Urbanek et al., 2007). The overall porosity was similar in soils from both sites (56 and 59% in CB and SG soils respectively), but the CB soil had a higher silt fraction and visible aggregates, still present after sample preparation, suggesting dual porosity behaviour. Pore-size distribution influences water flow through the soil matrix with larger pores facilitating rapid infiltration (Kutílek, 2004;

Smith et al., 2003) and, therefore, rapid movement of CO₂. The quick re-filling of larger pores first resulted in the spike observed in CB-WR, which is also supported by the quick and sharp peak (only 3 min after the start of wetting) in CB-NWR. The contribution of larger pores to the cumulative infiltration is especially pronounced in water-repellent soils, where preferential flow through larger pores has been estimated to contribute to up to 70 to 95% of the total infiltration through a water-repellent soil surface (Nyman et al., 2013). In the SG-NWR soil, the lower spike, but of longer duration (5.5 min after the start of wetting), suggests a relatively uniform re-filling of pores as a result of more homogeneous pore-size distribution.

This study has highlighted the substantial differences in CO₂ efflux upon rewetting between wettable and water-repellent soils. Given that the pre-treatment of soil material altered the internal soil structure and is likely to have affected their water flow patterns, the magnitude of the observed contrast in CO₂ efflux between wettable and water-repellent soils may differ somewhat to that of undisturbed field soils.

This study supports previous evidence that SWR potentially has a major impact on soil C dynamics (Goebel et al., 2011; Sánchez-García et al., 2020b; Urbanek and Doerr, 2017), however, the effects that changes in hydrological properties caused by SWR might have on the C flux is an area that still requires further attention. Our results suggest that in highly water-repellent soils, pore-size distribution played a major role in the release of CO₂ after wetting, but how common this response is under different factors like soil type, rainfall intensity or the degree of water repellency remains unclear.

3.5. Conclusions

This study shows that changes in the water-filled pore-space upon wetting, caused by SWR, reduces the short-term physical release of CO₂ in water-repellent soils. The high percolation concentrated along preferential paths resulted in low water retention in the soil and, therefore, low refilling of air-filled pores with infiltrating water. The CO₂ efflux was proportional to the amount of water retained in the soil after wetting. The pre-treatment of soil samples altered the soil structure so the CO₂ efflux in wettable and water-repellent soils might differ slightly in undisturbed soils. Our results also show that, upon wetting, some of the gas stored in the pore-space is displaced towards deeper areas of the soil profile and it is not released instantly. Under natural conditions, this downward flux might contribute to air entrapment below the wetting front, which could be released at a later stage.

Although SWR is a common characteristic of many soils, we are only beginning to understand the effects that water repellency-induced changes in soil hydrology might have on the overall soil C flux and current models remain unable to adequately reflect the dynamic nature of soil hydrological functions. Given that SWR is likely to become more common and severe with ongoing environmental change, future studies would be beneficial to further understand the longer-term effects of SWR on the overall soil C balance.

Chapter 4. Wildland fire ash enhances short-term CO₂ flux from
soil in a Southern African savannah

Carmen Sánchez-García, Cristina Santín, Stefan H. Doerr, Tercia Strydom, Emilia Urbanek

Under second revision in: Soil Biology and Biochemistry

4.1. Introduction

Fires in savannahs currently represent ~62% of the total global CO₂ emissions from vegetation fires due to their high frequency and the large annual area burnt that these extensive ecosystems exhibit (van der Werf et al., 2017). Fire in African savannahs is a recurrent intrinsic ecological driver with a <10 year fire return interval and, considering that African savannahs cover half of the continent, understanding the role of fire in carbon (C) dynamics in these fire-prone ecosystems is essential (Bird et al., 2000; Shackleton & Scholes, 2000).

Soil stores the largest pool of terrestrial C, of which approximately two-thirds is soil organic C (SOC; Stockmann et al., 2013). Fire can substantially alter the soil C pool directly, by SOC combustion during soil heating or by modifying SOC characteristics and composition, and indirectly, by altering processes that affect the fluxes and composition of C, like post-fire changes in vegetation cover and soil erosion (Coetsee et al., 2010; Santín and Doerr, 2018). During a fire, some of the burnt biomass is converted into recalcitrant forms of C (known as pyrogenic C, PyC), which are present in post-fire materials such as the ash layer, and can represent a C sink (Santín et al., 2015).

The CO₂ flux from soils is the largest C flux to the atmosphere from terrestrial ecosystems (Longdoz et al., 2000). Fire can influence soil CO₂ fluxes by limiting microbial activity through heating or by altering soil chemical properties that are essential for microbial functioning such as nutrient pools (Jensen et al., 2001; Matáix-Solera et al., 2009). Increases in CO₂ fluxes from burnt savannah soils compared with unburnt ones have been observed in response to precipitation events (Andersson et al., 2004; Castaldi et al., 2010; van Straaten et al., 2019) when sufficient soil moisture is available to mobilise nutrients and reactivate microbial activity (Fan et al., 2015). Increased availability of soil nutrients, such as inorganic nitrogen, calcium, magnesium or phosphorous, is common after a fire, with wildland fire ash being a major nutrient source (Bodí et al., 2014; Shakesby et al., 2015; Singh, 1994).

It is widely assumed that ash deposition stimulates soil respiration due to its fertilization effect, facilitating the supply of readily available nutrients (e.g. Matáix-Solera et al., 2009). Enhanced soil CO₂ fluxes in laboratory-based studies have been reported after the addition of lab-produced ash to burnt soils (Badia & Marti, 2003; Raison & McGarity, 1980) and after the fertilization of the forest floor with wood-ash (Fritze et al., 1994; Perkiomaki et al., 2003; Zimmerman & Frey, 2002). In a recent field and laboratory study in a burnt eucalyptus and pine stand in central Portugal, we observed a larger increase in the CO₂ flux following wetting of burnt soil in which a surface ash layer was intact compared with burnt soils in which the ash

layer had been experimentally removed, but the specific contribution of the ash layer to CO₂ fluxes could not be isolated from other factors such as vegetation cover or soil texture (Sánchez-García et al., 2020b). In addition to its high nutrient content, the ash layer often contains PyC, which is relatively resistant to environmental degradation enabling it to act as a long-term C sink (Bodí et al., 2014; Santín et al., 2016). Globally, savannah fires are the largest source of PyC because of the high fire frequency common in these ecosystems (Jones et al., 2019). However, rapid degradation of some forms of PyC has been previously reported from both wildfire-produced PyC (Bird et al., 1999; Zimmerman et al., 2012) and after the application of laboratory-produced PyC, like biochar, to soil (Hilscher et al., 2009; Jones et al., 2011; Naisse et al., 2015).

Although ash is a ubiquitous, direct product of vegetation fires, its role in post-fire soil C fluxes has been only sporadically considered (Forbes et al., 2006; Bodí et al., 2014). This may be in part due to its often rapid disappearance from the burnt areas, by its incorporation into the soil or redistribution or loss by wind and water erosion, prior to the initiation of most field studies (Santín et al., 2016). In addition, differences in the production conditions between naturally-produced ash (thereafter termed 'wildland fire ash') and artificially-produced ash (thereafter termed 'lab ash'), such as the duration of laboratory pyrolysis experiments or oxygen availability, can result in ash of different physico-chemical characteristics (Santín et al., 2017). In this study we refer to 'wildland fire ash' as the particulate ash residue produced naturally during experimental landscape fires (Bodí et al., 2014). To our knowledge, only two previous studies have investigated the input of naturally-produced ash on soil CO₂ fluxes and the results were inconclusive. Enhanced CO₂ fluxes after the input of wildland fire ash were reported from African savannah soils by Andersson et al. (2004); whereas García-Oliva et al. (1999) observed a reduction in CO₂ fluxes from soils with wildland fire ash, from a tropical deciduous forest in Mexico, suggesting that chemical changes induced by the input of ash inhibited microbial activity.

Therefore, evidence of the role of wildland fire ash on post-fire C fluxes is sparse and the response of soil CO₂ fluxes to the input of wildland fire ash remains poorly understood. Here we address this knowledge gap and aim at better understanding the effects of savannah fires on CO₂ fluxes from soils. The objective of the study was to investigate the effects of fire and wildland fire ash on CO₂ fluxes from savannah soils. We hypothesized that: I) the input of wildland fire ash to post-fire savannah soil will stimulate CO₂ fluxes, and II) the effect of fire will lead to enhanced CO₂ fluxes when soils are wetted.

4.2. Research design and methods

4.2.1. Study sites

The study comprises a series of CO₂ flux incubation experiments on homogenised natural soil and ash materials (< 2 mm fraction) conducted under controlled laboratory conditions. Samples were collected immediately before (pre-fire soils) and after (post-fire soils and ash) large-scale experimental fires conducted in the Kruger National Park (KNP; South Africa) towards the end of the dry season in August 2018. The locations used for the study are part of the ongoing long-term experimental burn plots (EBPs) at KNP established in 1954 to study the impact of different fire regimes across representative South African savannah landscapes (Biggs et al., 2003). Three plots were selected for the study. Two of the plots were located in the Pretoriuskop area (mean annual rainfall of 705 mm), a Lowveld Sour Bushveld landscape on sandy granitic soils, which included one plot burnt annually (hereafter known as PB1; lat./long.: 25° 08' 24''S; 31° 12' 26''E) and a second plot burnt triennially (hereafter known as PB3; lat./long.: 25° 08' 06''S; 31° 12' 24''E). The dominant grass species were *Hyperthelia dissoluta*, *Themeda triandra* and *Setaria sphacelata*. The main tree species were *Dichrostachys cinerea* and *Terminalia sericea*. The third plot was located in the Mopani area (mean annual rainfall of 451 mm), a *Colophospermum mopane* shrubveld on clayey basaltic soil, which has been burnt annually (hereafter known as MB1; lat./long.: 23° 33' 48''S; 31° 27' 24''E). The dominant grass species was *Bothriochloa radicans* and the dominant tree species was *Colophospermum mopane*.

4.2.2. Experimental fires and soil and ash sampling

For soil and ash sampling and fire behaviour monitoring, a 30 x 30 m subplot was selected within the experimental burn plot at both PB1 and PB3 (Fig. 4.1). These subplots were located more than 20 m from the edge of the burn plots to avoid any edge effects (Smit & Asner, 2012). In MB1, locating a subplot with enough fuel continuity to ensure a successful burn was challenging, therefore, a smaller subplot of 20 x 20 m with sufficient fuel was selected (Fig. 4.1). Before conducting the fires, within each plot, three parallel transects were established, 30 m long and 15 m apart in PB1 and PB3, and 20 m long and 5 m apart in MB1. To monitor temperatures during the fire, K-type thermocouples with dataloggers (Lascar, Easylog) were installed along each transect at four sampling points, at 9 m intervals in PB1 and PB3 and 5 m intervals in MB1. At each sampling point (n = 12 per plot: Fig. 4.1), one thermocouple was

placed in the grass, 3 – 5 cm above the ground, and another in the mineral soil at ~1 cm below the surface. In addition, between the three sampling transects, two ‘control’ transects were used for taking soil samples before the fire without disrupting the post-fire sampling transects (Fig. 4.1). Before the fire, the top 0 - 1 cm soil layer was sampled along these ‘control’ transects at 3 m intervals in PB1 and PB3 and 1 m intervals in MB1 (n = 20), using a 20 x 20 cm sampling frame and after removal of the grass. Immediately after the fire, the ash layer was brushed off the surface and the top 0 - 1 cm soil layer was sampled along the three sampling transects at the same points where the thermocouples had been placed (n = 12) also using a 20 x 20 cm frame. At each plot, three composite ash samples were also taken, based on material collected from several locations within each burnt plot (approximately 500 g per sample). The fire characteristics are given in Table 4.1.

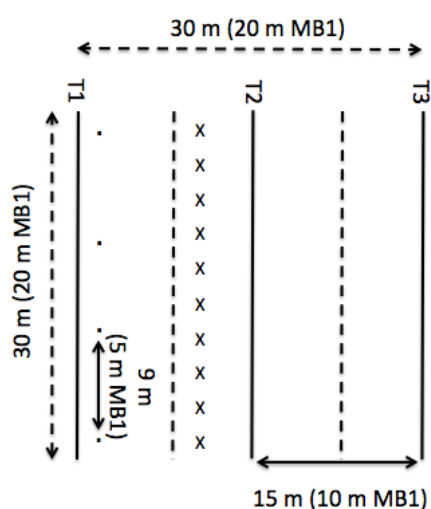


Fig. 4.1. Experimental plot diagram for PB1 and PB3 plots (and dimensions for the MB1 plot in brackets). Solid lines represent the experimental transects and dashed lines represent the control transects. Dots along the experimental transects represent the locations of the thermocouples and crosses along the control transect represent soil sampling locations before the fire.

Table 4.1. Experimental fire characteristics including atmospheric conditions (wind speed, air temperature (Air T) and relative humidity (RH)), maximum temperature range (Tmax) registered in the soil surface and grass (n = 12), residence times > 300 °C, and details of fire impacts on vegetation. Full details of temperatures reached during the experimental fires and residence times in the soil surface and grass are provided in Supplementary Table S1.

Site	Date	Atmospheric conditions			Tmax (°C)		Residence time > 300 °C (s)*		Fire impacts on vegetation
		Wind speed (m s ⁻¹)	Air T (°C)	RH (%)	Soil surface	Grass	Soil surface	Grass	
PB1	19/08/18	1.8 – 2.7	26	41	40 - 225	484 – 744	0	23 ± 20	Fire burnt entire experimental plot with complete combustion of fine fuels and no unburnt grass left. Woody fuels were mostly unaffected and wood on the ground (down wood) and bark from standing trees remained uncharred.
PB3	19/08/18	1.8 – 2.7	31	30	40 - 182	651- 918	0	54 ± 38	
MB1	23/08/18	2.2 – 3.1	31	41	40 - 498	452 - 850	15 ± 24	51 ± 40	Most (> 90%) of the fine fuels on the ground were burnt. Coarser woody fuels remained largely unaffected, whereas most of the green and brown leaves of the shrub were consumed.

* Temperature threshold above which organic materials tend to transform into more aromatic and recalcitrant forms (Santín et al., 2016).

4.2.3. Laboratory experiments and analysis

4.2.3.1. CO₂ flux

For the laboratory experiments, the following sample materials were used from each of the three burn plots: a) a pre-fire composite soil sample per site formed by combining equal weights of the samples collected before the fire from each site (n = 20); b) a post-fire composite soil sample per site formed by combining equal weights of the samples collected after the fire from each sampling location (n = 12) and c) a composite ash sample per site formed by combining the three ash samples. All soil and ash samples were sieved to < 2 mm to remove larger debris. To study the effect of fire and the impact of naturally-produced ash (wildland fire ash) on CO₂ fluxes, we used the following treatments: pre-fire soil (PreF), post-fire soil without ash (PostF) and post-fire soil with added ash (PostF_wA). We included three replicates of these three treatments from each site (PB1, PB3 and MB1), resulting in 27 separate samples for flux measurement. The 70 g of soil material for the PreF and PostF treatment were carefully placed into gas-tight plastic containers of 9 cm diameter and 11 cm height. For the post-fire soil with added ash (PostF_wA), 7 g of ash was mixed with 70 g of post-fire soil from their respective plots. The ash load (1051 g m⁻²) was substantially higher than that observed in the field (~90 g m⁻², unpublished data), but selected in order to be comparable with other PyC/ash-soil incubation studies (e.g. Gómez-Rey et al., 2012; Smith et al., 2010). The CO₂ flux measurements were conducted by connecting each soil container to an infrared CO₂ gas analyser system (IRGA) (Li-8100A, Li-COR Inc., Lincoln, NE, USA) via a multiplexer (Li-8150, Li-COR Inc., Lincoln, NE, USA) to allow an automated measurement of the CO₂ flux from each sample every hour. Ambient air was continuously flushed between measurements to prevent high CO₂ concentrations from developing in the containers. The measurement of the CO₂ concentration in each container lasted 2 min with an additional 30 s for pre- and post-purge. The measurements of the soil CO₂ flux started with air-dried samples for the first 24 h, then the samples were wetted to 60% of water-holding capacity (WHC) to ensure moisture availability while avoiding saturation. The wetting was achieved by spraying deionised water from above. The CO₂ flux monitoring was continued for 28 days. Soil moisture (60% WHC; i.e. 10% and 18% volumetric soil water content for the PB and MB1 soils respectively) and temperature (~20 °C) were maintained throughout the observations, with any minor moisture loss caused by evaporation being adjusted daily according to the weight difference in the samples from the previous day. A small number of shoots that germinated from the soil during the incubations were quickly removed by clipping to eliminate any root and shoot respiration.

The CO₂ concentration data over time was fitted exponentially; excluding the initial 30 s. Any CO₂ flux data ($\mu\text{mol m}^{-2} \text{s}^{-1}$) with a coefficient of $R^2 \leq 0.95$ was discarded. This applied to < 3% of the total measurements, which correspond predominantly to dry soil before wetting where the CO₂ flux was 0 or close to 0. Therefore, discarding these values does not affect the results. The cumulative flux ($\mu\text{mol m}^{-2}$) was calculated as the total CO₂ flux emitted during the whole duration of the observations (28 d). Carbon respired was calculated by converting cumulative flux ($\mu\text{mol m}^{-2}$) to g C m^{-2} .

4.2.3.2. Chemical Analysis

The pH and electrical conductivity (EC) of soil and ash samples were determined in water at a soil/ash-to-water mass ratio of 1:2.5 after stirring and waiting for 10 min (Buurman et al., 1996). pH was measured with a Crison micropH 2000 pH meter, with buffer solutions of pH 4, 7 and 9. EC was measured with a Crison GLP 31 apparatus, calibrated with 0.1 and 0.01 M potassium chloride (KCl) solutions (12.88 mS cm^{-1} and $1413 \mu\text{S cm}^{-1}$, respectively).

Total Nitrogen (TN) and Carbon (TC) concentrations were determined using a Leco TruSpec CHN. The total concentration of aluminium (Al), calcium (Ca), cobalt (Co), chromium (Cr), copper (Cu), iron (Fe), magnesium (Mg), manganese (Mn), nickel (Ni), and zinc (Zn) were determined in extracts obtained by acid digestion (HNO_3/HCl , ratio v/v 3:1; at $180 \text{ }^\circ\text{C}$ for 45 min in an Ethos Easy Milestone Microwave) and measured by Atomic Absorption in a PerkinElmer PinAAcle 500 Atomic Absorption Spectrometer. Total phosphorus (P) was measured in the same extracts by colorimetry in a Jasco V360 spectrophotometer.

Water-soluble elements were extracted following the leaching test method described in Hageman (2007). Two g of sample were weighed into 50 ml bottles. Then, 40 ml ultrapure water (sample: water ratio 1:20) was added and the bottles were capped and shaken for 5 min. After shaking, the contents were allowed to settle for 10 min. The supernatants were vacuum-filtered through $0.45 \mu\text{m}$ cellulose nitrate membranes. Water-soluble organic carbon (WSOC), phosphate (PO_4^{2-}) and ammonium (NH_4^+) were then measured by colorimetry in a Jasco V360 spectrophotometer. Water-soluble nitrate (NO_3^-) was quantified by liquid ion chromatography (Dionex Series 4500i Chromatographer).

4.2.3.4. TG-DSC analysis

Thermogravimetry-Differential Scanning Calorimetry (TG-DSC) was performed in order to examine thermal recalcitrance in the soil and ash material. The analyses were conducted in a simultaneous Thermal Analyzer (STA) 6000 PerkinElmer. Ground samples (50-70 mg) were placed in a ceramic crucible and heated under dry air (under O₂ flux; flow rate, 50 mL⁻¹) with increasing temperature from 50 to 600 °C at a heating rate of 10 °C min⁻¹ while continuously monitoring the combustion rate and sample mass change rate. For each DSC thermograph, the area in the 150 - 600 °C region, where the combustion of organic matter (OM) occurs, was divided into three temperature sections representing different levels of resistance to thermal oxidation (Merino et al., 2015): labile OM, mainly comprising carbohydrates, proteins and other labile aliphatic compounds (150 < T1 < 375 °C); recalcitrant OM, such as lignin or other polyphenols (375 < T2 < 475 °C); and highly recalcitrant OM, such as polycondensed aromatic forms (475 < T3 < 600 °C). The resulting partial heats of combustion, representing these three regions were calculated as Q1, Q2 and Q3, respectively.

4.2.4. Data analysis

The non-parametric Mann-Whitney U-test was used to test for statistical differences in the CO₂ fluxes (accepted at p < 0.05) between the incubation treatments and to test for differences in chemical composition and thermolability. The Spearman's rank correlation coefficient (rho) was used to test for linear correlations between the CO₂ flux and chemical properties. The tests were performed with Microsoft Excel 2011. The correlation tests amongst the thermogravimetry indicators and CO₂ fluxes were not performed since thermogravimetry data for the PostF_wA treatment were not available, as they were only obtained for the post-fire soil and the ash samples individually.

4.3. Results

4.3.1. CO₂ flux evolution with time

For all the analysed samples, the CO₂ flux before wetting was below 0.1 μmol m⁻² s⁻¹. Following wetting, the CO₂ flux increased in all samples (i.e. PreF, PostF and PostF_wA) after a lag phase of 14 to 23 h in the PB1 and PB3 soils and ~29 h in the MB1 soil (Fig. 4.2). With the addition of ash to the post-fire soil (PostF_wA), the lag phases in the PB1, PB3 and MB1 soils were 8, 9 and 25 h shorter than in the pre-fire soil respectively. After the lag phase, the CO₂ fluxes quickly

reached a peak (between 1 and 29 h) in all samples, except in the MB1 PreF soil where no distinct peak was detected (Fig. 4.2). The CO₂ pulse in pre-fire (PreF) soils was low (mean $\leq 1 \pm 0.18 \mu\text{mol m}^{-2} \text{s}^{-1}$), while post-fire (PostF) soils had a significantly higher pulse ($p < 0.001$) with the mean ranging between 1.5 ± 0.08 and $2.5 \pm 0.24 \mu\text{mol m}^{-2} \text{s}^{-1}$ in the PB1 and PB3 soils, respectively (Fig. 4.2).

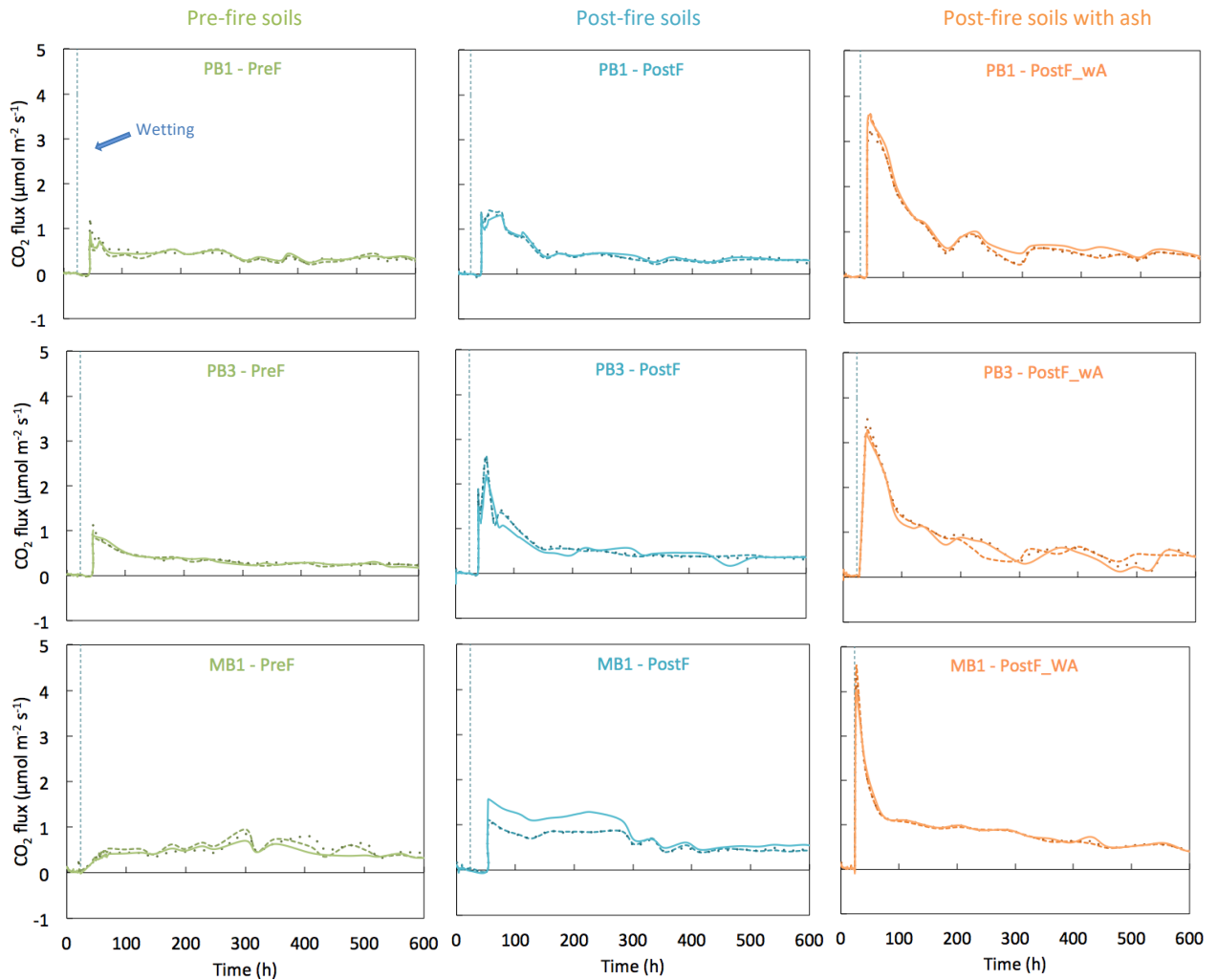


Fig. 4.2. Response of CO₂ flux to wetting of pre (PreF) and post-fire soils (PostF) and post-fire soils with added ash (PostF_wA). Solid, dotted and dashed lines represent the three replicates. The blue dashed vertical line represents the start of the wetting, 24 h after the start of measurements.

The addition of ash to the post-fire soils (PostF_wA) resulted in an even higher pulse in all samples ($p < 0.001$), reaching a mean of $4.5 \pm 0.8 \mu\text{mol m}^{-2} \text{s}^{-1}$ in the MB1 soil and 3.5 ± 0.19 and $3.3 \pm 0.14 \mu\text{mol m}^{-2} \text{s}^{-1}$ in the PB1 and PB3 soils (Fig. 4.2). The size of the pulse in the PB1

and PB3 PostF_wA soils was triple that of the PreF soils, but the CO₂ pulse observed with the input of ash was especially high for the MB1 soil; nearly 11 times higher than in the MB1 PreF soils. The CO₂ fluxes decreased quickly after reaching their peak and the pulse was over within the following 34 to 130 h. The CO₂ fluxes remained low thereafter ($< 0.5 \mu\text{mol m}^{-2} \text{s}^{-1}$) in all soils until the end of the observations, 648 h after the beginning of wetting (Fig. 4.2).

4.3.2. Cumulative CO₂ flux and respired C

The cumulative flux in the PreF soils ranged between 594 and 869 mmol m⁻² in the PB3 and MB1 soil respectively (Fig. 4.3). In the PostF soils, the cumulative flux was 25, 36 and 97% higher in the PB1, MB1 and PB3 soils respectively ($p < 0.001$; Fig. 4.3). The addition of ash to the post-fire soils (PostF_wA) doubled the cumulative flux of the PreF soils in the PB1 and MB1 (mean 1707 ± 98 and 1718 ± 66 mmol m⁻² respectively) and trebled PreF values in the PB3 soil (mean 1772 ± 56 mmol m⁻²; $p < 0.001$). The total C released from the PostF_wA soil was approximately 21 g C m⁻² (i.e. 2 to 3 times higher than in the PreF soils), comprising 3 - 5% of the total carbon (TC) present in the sample (soil + ash) (Table 4.2).

Table 4.2. Carbon (C) respired as CO₂ (CO₂-C; g C m⁻²) during the 28 day observation period and during the CO₂ pulse expressed in g of C and as a percentage of the total C (TC). Values are the arithmetic mean (n = 3) with standard deviation in brackets.

		Total CO ₂ -C released entire observation (g C m ⁻²)	CO ₂ -C released entire observation (g)	CO ₂ -C released pulse only (g)	CO ₂ -C released entire observation (% of TC)	CO ₂ -C released pulse only (% of TC)
PB1	PreF	9.8 (0.6)	0.065 (0.004)	0.007 (0.001)	7.9 (0.4)	0.8 (0.1)
	PostF	12.3 (0.4)	0.082 (0.002)	0.029 (0.002)	7.8 (0.3)	2.8 (0.2)
	PostF_wA	20.5 (1.2)	0.136 (0.008)	0.056 (0.006)	5.4 (0.3)	2.2 (0.2)
PB3	PreF	7.4 (0.3)	0.049 (0.002)	0.011 (0.001)	4.5 (0.2)	1.0 (0.1)
	PostF	14.6 (0.3)	0.097 (0.002)	0.032 (0.004)	6.4 (0.1)	2.1 (0.3)
	PostF_wA	21.3 (0.7)	0.142 (0.004)	0.043 (0.002)	4.8 (0.2)	1.4 (0.1)
MB1	PreF	9.5 (0.2)	0.063 (0.001)	0.010 (0.001)	3.1 (0.1)	0.5 (0.1)
	PostF	12.9 (0.8)	0.086 (0.005)	0.021 (0.004)	3.8 (0.2)	1.0 (0.2)
	PostF_wA	20.6 (0.8)	0.137 (0.005)	0.032 (0.001)	3.3 (0.1)	0.7 (0)

Table 4.3. Spearman's rank correlation (Spearman's rho) between CO₂ flux (size of the pulse and cumulative flux) and selected characteristics of the PreF, PostF and PostF_wA samples in mg kg⁻¹ (total C and N, and dissolved organic carbon (DOC), NH₄⁺, NO₃⁻ and PO₄; n = 9). Values with an asterisk show significant differences (at p < 0.05).

	Size of CO ₂ pulse (μmol m ⁻² s ⁻¹)	Cumulative CO ₂ flux (mmol m ⁻²)	TC (g kg ⁻¹)	TN (g kg ⁻¹)	DOC (mg kg ⁻¹)	NH ₄ ⁺ (mg kg ⁻¹)	NO ₃ ⁻ (mg kg ⁻¹)	PO ₄ (mg kg ⁻¹)
Size of CO ₂ pulse (μmol m ⁻² s ⁻¹)	1.000							
Cumulative CO ₂ flux (mmol m ⁻²)	0.917*	1.000						
TC (g kg ⁻¹)	0.667*	0.767*	1.000					
TN (g kg ⁻¹)	0.350	0.433	0.85*	1.000				
DOC (mg kg ⁻¹)	0.833*	0.95*	0.633	0.317	1.000			
NH ₄ ⁺ (mg kg ⁻¹)	0.717*	0.600	0.133	-0.133	0.617	1.000		
NO ₃ ⁻ (mg kg ⁻¹)	0.067	0.017	0.500	0.717*	-0.167	-0.083	1.000	
PO ₄ (mg kg ⁻¹)	0.583	0.667*	0.867	0.714	0.733	0.150	0.283	1.000

The cumulative flux released during the pulse only comprised up to 23% of the total cumulative flux in the PreF soils, which constituted up to 1% of the TC (Table 4.2). Up to 36 and 41% of the total cumulative flux was released during the pulse in the PostF and PostF_wA respectively, accounting for up to 3% of TC in the PostF soil and up to 2% of TC in the PostF_wA soil (Table 4.2).

The cumulative flux was positively correlated to dissolved organic carbon (DOC) and total carbon (TC; Fig. 4.4). The size of the CO₂ pulse was also significantly correlated to cumulative CO₂ flux, TC, DOC and NH₄⁺. TC was significantly correlated to TN and PO₄, and TN was significantly correlated with NO₃⁻ (Table 4.3).

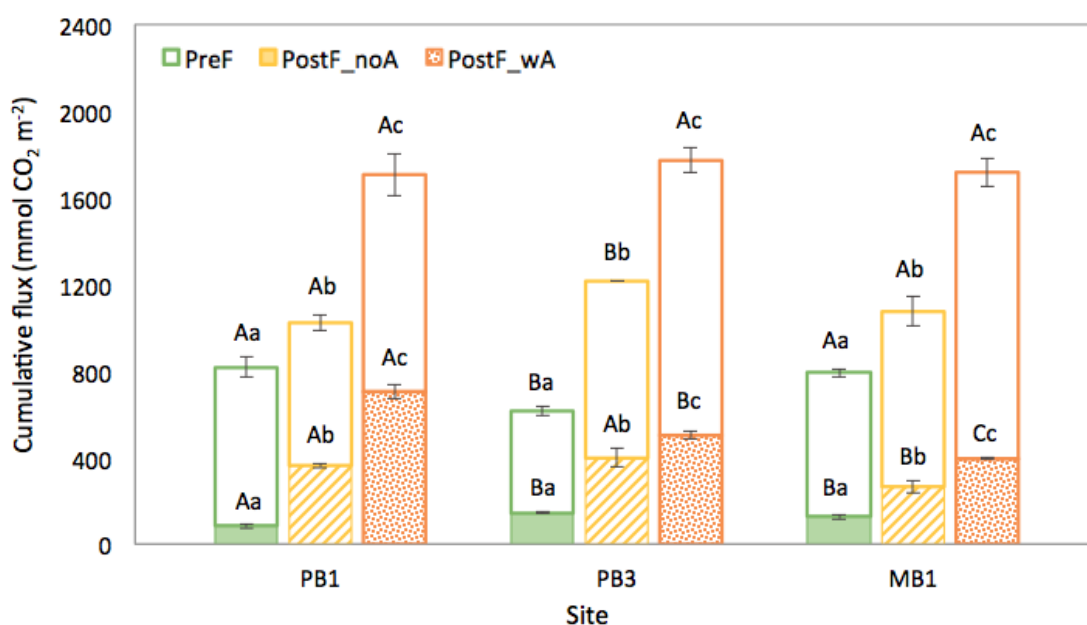


Fig. 4.3. Cumulative flux for the duration of the observations (28 d) (total columns) and proportion of the cumulative flux released only during the CO₂ pulse (filled columns) in the pre-fire (PreF) and post-fire soils (PostF) and in the post-fire soils with added ash (PostF_wA). Values represent the mean (n = 3) with standard deviation bars. Different lowercase letters (a – c) within the same site indicate significant differences between incubation treatments and different uppercase letters (A – C) indicate significant differences between sites for each treatment at p < 0.05. Letters above the unfilled columns represent differences between the total cumulative flux and letters above the filled columns represent differences between the cumulative flux released during CO₂ pulse.

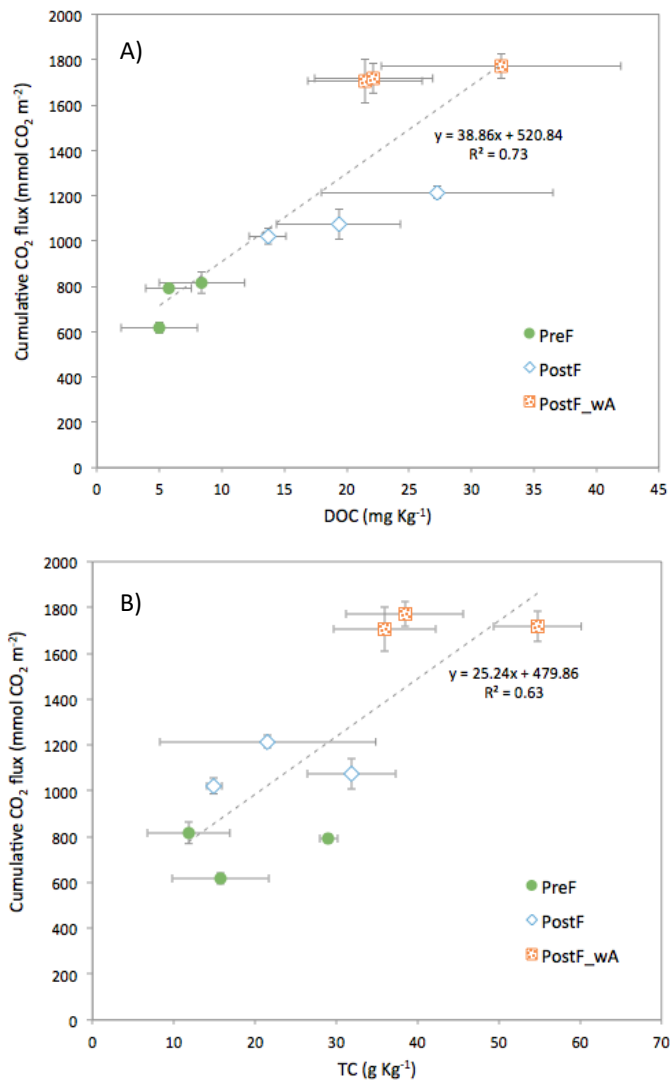


Fig. 4.4. A) Relationship between cumulative flux and dissolved organic carbon (DOC) ($p < 0.001$) and B) relationship between cumulative flux and total carbon (TC) ($p = 0.016$). Values are the arithmetic mean ($n = 3$) with standard deviation bars.

4.3.3. Chemical properties of soil and ash

In the soils statistically significant differences were observed between PreF and PostF samples in the three studied sites in pH, electrical conductivity (EC), dissolved organic carbon (DOC), water-soluble ammonium (NH_4^+), nitrate (NO_3^-), phosphate (PO_4), and total chromium (Cr), copper (Cu) and phosphorus (P). After the fire, in the PB3 soil, a significant increase was found in both pH (from 6.5 to 7.5) and also water-soluble PO_4 (from 0.4 to 2.3) (Table 4.4). The EC in the PostF soils was double the PreF values in the MB1 soil and three times higher than in the

PB3 soil. With regards to DOC, a significant increase was detected in all PostF soils, which was particularly prominent in the MB1 soil where DOC values were 5 times higher than PreF ones (8.4 to 13.7 mg kg⁻¹ in the PB1 soil, 5.0 to 27.2 mg kg⁻¹ in the PB3 soil and 5.7 to 19.4 mg kg⁻¹ in the MB1 soil). Contrasting trends were observed between water-soluble NH₄⁺ and NO₃⁻ amongst the soils. While the concentration of water-soluble NH₄⁺ was significantly enhanced in the PB3 soil (from 0.1 to 0.6 mg kg⁻¹); the concentration of water-soluble NO₃⁻ increased (from 0.4 to 0.8 mg kg⁻¹) and decreased (1.5 to 0.9 mg g⁻¹) significantly in the PB1 and MB1 soil, respectively (Table 4.4). Regarding total Cr, a significant decrease was found in the PB1 and PB3 PostF soils (from 40 to 25 mg kg⁻¹ and from 59 to 41 mg kg⁻¹, respectively). Total Cu increased significantly in the PB1 PostF soil (from 6 to 8 mg kg⁻¹) and a significant increment in total P was observed in the MB1 soil after the fire (from 1217 to 1437 mg kg⁻¹).

Table 4.4. Chemical properties of the pre-fire (PreF) and post-fire (PostF) soils and of the ash. Values are the arithmetic mean (n = 3) with standard deviation in brackets. Values with an asterisk show significant differences (at p < 0.05) between pre and post-fire soil.

		pH	EC (μS cm ⁻¹)	DOC (mg kg ⁻¹)	NH ₄ ⁺ (mg kg ⁻¹)	NO ₃ ⁻ (mg kg ⁻¹)	PO ₄ (mg kg ⁻¹)
	PreF	6.4 (0.2)	60.2 (25.8)	8.4 (3.4)	0.2 (0)	0.4 (0.1)	0.5 (0.3)
PB1	PostF	7.0 (0.5)	99.7 (24.9)	13.7* (1.5)	0.7 (0.4)	0.8* (0.2)	1.2 (0.7)
	Ash	9.8 (0.2)	5543.3 (605.8)	100.4 (36.1)	0.5 (0.1)	4.7 (1.3)	6.7 (2.7)
	PreF	6.7 (0.1)	68.9 (39)	5.0 (3.1)	0.1 (0)	0.7 (0.2)	0.5 (0)
PB3	PostF	7.5* (0.5)	206.4* (37.1)	27.2* (9.3)	0.6* (0.2)	0.4 (0.2)	2.3* (0.3)
	Ash	10.0 (0.1)	4776.7 (631.7)	84.4 (12.2)	0.4 (0)	3.2 (0.4)	6.2 (1.7)
	PreF	7.9 (0.1)	139.4 (22.2)	5.7 (1.9)	0.1 (0)	1.5 (0.4)	2.0 (0.5)
MB1	PostF	7.6 (0.4)	258.0* (43.7)	19.4* (5)	0.2 (0.1)	0.9* (0.1)	2.4 (0.6)
	Ash	9.9 (0)	2877.7 (965.3)	50.3 (2.2)	0.2 (0)	1.6 (0.3)	149.3 (29.9)

Regarding the ash samples, pH values were always around 10 (Table 4.4). EC in the ash from both the PB1 and PB3 sites was twice that of the MB1 site ($p = 0.015$). The TC ranged between 20,900 and 28,600 mg kg^{-1} in the PB3 and MB1 sites respectively. The TN in the MB1 ash was nearly half that in the PB1 ash ($p = 0.004$) (Table 4.5). The C:N ratio in the MB1 site was up to 2 and 2.5 times higher than in the PB1 and PB3 sites respectively ($p < 0.001$ in both cases). The DOC ranged between 50 and 100 mg kg^{-1} in the MB1 and PB1 sites, respectively (Table 4.4). Regarding inorganic N, both the concentrations of water-soluble NH_4^+ and NO_3^- were significantly higher in the PB soils than in the MB1 soils ($p = 0.005$, $p = 0.016$ for NH_4^+ in the PB1 and PB3 soils respectively; $p = 0.014$, $p = 0.005$ for NO_3^- in the PB1 and PB3 soils respectively). The concentration of water-soluble PO_4 was especially high in the ash from the MB1 site ($p = 0.001$ in both cases) with an average of 149 mg kg^{-1} compared with 6.7 and 6.2 mg kg^{-1} in the PB1 and PB3 sites (Table 4.4).

Table 4.5. Elemental analysis (mg kg⁻¹) of the pre-fire (PreF) and post-fire (PostF) soil and the ash. Values are the arithmetic mean (n = 3) with standard deviation in brackets. Values with an asterisk show significant differences (at p < 0.05) between pre and post-fire soil.

		C:N		TC		TN		Al		Ca		Co					
	PreF	16	(3)	11797	(5100)	750	(400)	14449	(2821)	481	(337)	4	(1)				
PB1	PostF	16	(4)	14963	(1000)	943	(200)	14643	(1530)	723	(93)	4	(0)				
	Ash	39	(2)	248267	(45700)	6287	(1000)	9852	(1530)	34226	(1262)	19	(1)				
	PreF	16	(0)	15730	(6000)	990	(400)	12601	(3703)	999	(662)	5	(2)				
PB3	PostF	19	(3)	21543	(13300)	1147	(600)	10867	(668)	1419	(607)	4	(1)				
	Ash	50	(3)	208967	(16800)	4203	(600)	9917	(2709)	43281	(4976)	8	(11)				
	PreF	15	(0)	29050	(1100)	1977	(100)	36248	(1406)	17700	(666)	37	(1)				
MB1	PostF	16	(1)	31850	(5500)	2047	(400)	35153	(2200)	16606	(1126)	38	(1)				
	Ash	93	(5)	286133	(6500)	3080	(100)	3695	(329)	17870	(2724)	4	(1)				
		Cr		Cu		Fe		Mg		Mn		Ni		P		Zn	
	PreF	40	(3)	6	(1)	14732	(1766)	356	(96)	193	(42)	2	(1)	97	(34)	11	(2)
PB1	PostF	25*	(1)	8*	(0)	18219	(2672)	393	(64)	218	(3)	2	(1)	125	(31)	11	(1)
	Ash	51	(13)	32	(1)	6551	(1521)	7373	(420)	1297	(58)	8	(1)	3902	(272)	164	(13)
	PreF	59	(3)	7	(1)	10656	(954)	397	(105)	244	(34)	8	(3)	128	(19)	11	(2)
PB3	PostF	41*	(6)	8	(1)	9735	(1646)	482	(64)	246	(13)	8	(1)	149	(22)	9	(3)
	Ash	65	(17)	29	(9)	7256	(2007)	8936	(1026)	1435	(252)	14	(3)	4687	(515)	182	(27)
	PreF	353	(15)	75	(1)	57773	(1277)	20740	(651)	949	(3)	348	(8)	1217	(84)	78	(1)
MB1	PostF	353	(8)	77	(4)	57298	(945)	21135	(192)	941	(29)	349	(8)	1437*	(71)	164	(13)
	Ash	57	(1)	22	(1)	6125	(430)	6872	(590)	252	(21)	44	(2)	5861	(1040)	129	(15)

Table 5.5. (continued)

4.3.4. Differential scanning calorimetry (DSC) and thermogravimetry (TG) analysis

The DSC thermographs revealed a first peak (T_{1Q}) in the range of 346 – 353 °C and a second, less prominent peak (T_{2Q}) at 376 – 399 °C (Fig. S4). Further analysis of the thermograms of the pre-fire samples show that the majority of the energy was released in the Q1, which represents the labile OM category (Table 4.6; Campo & Merino, 2016).

The thermograms of the soils sampled after the fire maintained the shape of the pre-fire samples with a peak at 341 – 346 °C (Fig. S4). T_{50Q} rose slightly but not significantly in both the PB1 and PB3 soil after the fire (371 - 388 °C in the PB1 soil and 304 - 355 °C in the PB3 soil), but did not differ from pre-fire values in the MB1 soil (Table 4.6). With regards to the Q values, no significant differences were observed in the soils before and after the fire. The Q1 thermolability remained the most dominant category for all three soils.

The DSC thermograms of the ash samples showed distinctive characteristics when compared with the pre- and post-fire soil samples (Fig. S4). A prominent peak was detected at much higher temperatures than in the soil samples, around 438 – 464 °C. Most of the OM in the ash samples was classified into the Q2 category (43 - 56%) representing recalcitrant OM, with 21 - 29% of the DSC thermogram's area in the labile Q1 category. The ash from the PB1 site showed the highest thermolability (Q1 = 29% and Q3 = 15%) while the lowest thermolability was observed in the MB1 site (Q1 = 21% and Q3 = 25%; Table 4.6). Detailed values of the TG-DSC analysis are shown in Table S2.

Table 4.6. Main TG-DSC parameters for the pre-fire (PreF) and post-fire soil (PostF) and in the ash. T50_q: temperature at which sample has released half of its total stored energy; Q1, Q2 and Q3: percentage of heat released in each group of thermal oxidation (150 – 375 °C; 375 – 475 °C; 475 – 600 °C respectively).

Site	Treatment	T50 _q [°C]		Q1 [%]		Q2 [%]		Q3 [%]	
PB1	PreF	371.3	(25.9)	44.9	(12.6)	31.7	(6.6)	23.3	(9.5)
	PostF	387.7	(27.1)	42.1	(10.3)	34.7	(7.7)	23.2	(18)
	Ash	414.3	(2.6)	29.4	(1.4)	55.9	(1.1)	14.6	(1.9)
PB3	PreF	304.0	(133.5)	40.9	(0.7)	35.9	(8)	23.2	(7.7)
	PostF	355.0	(35.5)	53.0	(12.4)	35.2	(9.8)	11.8	(4.1)
	Ash	419.0	(3.2)	26.3	(2.6)	56.4	(0.2)	17.3	(2.5)
MB1	PreF	342.0	(1.7)	53.6	(2.6)	33.2	(1.6)	13.1	(4.3)
	PostF	343.0	(3.6)	53.3	(2.8)	33.7	(0.4)	13.0	(2.9)
	Ash	433.8	(4.4)	21.2	(2.6)	53.4	(1.6)	25.4	(3.5)

4.4. Discussion

The post-fire soils showed an increased CO₂ flux for all samples within 3 to 29 h after the start of the wetting. The additional input of wildland fire ash stimulated this CO₂ release by 2 to 3 times compared with the pre-fire and post-fire soils (without ash; Fig. 4.3). Enhanced CO₂ fluxes following wetting of soils after fire have been reported previously, either during rainfall simulation experiments (e.g. Pinto et al., 2002; Castaldi et al., 2010) or after actual rainfall events (e.g. Pinto et al., 2002; van Straaten et al., 2019). In a previous field study, we also observed a rapid increase in the CO₂ flux following a rainfall simulation in a recently burnt pine and eucalyptus stand in Portugal and larger CO₂ fluxes in plots with ash compared with those in which the ash layer was removed, although the specific effect of ash could not be isolated from that of vegetation cover and soil texture (Sánchez-García et al., 2020b). Enhanced soil CO₂ fluxes with the experimental addition of ash have also been observed previously (e.g. Badia and Marti, 2003; Raison and McGarity, 1980; Hogg et al., 2011). For example, in an

incubation experiment Badia & Marti (2003) observed a 10% increase in respiration with the addition of laboratory-produced ash to artificially burnt soils from NE-Spain. Our results are in line with Andersson et al. (2004) who, to our knowledge, conducted the only previous study isolating the effects of wildland fire ash on C fluxes. They reported CO₂ fluxes twice as high in burnt loamy soils with added wildland fire ash than in recently burnt soils from African savannah woodland during a field experiment.

The high temporal resolution of the observations in our study shows that up to 40% of the total C respired from soils with ash occurred during a short period, just hours after the wetting of post-fire soils. Ash is rich in organic C and soluble nutrients readily available for mineralization like N and P (Tables 4.4 and 4.5; Bodí et al., 2014) and has been shown to stimulate vegetation regrowth on fire-affected soils compared with other soils (Kutiel and Naveh, 1987; Vlamis and Gowans, 1961). In addition, the high pH commonly observed in ash (~10 in this study) is a determining factor in the solubility of nutrients, and ash input to the soil reduces soil acidity and enhances nutrient availability (Jensen et al., 2001; Perkiomaki et al., 2003), which can boost microbial activity resulting in higher respiration rates (Fritze et al., 1994; Zimmerman & Frey, 2002). It is important to note that in order for our results to be replicable, we produced homogeneous samples of the post-fire soil with ash. However, under natural conditions, some ash will be redistributed by wind and water and likely accumulate preferentially in depositional areas in the landscape or be incorporated in the soil by bioturbation or percolating rainfall (Bodí et al., 2014).

A lower CO₂ flux was emitted from the post-fire soils without ash, but this was still significantly higher than that emitted from the pre-fire soils (Fig. 4.3). Only slight and non-significant differences in soil thermal recalcitrance were observed between pre- and post-fire soils, which along with the generally low temperatures registered in the soil during the fires (Table 4.1), indicate that the fire itself had little direct impact on the soil. We suspect that the small differences observed between the pre and post-fire soil without ash addition, mostly result from some residual ash being incorporated in the post-fire mineral soil surface sampled after the removal of the ash layer. Examining post-fire soil without ash is unlikely to reflect natural conditions except in those patches in which ash has been removed by erosion.

The total CO₂ released from the samples was positively correlated to TC and DOC (Table 4.3). Similar trends were reported by Badia and Marti (2003) and Dicen et al. (2020) in their laboratory incubation studies using artificially burnt soil. However, the DOC in our samples (≤ 0.002 g C in all cases, data not shown) is an order of magnitude lower than the total C respired

(Table 4.2). Ash is a very good source of easily mineralizable C (Table 4.4) and it is likely that microorganisms rely on the DOC initially, since this C pool can be accessed immediately by microorganisms (Jones et al., 2011), after which microbes will utilise more stable forms of C (Hilscher et al., 2009). Another explanation could be that microorganisms do not mineralize the labile C in the ash directly but use the nutrients in the ash to mineralize C from the native soil organic matter, a process also known as the priming effect (Maestrini et al., 2014).

It is important to note that the organic carbon in vegetation fire ash is mostly present in the form of pyrogenic C (Santín et al., 2020). Even though PyC is considered highly resistant to microbial degradation, the labile pool, made of readily available compounds, can undergo fairly rapid degradation during the initial stages of mineralisation (Santín et al., 2016). The labile PyC fraction in our samples ranged between 41 and 54% in the soil and between 21 and 29% in the ash so this relatively large labile PyC pool (as indicated by the Q1% in Table 4.5) might be easily accessed by microbes. High wildfire PyC degradation rates have previously been reported in savannah soils from Zimbabwe (Bird et al., 1999) and Australia (Zimmerman et al., 2012). Similarly, during a laboratory incubation experiment, Hilscher et al. (2009) observed a complete consumption of the PyC's labile fraction (lab-produced) within the initial 30 days of the incubation.

The CO₂ pulse observed after the wetting was preceded by a lag phase of very low CO₂ flux lasting between 14 to 29 h (Fig. 4.2). Rewetting of dry soils is commonly associated with a large flush of CO₂ from the soil to the atmosphere, known as the Birch effect (Birch, 1958), and has been extensively observed in both burnt and unburnt soils (Jarvis et al., 2007; Sánchez-García et al., 2020b; Thomas et al., 2014). The lag phase (i.e. the period of very low microbial respiration between the start of wetting and the reactivation of microbial activity) is characteristic of soils in which microbial activity has been affected by a disturbance, such as a drought or a fire (Göransson et al., 2013; Meisner et al., 2015; Zhuravleva et al., 2011). In burnt soils, the duration of the lag phase (the microbial activity recovery time after the fire) is linked to heat exposure, since soil temperatures > 80 °C may kill many microorganisms with most of them disappearing completely at 115 – 150 °C (Mataix-Solera et al., 2009). During the experimental fires in this study, only a few points registered $T_{max} > 80$ °C (Supplementary Table S1), therefore, considering that our studied samples were composite samples, we expect that heating did not lead to high rates of microbial mortality in our soils and suggest that the lag phase is likely a consequence of the dry conditions before wetting. These observations are in line with Pinto et al. (2002) and Zepp et al. (1996) who also observed very low or negligible effects of fire on CO₂ fluxes. The length of the lag phase observed in this study is in line with

those reported in dry unburnt soil. For instance, Meisner et al. (2017) and Göransson et al. (2013) reported lag phases of 15 to 20 h and of 16 h, respectively, following wetting of dry soil.

Shorter lag phases were observed in all the post-fire soils with added ash, likely in response to the input of readily available nutrients from the ash, which might have favoured a quicker microbial reactivation (Fig. 4.2). An exceptionally short lag phase of only 3 h was observed in the MB1 post-fire soil with ash along with a higher CO₂ pulse than in the other two soils. The MB1 soil exhibited higher nutrient content than both PB soils (Table 4.4 and 4.5), which could possibly lead to a quicker recovery of microbial activity and boost the regrowth of vegetation after the fire. Yet no differences in the duration of the lag phase were observed amongst the pre- and post-fire soil without ash in this soil. The very short lag phase in the MB1 post-fire soil with ash may have been a response to the high available P in the ash from this site (i.e. water soluble PO₄; Table 4.5). Similar levels of total P to those reported in this study were reported by Feig (2004) in soils from the same location. P is one of the most limiting nutrients in savannahs (Feig, 2004). Large inputs of P can result in its adsorption to soil particles and the desorption of previously bonded OM, which can increase the amount of DOC within only 1 h after the addition of P resulting in a larger CO₂ pulse (Meisner et al., 2015; Spohn & Schleuss, 2019). In addition, the increase in available P might accelerate the reactivation of heterotrophic bacteria in soil, a group of bacteria that generally recovers quickly after a fire (Matáix-Solera et al., 2009) and which could be a contributing factor for the quick and large CO₂ pulse observed in the MB1 soil after the addition of ash.

The mean CO₂ fluxes observed in the post-fire soil with added ash are similar to those reported from fire-affected soil in other arid or semi-arid ecosystems. For instance, Vargas et al. (2012) reported soil CO₂ fluxes in a similar range to those observed in this study (between 0 and 1 μmol m⁻² s⁻¹) following a wildfire in an arid grassland in New Mexico (USA). Meigs et al. (2009) and Irvine et al. (2007) in wildfire-burnt semi-arid mixed conifer and ponderosa pine stands in Oregon reported higher annual CO₂ fluxes (~300 g C m⁻² y⁻¹ in both cases), but in the same order of magnitude, as those estimated for this study. In contrast, double the mean CO₂ fluxes (~2 g CO₂ m⁻² d⁻¹) as those observed in this study (~0.8 g C m⁻² d⁻¹) were reported by Wüthrich et al. (2002) over the month following an experimental fire in a sweet chestnut forest in southern Switzerland.

When compared with unburned savannahs, average CO₂ fluxes observed in the post-fire soil with wildland fire ash are similar to those reported by Zepp et al. (1996) who observed mean fluxes of approximately 1 g C m⁻² d⁻¹ after light *in-situ* wetting of the soil in a semi-arid

savannah also from the Kruger National Park (South Africa), whilst our daily flux in the post-fire soil with added ash averaged $0.8 \text{ g C m}^{-2} \text{ d}^{-1}$. In contrast, the CO_2 flux reported in the post-fire soil with wildland fire ash is lower, but in the same order of magnitude, as those reported by Castaldi et al. (2010) and Pinto et al. (2002), both during *in-situ* observations in a grass and shrub savannah in the Region of Congo (central Africa) and in a Brazilian savannah (central Brazil) respectively.

It is worth noting that up to 41% of the total CO_2 flux from the post-fire soil with added ash was released during the CO_2 pulse observed after wetting (i.e. the Birch effect), which indicates the importance of high frequency observations following the wetting of fire-affected soil. During field observations, bursts of CO_2 following rainfall events were reported in burnt African savannah soils by Andersson et al. (2004). In African savannahs, the CO_2 flux emitted during pulses in response to rainfall is estimated to account for up to a fifth of the annual CO_2 flux from soils (Fan et al., 2015) and soil moisture is one of the main controllers on the CO_2 fluxes from these semi-arid ecosystems (Zepp et al., 1996). After a fire, the first wetting mobilises soil nutrients from both the soil and ash, reactivates microbial activity and facilitates the release of stored CO_2 in the soil pores resulting in a short, yet intense, mineralisation period which explains the large CO_2 flush observed in this study (Matáix-Solera et al., 2014; Sánchez-García et al., 2020b).

It is important to highlight that the ash load applied in this study was substantially higher than that generated from the experimental burns in the field. The outcomes should thus be seen as indicative only, and we expect the CO_2 flux response to be less pronounced under field conditions. However, our observations with wildland fire ash support the increased CO_2 response previously observed by studies where artificially produced ash has been used (e.g. Badia and Marti, 2003; Raison and McGarity, 1980). Additionally, our results show that nearly half of the CO_2 emissions observed in the post-fire soils with added ash occurred soon after soil wetting. It is unlikely that under field conditions the soil moisture would remain constant for long periods of time following wetting of burnt soil (e.g. Vargas et al., 2012), instead another period of dry weather might follow, with subsequent fluctuation in the CO_2 fluxes after each drying-wetting cycle. Capturing these “hot moments” of CO_2 release after a wildfire, and while the layer of ash is still on the soil surface, is challenging. Missing these large spikes in CO_2 flux can lead to unrealistic estimates of post-fire C dynamics and highlights the need to (i) increase the frequency of observations and (ii) for models to reflect this high variation in the CO_2 fluxes. This becomes especially relevant in ecosystems with high fire frequency like savannahs, which contribute most to global CO_2 emissions from vegetation fires each year (van

der Werf, et al., 2017) and where fire occurrence is already being altered by climate change (Zubkova et al. 2019; Wei et al., 2020).

4.5. Conclusions

The results from this incubation study show that the presence of wildland fire ash significantly enhanced soil CO₂ fluxes when compared with pre-fire soils and post-fire soils without ash, and indicate that ash plays a quantitatively important role in post-fire C emissions. We suggest that the high content of readily available nutrients observed in the ash boosted the soil respiration. Even though most of the organic C in the wildland fire ash is in the form of PyC, which is considered highly resistant to degradation, there is a substantial labile pool within PyC in the ash examined here, which may provide readily accessible compounds for microorganisms.

The results also show that heating from the fires did not substantially affect the soil and that the recovery of soil respiration after the fire was mostly controlled by soil moisture. Approximately 40% of the total C emissions during the 28-day observation period occurred during a short-lived period of up to 130 h following the wetting of the dry samples.

Our findings, although based on homogenised wildland fire ash and pre- and post-fire soil material, indicate that overlooking wildland fire ash in post-fire soil studies is unlikely to reflect natural conditions, and might result in an underestimation of post-fire C fluxes. This is especially relevant in ecosystems with high fire frequencies such as savannahs. We expect a similar response of soil C fluxes to the presence of wildland fire ash in other post-fire environments but the magnitude of this response, which we anticipate will depend on factors including fire characteristics, vegetation, soil type and climatic conditions during the post-fire period, needs to be confirmed by future studies.

Chapter 5. General discussion

The results from each experimental chapter are discussed in detail at the end of each chapter. The main aim of this chapter is to summarise the principal findings of the thesis, discuss them in a wider context and suggest new directions for future work. The experimental work in this thesis aimed to study i) the effect of SWR on the magnitude and timing of the flush of CO₂ typically observed after wetting of dry soil (i.e. the “Birch effect”); ii) the main factors controlling the magnitude and duration of the Birch effect in water-repellent soils; iii) the role of wildland fire ash on the short-term release of post-fire soil CO₂ flux

SWR is a very common soil property of dry and fire-affected soils, and under low moisture conditions most soils will show some degree of repellency (Doerr et al., 2000). SWR is, in most dry soils, the norm rather than the exception, and it is predicted to become even more common as climate change increases the severity and frequency of droughts in some regions of the world (Goebel et al., 2011). Although previous studies such as those by Lado-Monserrat et al. (2014) and Muhr and Broken (2009) point to SWR as a possible explanation for the unexpectedly low CO₂ flux following wetting of dry soils, this hypothesis had never been tested before this research. Evidence that the amount of wetting and the overall increase in SWC are good indicators of the magnitude of the Birch effect has been challenged in this research.

Throughout this thesis clear CO₂ flux responses to wetting of dry and fire-affected soil have been observed under wettable conditions, but the timescale of this response differs based on the sources of the CO₂ released. The results presented here challenge the conceptual notion that the Birch effect comprises one large CO₂ pulse, suggesting that it may involve two spikes of different magnitude occurring at different timescales; an initial one of physicochemical origins (timescale: seconds to minutes after wetting), and a larger one underpinned by the recovery of microbial activity (timescale: hours to days after wetting).

One of the main objectives of this research was to enhance understanding of the role of wildland fire ash (i.e. ash produced naturally during vegetation fires) in post-fire CO₂ fluxes, with a particular focus on the initial post-fire recovery time. As much as 4% of the global vegetated land surface burns every year, and the area burned is projected to increase in many regions of the world due to climate change (Doerr and Santín, 2016). However, evidence of the effects of wildland fire ash on key post-fire hydro-geomorphological and biogeochemical processes remains scarce due to the short timeframe in which ash remains in the landscape after a fire (Santín et al., 2016). Its rapid redistribution, often occurring before the start of the field investigations, means that its role in post-fire soil C fluxes has been only sporadically considered (Bodí et al., 2014; Forbes et al., 2006). The results from the experiments involving

fire-affected soils, although using artificially high ash loads (x10 of that observed under field conditions) (Chapter 4), unequivocally showed that wildland fire ash plays a key role in contributing to post-fire CO₂ fluxes.

5.1. Soil water repellency and the Birch effect

5.1.1. Preferential flow and limited wetting: the main controllers of the Birch effect

In all of the measurements involving water-repellent soils in this study, SWR reduced the magnitude of the Birch effect mostly as a result of limited soil wetting and rapid percolation, both typically observed under water-repellent conditions (Chapters 2 and 3). Rapid water percolation upon wetting (within 2 to 3 min of the start of wetting) due to preferential infiltration resulted in up to 95% of the total water applied percolating quickly through the soil, refilling only a minimal volume of air-filled pores and resulting in low CO₂ flux. This suggests that water moved through the same infiltration paths, regardless of the amount of water added, with only a small proportion of the soil matrix conducting water. This pattern, typical of water-repellent soils, is made most apparent in the SWC distribution analysis of the water-repellent and fire-affected soils from Chapter 2. In this case only slight and uneven wetting was observed even when enough water was added to cause saturation of the soil pore-space.

The preferential infiltration patterns observed in the experiments with water-repellent soils (Chapters 2 and 3) are reflective of those typically observed under field conditions where water often bypasses the first cm of the top soil and moves towards deeper areas of the soil profile (Doerr et al., 2000; Ritsema and Dekker, 1994). An exception was observed at the burnt site with ash and water-repellent soil (BwA, Chapter 2), where the layer of wettable ash covering the soil surface intercepted a large fraction of the added water due to its high water-storing capacity. The wet layer of ash contributed to the breakdown of the extremely water-repellent soil below facilitating infiltration and, subsequently, enhancing the release of CO₂. Other mechanisms by which the ash layer contributes to CO₂ fluxes are discussed in more detail in section 5.3 of this chapter.

5.1.2. Further implications of SWR on soil CO₂ flux

The rewetting rate and the overall increase in SWC after wetting have previously been used as predictors of the magnitude of the CO₂ pulse following wetting (Borken and Matzner, 2009; Lado-Monserrat et al., 2014). However, the observations presented in this thesis suggest that

in water-repellent soils these two parameters may not be good indicators of the magnitude of the Birch effect and should be re-evaluated. This is an important observation from this research and is likely to be particularly relevant in extremely water-repellent soils.

This notion became apparent when examining the effect of different rewetting rates on the Birch effect from water-repellent soils (Chapter 3). While under wettable conditions CO₂ fluxes proportionally increased with the increase in the rewetting rate (limited by saturation), in water-repellent soils disproportionately high CO₂ fluxes were detected with high rewetting rates despite very low water retained in the soil after wetting. This suggests that CO₂ dynamics below ground, within the soil matrix, differ in wettable and water-repellent soils. It is likely that preferential flow induces pressure increase along the preferential path, while the dry areas of air-filled pores act as degassing channels facilitating gas exchange and explaining the observation of surprisingly high CO₂ fluxes. As part of this research, preliminary work was carried out towards mapping the distribution of CO₂ within the pore-space in real time (material not shown). However, further work is needed to develop a methodology to obtain real-time visualisations of changes in CO₂ concentration with wetting in the pore-space.

The high spatial variability in wetting flow pathways typical of water repellent soils had a direct effect on the CO₂ response to wetting. CO₂ flux following wetting was particularly susceptible to the high spatial variability in SWR observed, especially, in the intact core samples used in Chapter 2 (Fig. 2.6), which resulted in variable CO₂ flux responses for each replicate. As opposed to this, less variable responses of CO₂ flux to wetting were observed in the homogeneous water-repellent soils from Chapter 3. The relatively homogeneous water-repellent soil surface observed in the soils used in Chapter 3 provided fewer opportunities for water to penetrate through the soil surface. Heterogeneous moisture distribution is innate to most soils and, in field conditions, depends on a number of factors such as soil texture, structure, stone content or the presence of cracks and roots. Some hydrological processes, like preferential flow, are often more pronounced in water-repellent soils than in wettable ones (Nyman et al., 2010). Representing spatial variability is especially important when modelling the CO₂ flux response to wetting in water-repellent soils. Failing to consider this is unlikely to represent natural conditions.

The results presented in this thesis focus on the CO₂ flux response to the first rainfall after a dry period but subsequent cycles of drying and wetting can still result in a series of CO₂ pulses from soil to the atmosphere (Sponseller, 2007). However, the magnitude of the CO₂ pulse has been shown to decrease with consecutive drying-wetting cycles (Fierer and Schimel, 2002).

This pattern was observed in experiments with water-repellent soils in the burnt sites from Portugal (Chapter 2) during an additional fieldwork campaign six weeks after the first one (i.e. December 2017; results not shown), and following the same methodology. In December, a distinctively lower CO₂ flux response to wetting than in October was observed. This difference can be attributed to an increased SWC in the December campaign, compared with the very dry conditions in October, as a result of small rainfall events occurring days before the fieldwork. In addition, no marked differences in CO₂ pulse between wettable and water-repellent soils were observed in December most likely due to a reduction in SWR as a result of the increase in SWC (Dekker and Ritsema, 1994).

5.2. Sources of the Birch effect and the importance of high frequency observations

5.2.1. A dual response to wetting

The different approaches to measuring CO₂ fluxes followed in this research (short-term vs. longer-term CO₂ flux following wetting) allowed the observation of two very different CO₂ flux responses to wetting. The magnitude and timing of the CO₂ pulse differed considerably between the experiments focusing on the short-term phase after wetting (Chapters 2 and 3), and experiments focusing on the longer-term CO₂ flux response described in Chapter 4. This is very likely a reflection of the different sources of CO₂ flux (physicochemical vs. biological) underpinning the different responses.

The results from the experiments involving continuous CO₂ flux measurements for 28 d (Chapter 4) revealed a substantially higher pulse, within 130 h after wetting, than those observed in the experiments focusing on the initial phase of the wetting (Chapters 2 and 3). The timing and magnitude of this CO₂ flux response coincides with the commonly observed microbial recovery time following a soil disturbance such as a drought or a fire (e.g. Göransson et al., 2013; Meisner et al., 2015; Zhuravleva et al., 2011). Fully identifying the different sources of the CO₂ flux is not possible based on the work carried out here, and would require further investigations combining the experiment designs of all three approaches followed in this thesis. However, the lag phase (i.e. the time between wetting and the reactivation of microbial activity) in the soils from chapter 4 is similar to that previously reported in dry unburnt soil (Göransson et al., 2013; Meisner et al., 2017), indicating that the CO₂ pulse mostly originated from microbial respiration.

A large difference in the response and timing of the CO₂ release from that reported in the longer-term CO₂ flux experiment (Chapter 4) was observed in the experiments focusing on the short-term release of CO₂ after wetting (i.e. within the 4 - 5 h following soil wetting, Chapters 2 and 3). In this case an immediate increase in CO₂ flux coinciding with the beginning of wetting was observed, reaching a peak during the wetting period and declining soon after the end of wetting. The immediate CO₂ flux response to wetting in dry fire-affected soils (Chapter 2) and in autoclaved soils (Chapter 3) suggests different sources of CO₂ than those suggested for the CO₂ response in the dry savannah soils (Chapter 4). Physicochemical mechanisms driven by water such as the physical displacement of CO₂ stored in the dry air-filled pores, and the desorption of CO₂ molecules replaced by water, are likely behind this rapid release of CO₂ (Inglima et al., 2009; Kemper et al., 1985; Liu et al., 2002). Physical displacement of CO₂-rich air from the pore-space upon infiltration has been previously suggested to explain short-lived increases in CO₂ flux after the flooding of a saltpan in northern Botswana (Thomas et al., 2014) and after rainfall in arid and semi-arid soils (Huxman et al., 2004).

The results from this research have shown that the immediate response to wetting, originating mainly from physicochemical sources, can be potentially large and makes up a substantial fraction of the total CO₂ released during a wetting event. For instance, in the experiment focusing on the initial phase of the wetting in post-fire soil (Chapter 2), it was quantified that nearly 80% of the total CO₂ flux released during the 5 h following wetting occurred during the short duration of the pulse. This conclusion supports previous observations by Maier et al. (2010) who estimated that up to a fifth of the total CO₂ released during heavy rainfall events originates from CO₂ stored in the dry pore-space.

Differentiating between these two different episodes of intense CO₂ release following wetting is essential when defining and quantifying C emissions from drying-wetting cycles. This dual pattern of CO₂ release comprising two clear CO₂ spikes following wetting may be more pronounced in soils that have undergone a disturbance such as an intense drought or a fire. The reactivation of microbial respiration which determines the time elapsed between both CO₂ pulses is primarily a function of the magnitude of the disturbance; i.e. the more severe the disturbance, the longer the recovery time (Meisner et al., 2017).

5.2.2. Capturing the entire CO₂ response to drying-wetting events

In the experiments conducted here it was found that as much as 40% of the total C respired during a 28 day observation period occurred during a short period of up to 130 h after wetting

(Chapter 4). However, because of the difficulty of measuring CO₂ fluxes during rainfall or artificial wetting experiments, it is very likely that the immediate CO₂ response to wetting is systematically missed. Even those studies aimed at capturing the early response of CO₂ to wetting (e.g. Inglima et al., 2009; Rey et al., 2017; Sponseller, 2007) often begin the observations 15 min after wetting at the earliest. For example, evidence of degassing of CO₂ stored in the pore-space was observed through the upward movement of bubbles after water addition in the site with flat terrain from the field experiments described in chapter 2. However, the complete CO₂ flux response could not be captured during *in situ* observations and only a downward trend, probably from the pulse, was observed. Similar observations were described by Thomas and Hoon (2010) after *in situ* artificial wetting of dry Kalahari sand soils. This immediate CO₂ response to wetting of dry soil was observed *in situ* during additional fieldwork carried out in the Cefn Bryn area as part of this research (soil described in Chapter 3) in the Gower peninsula (South Wales, UK) during the 2018 European summer drought (data not shown).

The large variability between wetting and the commencement of the CO₂ flux observations in drying-wetting studies may fail to reflect all the mechanisms underpinning the production and transport of CO₂ in response to wetting. In addition, eddy-covariance towers measuring CO₂ fluxes at the ecosystem level may also systematically miss, partly or entirely, the CO₂ flux response since data captured during heavy rainfall events are usually discarded and the resulting gaps filled with estimations. The common methods used to fill in the discarded data do a poor job in estimating CO₂ spikes from moisture-limited ecosystems, as stated in a recent study by Oliveira et al. (2021) from the same fire-affected area as the experiments described in Chapter 2.

5.3. Wildland fire ash is a key player in post-fire CO₂ fluxes

The indirect effects of ash on CO₂ flux dynamics following wetting was most apparent in the experiment comparing CO₂ fluxes from two burnt soils: one in which a thin layer of black ash remained untouched on the soil surface (BwA) and a second one in which the layer of black ash was removed (BnoA) exposing the bare soil (Chapter 2). The short-lived (i.e. seconds to minutes after wetting) CO₂ response observed in this experiment coincides with the short timescale at which main wetting-induced hydrological processes, such as ponding, infiltration and runoff generation, take place in fire-affected soils (Leighton-Boyce et al., 2007; Woods and Balfour, 2008). Following wetting more CO₂ was released from the BwA soil than from the

BnoA suggesting that ash indirectly contributed to post-fire CO₂ fluxes by facilitating infiltration into the dry soil matrix below (Fig. 3, Chapter 2). The wettable layer of ash covering the dry burnt soil intercepted and stored a large amount of the added water (Fig. 7, Chapter 2). The hydraulic pressure of the wet layer of ash over the dry soil is likely to have facilitated infiltration by initiating preferential flow in the larger pores; a mechanism previously observed by other researchers such as Nyman et al. (2010) and Wang et al. (2000).

The hydraulic effect of the ash layer is likely to have been more pronounced under water-repellent soil conditions due to ponding, which likely enhanced the hydraulic pressure exerted by the ash layer. In contrast, in the no-ash soil (BnoA), situated on a slope, water repellency reduced effective infiltration in the soil matrix due to runoff generation. A direct comparison between sites cannot be made due to the differences in the slope angle, which interferes with the hydrologic response to the wetting event. However, a hypothetical layer of wettable ash covering the BnoA soil would likely have resulted in runoff and substantial redistribution of the ash downslope after saturation of the thin ash layer; therefore limiting the hydraulic pressure exerted over the soil below (Ebel et al., 2012; Masiello and Berhe, 2020; Novara et al., 2011).

The direct contribution of ash to post-fire CO₂ fluxes was shown in the experiment designed to isolate the effect of wildland fire ash on post-fire CO₂ fluxes (Chapter 4). The input of ash to post-fire soil boosted soil respiration and enhanced CO₂ emissions by up to 3 times, compared to post-fire soil without ash, as a result of the high content of readily available nutrients in the ash. This response may be less pronounced under field conditions since the ash load applied in this experiment (Chapter 4) was substantially higher than that generated in the field, but still similar to that in previous incubation experiments (e.g. Gómez-Rey et al., 2012; Smith et al., 2010). The addition of ash also accelerated the recovery of post-fire soil respiration. This shows that ash is a significant player in post-fire C fluxes and should be taken into account in post-fire C studies.

Finally, the findings presented in this research highlight that using laboratory-produced ash as a proxy for naturally-produced ash can have critical implications when estimating post-fire C dynamics and may lead to underestimations of post-fire C emissions. Using laboratory-produced ash as a substitute for naturally-produced ash is a common practice in post-fire C studies, but these two ash types may have very different physico-chemical characteristics due to large differences in their production, mostly in oxygen availability and duration of laboratory pyrolysis (Santín et al., 2017). The total C respired over the 28 d observation was an order of magnitude higher than the labile C fraction in the ash (DOC). This indicates high levels

of C mineralization beyond the consumption of the easily accessible C. While identifying the source of the respired C would need an additional experiment it is likely that microbes consumed the easily accessible C, after which they consumed more stable forms of C, such as the PyC labile's fraction. Although PyC is considered resistant to mineralization the relatively large PyC labile fraction in the samples suggests that some of the PyC could have undergone quick degradation during the initial stages of mineralisation (Santín et al., 2016).

5.4. Recommendations for future work

1) More work is needed to improve understanding of the long-lasting implications of SWR on CO₂ flux. The results presented in this thesis revealed the important effect of SWR on C dynamics in drying-wetting events. However, future studies should focus on the longer-term effects of SWR on C dynamics, which remain poorly understood. It would be interesting to study the effects of subsequent rainfall events (i.e. series of wetting events following the first rainfall after the dry period) on CO₂ fluxes from water-repellent soils, and also at different stages of the post-fire period, beyond the first rainfall after the fire.

2) Representing spatial and temporal variability in SWC, and not only overall changes in SWC, is key when modelling C fluxes. It is therefore recommended that future studies focus on quantifying the effects of moisture variability on C dynamics. Emphasis should be put on integrating this spatial/temporal variability into more representative models. Alongside this, another research gap is the development and application of standard methods that enable the capture of short and intense moments of CO₂ release during drying-wetting events with high temporal resolution. A more integrative approach between fieldwork and remote sensing data (i.e. satellite and airborne generated) would be of particular interest by, for example, using satellite data from NASA's OCO-2 or drones with CO₂ and CH₄, and thermal infrared cameras sensors.

3) Future studies should also investigate the contribution to the Birch effect of the different sources of CO₂ under different soil conditions. The identification of the different sources of CO₂ release following wetting of dry soils alongside the microbial processes underpinning these events will help understand and predict the total contribution of different sources to annual C emissions. Closer interdisciplinary collaboration particularly between soil microbiologists, physicists, biochemists and the modelling community is likely to be beneficial in enhancing our understanding of the processes underlying rapid changes of CO₂ flux after soil wetting and quantify their role in global soil C budget.

4) Future studies focusing on fire-affected terrain should consider wildland fire ash in post-fire C investigations in order to produce more realistic outputs when estimating the effects of fire on C budgets. Given the commonly observed quick redistribution of ash in the landscape by wind and water, it is especially important to consider the time elapsed since the fire and the field investigations (i.e. time-since-fire).

Chapter 6. Conclusions

1) Despite both SWR and the Birch effect being characteristic of many dry soils, to the author's knowledge their interaction had never been studied before this research. The work presented in this thesis has clearly demonstrated that SWR is a controlling factor of the Birch effect and needs to be considered when studying C dynamics of drying-wetting events. This outcome is critically important because it challenges the common assumption that wetting dry soil unequivocally results in a large pulse of CO₂ to the atmosphere.

2) This research shows that the CO₂ response to drying-wetting events is more complex than previously assumed and comprise at least two transient periods of intense CO₂ release at different timescale; one of physicochemical origins and a second dominated by the recovery of microbial activity. This challenges the common notion that the Birch effect primarily comprises one large pulse of CO₂.

3) Capturing the complete CO₂ flux response to wetting is key in order to obtain a more precise understanding of the mechanisms underlying the release of CO₂ during drying-wetting events. The results from this research clearly show the need for capturing rapid changes of CO₂ flux in response to wetting and strongly highlight the importance of high frequency observations after the wetting of dry soil. In order to capture the CO₂ response it is important that future studies consider the effect of the timescale of observation and the application of high temporal CO₂ flux measurements, particularly during the short period after soil wetting.

4) Wildland fire ash, often overlooked in post-fire investigations, is a key player in post-fire C fluxes. Wildland fire ash indirectly affected CO₂ fluxes by influencing key hydrological behaviours and directly influenced it by adding easily accessible nutrients and labile C essential for microbial respiration.

Appendices

i) Supplementary material: Chapter 2

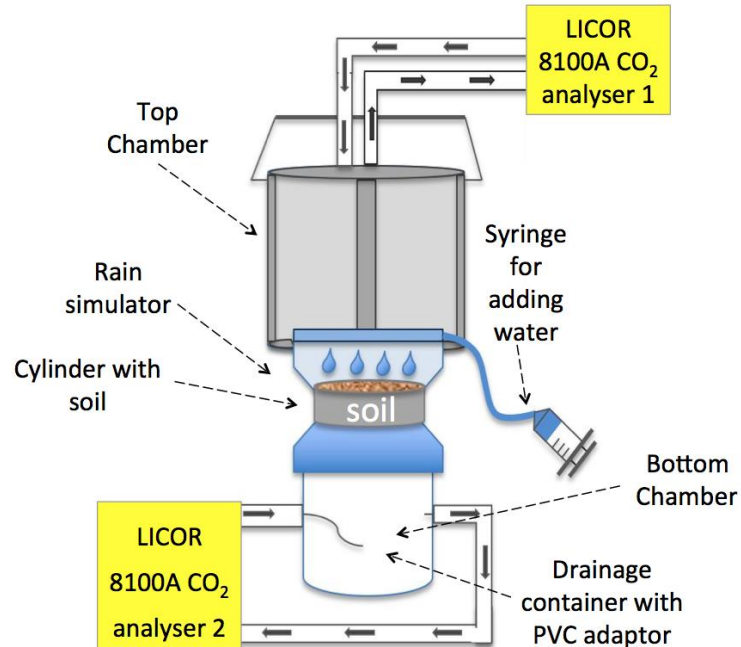


Fig. S1. Schematic illustration of rewetting and CO₂ analyser system.

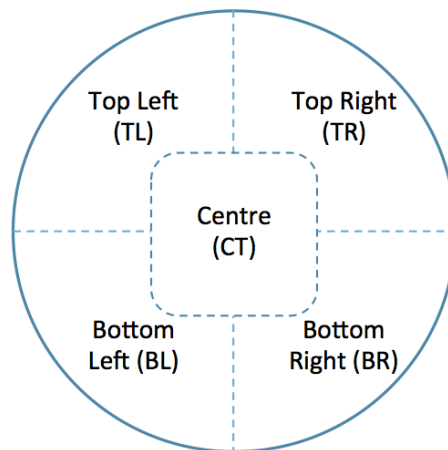


Fig. S2. Diagram showing the subsampling strategy on intact cores for each 1 cm layer.

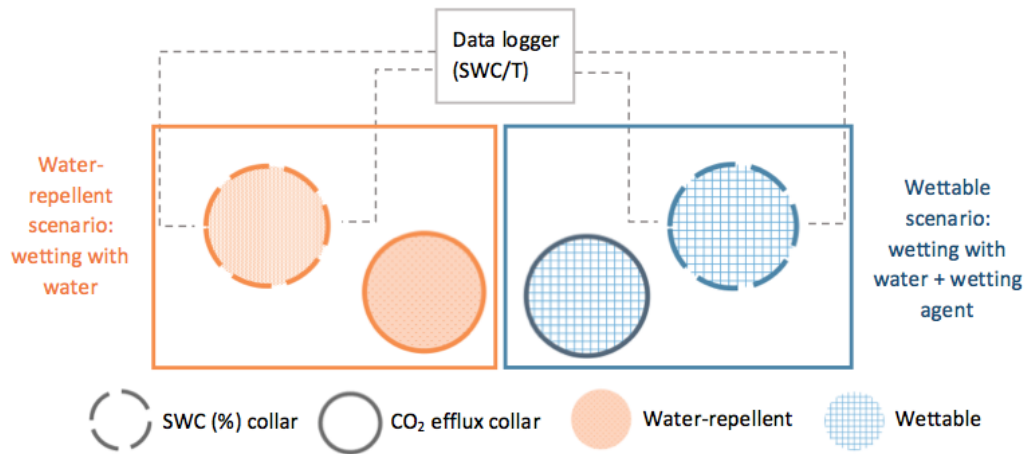


Fig. S3. Schematic representation of a field plot with two collars per wetting scenario.

ii) Supplementary material: Chapter 4

Table S.1. Maximum temperatures (Tmax) (°C) and residence times (seconds > 300 °C) registered during the experimental fires in the soil surface and in the grass (n = 12). Values in bold are the arithmetic mean (n = 12) with standard deviation in brackets. n.d. (no data) cells represent discarded values after errors in the sensors.

Sample n°	PB1				PB3				MB1			
	Soil surface		Grass		Soil surface		Grass		Soil surface		Grass	
	Tmax	Time > 300 °C	Tmax	Time > 300 °C	Tmax	Time > 300 °C	Tmax	Time > 300 °C	Tmax	Time > 300 °C	Tmax	Time > 300 °C
1	58	0	585	22	41	0	n.d.	n.d.	206	0	748	155
2	<40	0	574	12	73	0	803	41	<40	0	778	63
3	<40	0	618	12	73	0	918	139	498	62	685	75
4	<40	0	484	24	<40	0	n.d.	n.d.	75	0	667	29
5	<40	0	576	13	182	0	651	65	369	20	840	31
6	56	0	634	14	74	0	782	67	<40	0	796	73
7	95	0	729	15	<40	0	659	27	<40	0	849	25
8	44	0	722	73	n.d.	n.d.	702	37	365	27	n.d.	n.d.
9	59	0	577	11	<40	0	788	37	468	56	850	36
10	n.d.	n.d.	n.d.	0	<40	0	n.d.	n.d.	n.d.	n.d.	800	37
11	99	0	744	37	63	0	n.d.	n.d.	<40	0	751	22
12	225	0	554	42	<40	0	665	19	<40	0	452	19
Mean	72 (55)	0	618 (83)	23 (20)	64 (42)	0	746 (94)	54 (38)	198 (190)	15 (24)	747 (115)	51 (40)

Table S.2. Outcomes of DTG-DSC analysis in the pre-fire (PreF) and post-fire (PostF) soil and in the ash. Total organic matter (OM) loss, total energy (Q) released, Q': energetic net output, calculated as a result of combining both thermograms; Q50: 50% of the total energy released by the OM; T50_Q: temperature at which sample has released half of its total stored energy; Q1, Q2 and Q3: percentage of heat released in each group of thermal oxidation (150-37 °C; 375-475 °C; 475-600 °C); T1_Q, T2_Q, T3_Q: temperature at which each peak of heat combustion occurs; W50: weigh loss of 50%; T50_w: temperature at which 50% of the OM weight is lost; W1, W2, W3: % of OM weight loss in each group of resistance to thermal oxidation (150-37 °C; 375-475 °C; 475-600 °C); T1_w, T2_w, T3_w: temperature at which each peak of weight loss occurs.

Site	Treatment	Total OM loss [%]	Total Q released [J g ⁻¹]	Q' [J mg ⁻¹ OM]	Q50 [J g ⁻¹]	T50 _Q [°C]	Q1 [%]	Q2 [%]	Q3 [%]	T1 _Q [°C]	T2 _Q [°C]	T3 _Q [°C]	W50 [%]	T50 _w [°C]	W1 (%)	W2 (%)	W3 (%)	T1 _w [°C]	T2 _w [°C]	T3 _w [°C]
PreF	PB1	2.9	1851.8	63634.4	925.9	353.0	46.2	25.6	28.2	343.0	375.0	600.0	1.5	373.0	1.5	1.0	0.4	331.0	375.0	475.0
	PB3	3.3	2250.2	67451.5	1125.1	374.0	40.0	37.8	22.2	356.0	375.0	600.0	1.7	376.3	1.6	1.3	0.4	330.0	395.0	475.0
	MB1	7.8	10353.7	132893.7	5176.9	341.0	50.6	31.4	18.1	347.0	375.0	507.0	3.9	377.1	3.8	2.4	1.6	373.0	429.0	497.0
PostF	PB1	3.2	4390.5	138064.6	2195.2	419.0	30.2	25.8	44.0	350.0	403.0	600.0	1.6	375.8	1.6	1.2	0.4	330.0	448.0	475.0
	PB3	2.4	3788.0	156592.6	1894.0	314.0	67.1	23.9	9.0	335.0	375.0	600.0	1.2	370.5	1.2	0.9	0.3	329.0	393.0	475.0
	MB1	8.0	14414.9	179267.1	7207.4	339.0	50.4	33.9	15.7	347.0	435.0	507.0	4.0	378.6	3.9	2.5	1.7	341.0	433.0	497.0
Ash	PB1	34.9	22349.2	65079.4	11174.6	414.3	29.4	55.9	14.6	374.6	438.0	475.6	17.4	414.6	10.8	18.2	5.6	374.6	433.6	475.6
	PB3	28.7	16471.4	58017.0	8235.7	419.0	26.3	56.4	17.3	374.6	439.3	475.3	14.3	418.6	8.4	14.8	5.1	374.6	435.3	475.6
	MB1	35.0	22926.4	65503.2	11463.2	433.8	21.2	53.4	25.4	374.8	463.5	475.8	17.5	442.2	6.2	18.2	10.2	374.8	459.5	475.5

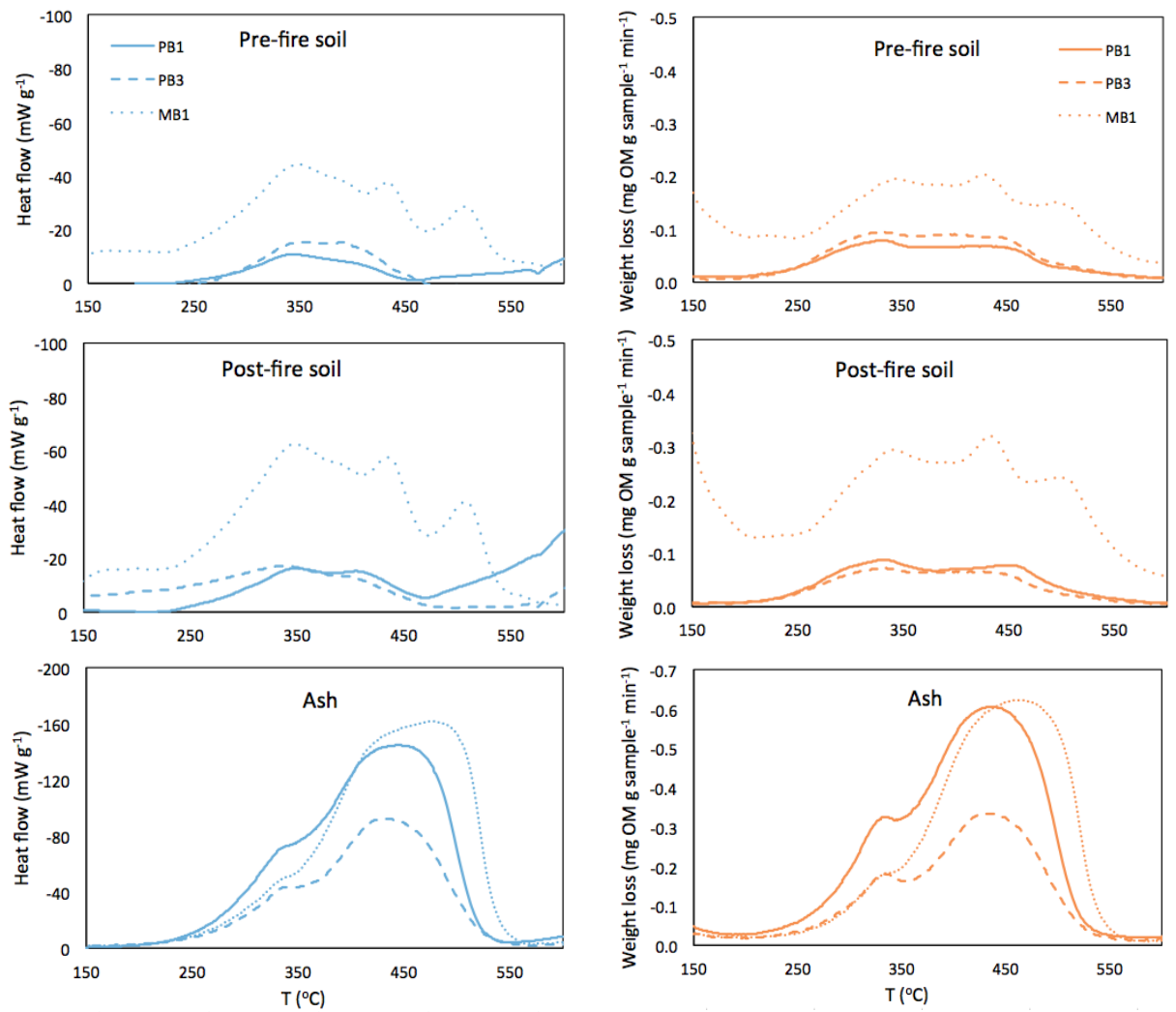


Fig. S4. Representative scanning calorimetry (left) and thermogravimetry (right) curves in the pre and post-fire soils and in the ash.

Bibliography

- Alcañiz, M., Outeiro, L., Francos, M., Úbeda, X. (2018). Effects of prescribed fires on soil properties: A review. *Science of The Total Environment*, 613–614, 944–957. <https://doi.org/https://doi.org/10.1016/j.scitotenv.2017.09.144>
- Alexis, M. A., Rasse, D. P., Rumpel, C., Bardoux, G., Péchot, N., Schmalzer, P., Mariotti, A. (2007). Fire impact on C and N losses and charcoal production in a scrub oak ecosystem. *Biogeochemistry*, 82, 201–216. <https://doi.org/10.1007/s10533-006-9063-1>
- Amiro, B. D., Macpherson, J. I., Desjardins, R. L., Chen, J. M., Liu, J. (2003). Post-fire carbon dioxide fluxes in the western Canadian boreal forest: evidence from towers, aircrafts and remote sensing. *Agricultural and Forest Meteorology*, 115, 91–107. [https://doi.org/https://doi.org/10.1016/S0168-1923\(02\)00170-3](https://doi.org/https://doi.org/10.1016/S0168-1923(02)00170-3)
- Andela, N., Morton, D. C., Giglio, L., Chen, Y., van der Werf, G. R., Kasibhatla, P. S., Randerson, J. T. (2017). A human-driven decline in global burned area. *Science*, 356, 1356–1362. <https://doi.org/10.1126/science.aal4108>
- Andersson, M., Michelsen, A., Jensen, M., Kjøller, A. (2004). Tropical savannah woodland: Effects of experimental fire on soil microorganisms and soil emissions of carbon dioxide. *Soil Biology and Biochemistry*, 36, 849–858. <https://doi.org/10.1016/j.soilbio.2004.01.015>
- Arcenegui, V., Mataix-Solera, J., Guerrero, C., Zornoza, R., Mataix-Beneyto, J., García-Orenes, F. (2008). Immediate effects of wildfires on water repellency and aggregate stability in Mediterranean calcareous soils. *Catena*, 74, 219–226. <https://doi.org/10.1016/j.catena.2007.12.008>
- Bachmann, J., Woche, S. K., Goebel, M.-O., Kirkham, M. B., Horton, R. (2003). Extended methodology for determining wetting properties of porous media. *Water Resources Research*, 39. <https://doi.org/https://doi.org/10.1029/2003WR002143>
- Bachmann, Jörg, Guggenberger, G., Baumgartl, T., Ellerbrock, R. H., Urbanek, E., Goebel, M. O., Fischer, W. R. (2008). Physical carbon-sequestration mechanisms under special consideration of soil wettability. *Journal of Plant Nutrition and Soil Science*. WILEY-VCH Verlag. <https://doi.org/10.1002/jpln.200700054>
- Badía, D., Martí, C. (2003). Effect of simulated fire on organic matter and selected microbiological properties of two contrasting soils. *Arid Land Research and Management*, 17, 55–69. <https://doi.org/10.1080/15324980301594>

- Badía, D., Martí, C., Aguirre, A. J., Aznar, J. M., González-Pérez, J. A., De la Rosa, J. M., Echeverría, T. (2014). Wildfire effects on nutrients and organic carbon of a Rendzic Phaeozem in NE Spain: Changes at cm-scale topsoil. *CATENA*, *113*, 267–275. <https://doi.org/https://doi.org/10.1016/j.catena.2013.08.002>
- Balser, T. C., Firestone, M. K. (2005). Linking microbial community composition and soil processes in a California annual grassland and mixed-conifer forest. *Biogeochemistry*, *73*, 395–415. <https://doi.org/10.1007/s10533-004-0372-y>
- Barnard, R. L., Osborne, C. A., Firestone, M. K. (2015). Changing precipitation pattern alters soil microbial community response to wet-up under a Mediterranean-type climate. *ISME Journal*, *9*, 946–957. <https://doi.org/10.1038/ismej.2014.192>
- Beisner, B., Haydon, D., Cuddington, K. (2003). Alternative stable states in ecology. *Frontiers in Ecology and the Environment*, *1*, 376–382. [https://doi.org/10.1890/1540-9295\(2003\)001\[0376:ASSIE\]2.0.CO;2](https://doi.org/10.1890/1540-9295(2003)001[0376:ASSIE]2.0.CO;2)
- Benavides, J. C., Vitt, D. H., Wieder, R. K. (2013). The influence of climate change on recent peat accumulation patterns of *Distichia muscoides* cushion bogs in the high-elevation tropical Andes of Colombia. *Journal of Geophysical Research: Biogeosciences*, *118*, 1627–1635. <https://doi.org/https://doi.org/10.1002/2013JG002419>
- Bertrand, I., Delfosse, O., Mary, B. (2007). Carbon and nitrogen mineralization in acidic, limed and calcareous agricultural soils: apparent and actual effects. *Soil Biology and Biochemistry*, *39*, 276–288. <https://doi.org/10.1016/j.soilbio.2006.07.016>
- Biggs, R., Biggs, H. C., Dunne, T. T., Govender, N., Potgieter, A. L. F. (2003). Experimental burn plot trial in the Kruger National Park: History, experimental design and suggestions for data analysis. *Koedoe*, *46*, 1–15. <https://doi.org/10.4102/koedoe.v46i1.35>
- Birch, H. F. (1958). The effect of soil drying on humus decomposition and nitrogen availability. *Plant and Soil*, *10*, 9–31. <https://doi.org/10.1007/BF01343734>
- Bird, M. I., Moyo, C., Veenendaal E. M., Frost, P. (1999). Stability of elemental carbon in a savanna soil total of the soil protected. *Global Biogeochemical Cycles*, *13*, 923–932.
- Bird, M. I., Veenendaal, E. M., Moyo, C., Lloyd, J., Frost, P. (2000). Effect of fire and soil texture on soil carbon in a sub-humid savanna (Matopos, Zimbabwe). *Geoderma*, *94*, 71–90. [https://doi.org/10.1016/S0016-7061\(99\)00084-1](https://doi.org/10.1016/S0016-7061(99)00084-1)
- Blake, G. R. (2008). Particle density. In W. Chesworth (Ed.), *Encyclopedia of Soil Science* (pp. 504–505). Dordrecht: Springer Netherlands. <https://doi.org/10.1007/978-1-4020-3995-504-505>

- Bodí, M. B., Doerr, S. H., Cerdà, A., Mataix-Solera, J. (2012). Hydrological effects of a layer of vegetation ash on underlying wettable and water repellent soil. *Geoderma*, 191, 14–23. <https://doi.org/10.1016/j.geoderma.2012.01.006>
- Bodí, M. B., Martin, D. A., Balfour, V. N., Santín, C., Doerr, S. H., Pereira, P., Cerdà, A., Mataix-Solera, J. (2014). Wildland fire ash: production, composition and eco-hydro-geomorphic effects. *Earth Science Reviews*, 130, 8252. <https://doi.org/10.1016/j.earscirev.2014.07.005>
- Bodí, M. B., Mataix-Solera, J., Doerr, S. H., Cerdà, A. (2011). The wettability of ash from burned vegetation and its relationship to Mediterranean plant species type, burn severity and total organic carbon content. *Geoderma*, 160, 599–607. <https://doi.org/10.1016/j.geoderma.2010.11.009>
- Bond-Lamberty, B., Peckham, S. D., Ahl, D. E., Gower, S. T. (2007). Fire as the dominant driver of central Canadian boreal forest carbon balance. *Nature*, 450, 89–92. <https://doi.org/10.1038/nature06272>
- Bond-Lamberty, B., Thomson, A. (2010). A global database of soil respiration data. *Biogeosciences*, 7, 1915–1926. <https://doi.org/10.5194/bg-7-1915-2010>
- Bond-Lamberty, B., Thomson, A. (2010). Temperature-associated increases in the global soil respiration record. *Nature*, 464, 579–582. <https://doi.org/10.1038/nature08930>
- Borken, W., Matzner, E. (2009). Reappraisal of drying and wetting effects on C and N mineralization and fluxes in soils. *Global Change Biology*, 15, 808–824. <https://doi.org/10.1111/j.1365-2486.2008.01681.x>
- Bradford, M. A., Davies, C. A., Frey, S. D., Maddox, T. R., Melillo, J. M., Mohan, J. E., Wallenstein, M. D. (2008). Thermal adaptation of soil microbial respiration to elevated temperature. *Ecology Letters*, 11, 1316–1327. <https://doi.org/10.1111/j.1461-0248.2008.01251.x>
- Brüggemann, N., Gessler, A., Kayler, Z., Keel, S. G., Badeck, F., Barthel, M., Bahn, M. (2011). Carbon allocation and carbon isotope fluxes in the plant-soil-atmosphere continuum: A review. *Biogeosciences*, 8, 3457–3489. <https://doi.org/10.5194/bg-8-3457-2011>
- Bruun, S., Clauson-Kaas, S., Bobuřská, L., Thomsen, I. K. (2014). Carbon dioxide emissions from biochar in soil: role of clay, microorganisms and carbonates. *European Journal of Soil*

Science, 65, 52–59. <https://doi.org/10.1111/ejss.12073>

- Buurman, P., Van Lagen, B., Velthorst, E. J. (1996). *Manual for soil and water analysis*. Backhuys publishers, Leiden, The Netherlands.
- Campbell, G. S., Jungbauer, J. D., Bidlake, W. R., Hungerford, R. D. (1994). Predicting the effect of temperature on soil thermal conductivity. *Soil Science*, 158. Retrieved from https://journals.lww.com/soilsci/Fulltext/1994/11000/PREDICTING_THE_EFFECT_OF_TEMPERATURE_ON_SOIL.1.aspx
- Campo, J., Merino, A. (2016). Variations in soil carbon sequestration and their determinants along a precipitation gradient in seasonally dry tropical forest ecosystems. *Global Change Biology*, 22, 1942–1956. <https://doi.org/doi:10.1111/gcb.13244>
- Canarini, A., Kiær, L. P., Dijkstra, F. A. (2017). Soil carbon loss regulated by drought intensity and available substrate: A meta-analysis. *Soil Biology and Biochemistry*, 112, 90–99. <https://doi.org/10.1016/j.soilbio.2017.04.020>
- Castaldi, S., de Grandcourt, A., Rasile, A., Skiba, U., Valentini, R. (2010). CO₂, CH₄ and N₂O fluxes from soil of a burned grassland in Central Africa. *Biogeosciences*, 7, 3459–3471. <https://doi.org/10.5194/bg-7-3459-2010>
- Cerdà, A., Doerr, S. H. (2008). The effect of ash and needle cover on surface runoff and erosion in the immediate post-fire period. *Catena*, 74, 256–263. <https://doi.org/10.1016/j.catena.2008.03.010>
- Certini, G. (2005). Effects of fire on properties of forest soils: A review. *Oecologia*, 143, 1–10. <https://doi.org/10.1007/s00442-004-1788-8>
- Chen, X., Wang, W., Luo, G., Ye, H. (2014). Can soil respiration estimate neglect the contribution of abiotic exchange? *Journal of Arid Land*, 6, 129–135. <https://doi.org/10.1007/s40333-013-0244-1>
- Chowdhury, N., Burns, R. G., Marschner, P. (2011). Recovery of soil respiration after drying. *Plant and Soil*, 348, 269–279. <https://doi.org/10.1007/s11104-011-0871-2>
- Christensen, S., Prieme, A. (2001). Natural perturbations, drying-wetting and freezing-thawing cycles, and the emission of nitrous oxide, carbon dioxide and methane from farmed organic soils. *Soil Biology*, 33, 2083–2091. [https://doi.org/10.1016/S0038-0717\(01\)00140-7](https://doi.org/10.1016/S0038-0717(01)00140-7)

- Coetsee, C., Bond, W. J., February, E. C. (2010). Frequent fire affects soil nitrogen and carbon in an African savanna by changing woody cover. *Oecologia*, 162, 1027–1034. <https://doi.org/10.1007/s00442-009-1490-y>
- Concilio, A., Ma, S., Ryu, S., North, M., Chen, J. (2006). Soil respiration response to experimental disturbances over 3 years. *Forest Ecology and Management*, 228, 82–90. <https://doi.org/10.1016/j.foreco.2006.02.029>
- Coumou, D., Rahmstorf, S. (2012). A decade of weather extremes. *Nature Climate Change*, 2, 491. <https://doi.org/https://doi.org/10.1038/nclimate1452>
- Cox, P. M., Betts, R. A., Jones, C. D., Spall, S. A., Totterdell, I. J. (2000). Acceleration of global warming due to carbon-cycle feedbacks in a coupled climate model. *Nature*, 408, 184–187. <https://doi.org/10.1038/35041539>
- Crowther, T. W., Todd-Brown, K. E. O., Rowe, C. W., Wieder, W. R., Carey, J. C., Machmuller, M. B., Bradford, M. A. (2016). Quantifying global soil carbon losses in response to warming. *Nature*, 540, 104–108. <https://doi.org/10.1038/nature20150>
- Czimczik, C. I., Schmidt, M. W. I., Schulze, E.-D. (2005). Effects of increasing fire frequency on black carbon and organic matter in Podzols of Siberian Scots pine forests. *European Journal of Soil Science*, 56, 417–428. <https://doi.org/https://doi.org/10.1111/j.1365-2389.2004.00665.x>
- Dacal, M., Bradford, M. A., Plaza, C., Maestre, F. T., García-Palacios, P. (2019). Soil microbial respiration adapts to ambient temperature in global drylands. *Nature Ecology and Evolution*, 3, 232–238. <https://doi.org/10.1038/s41559-018-0770-5>
- Davidson, E. A., Janssens, I. A. (2006). Temperature sensitivity of soil carbon decomposition and feedbacks to climate change. *Nature*, 440, 165–173. <https://doi.org/10.1038/nature04514>
- DeBano, L. . (1991). The effect of fire on soil properties. In *Proceedings management and productivity of western-Montane forest soils*. (pp. 151–155). Retrieved from [https://books.google.es/books?hl=es&lr=&id=PGTOhtl2380C&oi=fnd&pg=PA151&dq=fire+effect+soil+nutrients&ots=8koOpbPZ4V&sig=oorbQzjgSwTjxs9TQTpu2fPEKsY&redir_esc=y#v=onepage&q=fire effect soil nutrients&f=false](https://books.google.es/books?hl=es&lr=&id=PGTOhtl2380C&oi=fnd&pg=PA151&dq=fire+effect+soil+nutrients&ots=8koOpbPZ4V&sig=oorbQzjgSwTjxs9TQTpu2fPEKsY&redir_esc=y#v=onepage&q=fire%20effect%20soil%20nutrients&f=false)
- DeBano, L. (2000). The role of fire and soil heating on water repellency in wildland environments: a review. *Journal of Hydrology*, 231–232, 195–206.

[https://doi.org/10.1016/S0022-1694\(00\)00194-3](https://doi.org/10.1016/S0022-1694(00)00194-3)

- Dekker, L. W., Doerr, S. H., Oostindie, K., Ziogas, A. K., Ritsema, C. J. (2001). Water repellency and critical soil water content in a dune sand. *Soil Science Society of America Journal*, 65, 1667–1674. <https://doi.org/10.2136/sssaj2001.1667>
- Dekker, L. W., Ritsema, C. J. (1996). Preferential flow path in a water repellent clay soil with grass cover. *Water Resources Research*, 32, 1239–1249.
- Dekker, Louis W., Ritsema, C. J. (1995). Fingerlike Wetting Patterns in Two Water-Repellent Loam Soils. *Journal of Environmental Quality*, 24(2), 324–333. <https://doi.org/10.2134/jeq1995.00472425002400020016x>
- Delahaye, C. H., Alonso, E. E. (2002). Soil heterogeneity and preferential paths for gas migration. *Engineering Geology*, 64, 251–271. [https://doi.org/10.1016/S0013-7952\(01\)00104-1](https://doi.org/10.1016/S0013-7952(01)00104-1)
- Dicen, G. P., Rallos, R. V., Leonard, J., Navarrete, I. A. (2020). Vulnerability of soil organic matter to microbial decomposition as a consequence of burning. *Biogeochemistry*, 1. <https://doi.org/10.1007/s10533-020-00688-1>
- de Baets, S., van de Weg, M. J., Lewis, R., Steinberg, N., Meersmans, J., Quine, T. A., Hartley, I. P. (2016). Investigating the controls on soil organic matter decomposition in tussock tundra soil and permafrost after fire. *Soil Biology and Biochemistry*, 99, 108–116. <https://doi.org/https://doi.org/10.1016/j.soilbio.2016.04.020>
- de Jonge, H., Mittelmeijer-Hazeleger, M. C. (1996). Adsorption of CO₂ and N₂ on soil organic matter: Nature of porosity, surface area, and diffusion mechanisms. *Environmental Science and Technology*, 30, 408–413. <https://doi.org/10.1021/es950043t>
- de Nijs, E. A., Hicks, L. C., Leizeaga, A., Tietema, A., Rousk, J. (2018). Soil microbial moisture dependences and responses to drying-rewetting: the legacy of 18 years drought. *Global Change Biology*, 0–2. <https://doi.org/10.1111/gcb.14508>
- Dlapa, P., Bodí, M. B., Mataix-Solera, J., Cerdà, A., Doerr, S. H. (2013). FT-IR spectroscopy reveals that ash water repellency is highly dependent on ash chemical composition. *Catena*, 108, 35–43. <https://doi.org/10.1016/j.catena.2012.02.011>
- Doerr, S. H. (1998). On standardizing the ‘Water Drop Penetration Time’ and the ‘Molarity of an Ethanol Droplet’ techniques to classify soil hydrophobicity: a case study using medium textured soils. *Earth Surface Processes and Landforms*, 23, 663–668. [https://doi.org/10.1002/\(SICI\)1096-9837\(199807\)23:7<663::AID-ESP909>3.0.CO;2-6](https://doi.org/10.1002/(SICI)1096-9837(199807)23:7<663::AID-ESP909>3.0.CO;2-6)

- Doerr, S. H., Blake, W. H., Shakesby, R. A., Stagnitti, F., Vuurens, S. H., Humphreys, G. S., Wallbrink, P. (2004). Heating effects on water repellency in Australian eucalypt forest soils and their value in estimating wildfire soil temperatures. *International Journal of Wildland Fire*, 13, 157–163. <https://doi.org/10.1071/WF03051>
- Doerr, S. H., Ferreira, A. J. D., Walsh, R. P. D., Shakesby, R. A., Leighton-Boyce, G., Coelho, C. O. A. (2003). Soil water repellency as a potential parameter in rainfall-runoff modelling: experimental evidence at point to catchment scales from Portugal. *Hydrological Processes*, 17, 363–377. <https://doi.org/10.1002/hyp.1129>
- Doerr, S. H., Santín, C. (2016). Global trends in wildfire and its impacts: Perceptions versus realities in a changing world. *Philosophical Transactions of the Royal Society B: Biological Sciences*, 371. <https://doi.org/10.1098/rstb.2015.0345>
- Doerr, S. H., Shakesby, R. A., Blake, W. H., Chafer, C. J. (2006). Effects of differing wildfire severities on soil wettability and implications for hydrological response, 319, 295–311. <https://doi.org/10.1016/j.jhydrol.2005.06.038>
- Doerr, S. H., Shakesby, R. A., Macdonald, L. H. (2009). Soil Water Repellency: A Key Factor in Post-Fire Erosion? In *Fire effects on soils and restoration strategies* (Vol. 2).
- Doerr, S. H., Shakesby, R. A., Walsh, R. P. D. (2000). Soil water repellency: Its causes, characteristics and hydro-geomorphological significance. *Earth Science Reviews*, 51, 33–65. [https://doi.org/10.1016/S0012-8252\(00\)00011-8](https://doi.org/10.1016/S0012-8252(00)00011-8)
- Doerr, S. H., Thomas, A. D. (2000). The role of soil moisture in controlling water repellency: new evidence from forest soils in Portugal. *Journal of Hydrology*, 231, 134–147. [https://doi.org/10.1016/S0022-1694\(00\)00190-6](https://doi.org/10.1016/S0022-1694(00)00190-6)
- Dunn, P. H., Barro, S. C., Poth, M. (1985). Soil moisture affects survival of microorganisms in heated chaparral soil. *Soil Biology and Biochemistry*, 17, 143–148. [https://doi.org/https://doi.org/10.1016/0038-0717\(85\)90105-1](https://doi.org/https://doi.org/10.1016/0038-0717(85)90105-1)
- EFFIS, 2017. COPERNICUS – Emergency Management Service. https://effis.jrc.ec.europa.eu/static/effis_current_situation/public/index.html
- Falloon, P., Jones, C. D., Ades, M., Paul, K. (2011). Direct soil moisture controls of future global soil carbon changes: An important source of uncertainty. *Global Biogeochemical Cycles*, 25. <https://doi.org/10.1029/2010GB003938>
- Fan, Z., Neff, J. C., Hanan, N. P. (2015). Modeling pulsed soil respiration in an African savanna ecosystem. *Agricultural and Forest Meteorology*, 200, 282–292.

<https://doi.org/10.1016/j.agrformet.2014.10.009>

- Feig, G. T. (2004). *The Effect of Fire Regime on Soil Microbial Community Composition and Activity*. MSc Thesis, University of the Witwatersrand, Johannesburg.
- Fierer, N., Schimel, J. P. (2002). Effects of drying-rewetting frequency on soil carbon and nitrogen transformations. *Soil Biology and Biochemistry*, *34*, 777–787.
- Forbes, M. S., Raison, R. J., Skjemstad, J. O. (2006). Formation, transformation and transport of black carbon (charcoal) in terrestrial and aquatic ecosystems. *Science of the Total Environment*, *370*, 190–206. <https://doi.org/10.1016/j.scitotenv.2006.06.007>
- Fox, D. M., Darboux, F., Carrega, P. (2007). Effects of fire-induced water repellency on soil aggregate stability, splash erosion, and saturated hydraulic conductivity for different size fractions. *Hydrological Processes*, *21*, 2377–2384. <https://doi.org/https://doi.org/10.1002/hyp.6758>
- Franco, C. M. M., Clarke, P. J., Tate, M. E., Oades, J. M. (2000). Hydrophobic properties and chemical characterisation of natural water repellent materials in Australian sands. *Journal of Hydrology*, *231–232*, 47–58. [https://doi.org/https://doi.org/10.1016/S0022-1694\(00\)00182-7](https://doi.org/https://doi.org/10.1016/S0022-1694(00)00182-7)
- Fraser, F. C., Corstanje, R., Deeks, L. K., Harris, J. A., Pawlett, M., Todman, L. C., Whitmore, A. P., Ritz, K. (2016). On the origin of carbon dioxide released from rewetted soils. *Soil Biology and Biochemistry*, *101*, 1-5. <https://doi.org/10.1016/j.soilbio.2016.06.032>
- Friedlingstein, P., O’Sullivan, M., Jones, M. W., Andrew, R. M., Hauck, J., Olsen, A., ... Zaehle, S. (2020). Global Carbon Budget 2020. *Earth System Science Data*, *12*, 3269–3340. <https://doi.org/10.5194/essd-12-3269-2020>
- Fritze, H., Smolander, A., Levula, T., Kitunen, V., Mälkönen, E. (1994). Wood-ash fertilization and fire treatments in a Scots pine forest stand: Effects on the organic layer, microbial biomass, and microbial activity. *Biology and Fertility of Soils*, *17*, 57–63. <https://doi.org/10.1007/BF00418673>
- Ganot, Y., Dragila, M. I., Weisbrod, N. (2014). Impact of thermal convection on CO₂ flux across the earth–atmosphere boundary in high-permeability soils. *Agricultural and Forest Meteorology*, *184*, 12–24. <https://doi.org/https://doi.org/10.1016/j.agrformet.2013.09.001>
- García-Corona, R., Benito, E., de Blas, E., Varela, M. E. (2004). Effects of heating on some soil

physical properties related to its hydrological behaviour in two north-western Spanish soils. *International Journal of Wildland Fire*, 13, 195–199. Retrieved from <https://doi.org/10.1071/WF03068>

García-Oliva, F., Sanford, R. L., Kelly, E. (1999). Effect of burning of tropical deciduous forest soil in Mexico on the microbial degradation of organic matter. *Plant and Soil*, 206, 29–36. <https://doi.org/10.1023/A:1004390202057>

Gazze, S. A., Hallin, I., Quinn, G., Dudley, E., Matthews, G. P., Rees, P., Van Keulen, G., Doerr, S. H., Francis, L. W. (2018). Organic matter identifies the nano-mechanical properties of native soil aggregates. *Nanoscale*, 10, 520–525. <https://doi.org/10.1039/c7nr07070e>

Giovannini, G., Lucchesi, S. (1997). Modifications induced in soil physico-chemical parameters by experimental fires at different intensities. *Soil Science*, 162. Retrieved from https://journals.lww.com/soilsci/Fulltext/1997/07000/modifications__induced_in_soil_physico_chemical.3.aspx

Giovannini, G., Lucchesi, S. (1983). Effect of fire on hydrophobic and cementing substances of soil aggregates. *Soil Science*, 136. Retrieved from https://journals.lww.com/soilsci/Fulltext/1983/10000/effect_of_fire_on_hydrophobic_and_cementing.6.aspx

Giovannini, G., Lucchesi, S., Giachetti, M. (1987). The natural evolution of a burned soil: a three-year investigation. *Soil Science*, 143. Retrieved from https://journals.lww.com/soilsci/Fulltext/1987/03000/the_natural_evolution_of_a_burned_soil__a.9.aspx

Goebel, M. O., Bachmann, J., Reichstein, M., Janssens, I. A., Guggenberger, G. (2011). Soil water repellency and its implications for organic matter decomposition - is there a link to extreme climatic events? *Global Change Biology*, 17, 2640–2656. <https://doi.org/10.1111/j.1365-2486.2011.02414.x>

Goebel, M. O., Bachmann, J., Woche, S. K., Fischer, W. R. (2005). Soil wettability, aggregate stability, and the decomposition of soil organic matter. *Geoderma*, 128, 80–93. <https://doi.org/10.1016/j.geoderma.2004.12.016>

Goebel, M. O., Woche, S. K., Bachmann, J. (2012). Quantitative analysis of liquid penetration kinetics and slaking of aggregates as related to solid–liquid interfacial properties. *Journal of Hydrology*, 442–443, 63–74. <https://doi.org/10.1016/J.JHYDROL.2012.03.039>

Goebel, M. O., Woche, S. K., Bachmann, J., Lamparter, A., Fischer, W. R. (2007). Significance of

- wettability-induced changes in microscopic water distribution for soil organic matter decomposition. *Soil Science Society of America Journal*, 71, 1593–1599. <https://doi.org/doi:10.2136/sssaj2006.0192>
- Gómez-Rey, M. X., Madeira, M., Coutinho, J. (2012). Wood ash effects on nutrient dynamics and soil properties under Mediterranean climate. *Annals of Forest Science*, 69, 569–579. <https://doi.org/10.1007/s13595-011-0175-y>
- González-Pérez, J. A., González-Vila, F. J., Almendros, G., Knicker, H. (2004). The effect of fire on soil organic matter - A review. *Environment International*. <https://doi.org/10.1016/j.envint.2004.02.003>
- Göransson, H., Godbold, D. L., Jones, D. L., Rousk, J. (2013). Bacterial growth and respiration responses upon rewetting dry forest soils: Impact of drought-legacy. *Soil Biology and Biochemistry*, 57, 477–486. <https://doi.org/10.1016/j.soilbio.2012.08.031>
- Hageman, P. L. (2007). *U.S. Geological Survey Field Leach Test for Assessing Water Reactivity and Leaching Potential of Mine Wastes, Soils, and Other Geologic and Environmental Materials. U.S. Geological Survey Techniques and Methods*. Book 5, Chap. D3, 14 p. <https://doi.org/10.3133/tm5D3>
- Hamdi, S., Moyano, F., Sall, S., Bernoux, M., Chevallier, T. (2013). Synthesis analysis of the temperature sensitivity of soil respiration from laboratory studies in relation to incubation methods and soil conditions. *Soil Biology and Biochemistry*, 58, 115–126. <https://doi.org/10.1016/j.soilbio.2012.11.012>
- Hamman, S. T., Burke, I. C., Knapp, E. E. (2008). Forest Ecology and Management Soil nutrients and microbial activity after early and late season prescribed burns in a Sierra Nevada mixed conifer forest, 256, 367–374. <https://doi.org/10.1016/j.foreco.2008.04.030>
- Hart, S. C., DeLuca, T. H., Newman, G. S., MacKenzie, M. D., Boyle, S. I. (2005). Post-fire vegetative dynamics as drivers of microbial community structure and function in forest soils. *Forest Ecology and Management*, 220, 166–184. <https://doi.org/https://doi.org/10.1016/j.foreco.2005.08.012>
- Hartley, I. P., Hopkins, D. W., Garnett, M. H., Sommerkorn, M., Wookey, P. A. (2008). Soil microbial respiration in arctic soil does not acclimate to temperature. *Ecology Letters*, 11, 1092–1100. <https://doi.org/10.1111/j.1461-0248.2008.01223.x>

- Heaton, L., Fullen, M. A., Bhattacharyya, R. (2016). Critical Analysis of the van Bemmelen Conversion Factor used to Convert Soil Organic Matter Data to Soil Organic Carbon Data: Comparative Analyses in a UK Loamy Sand Soil. *Espaço Aberto*, 6, 35–44. <https://doi.org/10.36403/espacoaberto.2016.5244>
- Hendrickx, J. M. H., Flury, M. (2001). Uniform and preferential flow mechanisms in the vadose zone. In *Conceptual models of flow and transport in the fractured vadose zone*. (pp. 149–187). Washington, DC: Natl.Acad.Press.
- Hilscher, A., Heister, K., Siewert, C., Knicker, H. (2009). Mineralisation and structural changes during the initial phase of microbial degradation of pyrogenic plant residues in soil. *Organic Geochemistry*, 40, 332–342. <https://doi.org/10.1016/j.orggeochem.2008.12.004>
- Hogg, E. H., Lieffers, V. J., Wein, R. W. (2011). Potential Carbon Losses From Peat Profiles: Effects of Temperature, Drought Cycles, and Fire. *Ecological Society of America*, 2, 298–306. <https://doi.org/10.2307/1941863>
- Holden, S. R., Berhe, A. A., Treseder, K. K. (2015). Decreases in soil moisture and organic matter quality suppress microbial decomposition following a boreal forest fire. *Soil Biology and Biochemistry*, 87, 1–9. <https://doi.org/https://doi.org/10.1016/j.soilbio.2015.04.005>
- Horwath, W. R. (2008). Carbon cycling and formation of soil organic matter. In *Encyclopedia of Earth Sciences Series* (Third Edit, pp. 91–97). Elsevier Inc. <https://doi.org/10.1016/B978-0-08-047514-1.50016-0>
- Houghton, R. A., House, J. I., Pongratz, J., van der Werf, G. R., DeFries, R. S., Hansen, M. C., Ramankutty, N. (2012). Carbon emissions from land use and land-cover change. *Biogeosciences*, 9, 5125–5142. <https://doi.org/10.5194/bg-9-5125-2012>
- Huffman, E. L., MacDonald, L. H., Stednick, J. D. (2001). Strength and persistence of fire-induced soil hydrophobicity under ponderosa and lodgepole pine, Colorado Front Range. *Hydrological Processes*, 15, 2877–2892. <https://doi.org/https://doi.org/10.1002/hyp.379>
- Huxman, T., Snyder, K., Tissue, D., Leffler, A. J., Ogle, K., Pockman, W., Sandquist, D. R., Potts, D. L., Schwinning, S. (2004). Precipitation pulses and carbon fluxes in semiarid and arid ecosystems. *Oecologia*, 141, 254–268. <https://doi.org/10.1007/s00442-004-1682-4>
- Inglima, I., Alberti, G., Bertolini, T., Vaccari, F. P., Gioli, B., Miglietta, F., Cotrufo, M. F., Peressotti, A. (2009). Precipitation pulses enhance respiration of Mediterranean ecosystems: the balance between organic and inorganic components of increased soil

- CO₂ efflux. *Global Change Biology*, 15, 1289–1301. <https://doi.org/10.1111/j.1365-2486.2008.01793.x>
- Irvine, J., Law, B. E., Hibbard, K. A. (2007). Postfire carbon pools and fluxes in semiarid ponderosa pine in Central Oregon. *Global Change Biology*, 13, 1748–1760. <https://doi.org/10.1111/j.1365-2486.2007.01368.x>
- IUSS Working Group WRB. 2015. World Reference Base for Soil Resources 2014, update 2015 International soil classification system for naming soils and creating legends for soil maps. World Soil Resources Reports No. 106. FAO, Rome.
- IUSS Working Group WRB 2016. World Reference Base for Soil Resources 2006. In: World Soil Resources Reports No. 103. FAO, Rome.
- Janssens, I. A., Freibauer, A., Ciais, P., Smith, P., Nabuurs, G. J., Folberth, G., Dolman, A. J. (2003). Europe's Terrestrial Biosphere Absorbs 7 to 12% of European Anthropogenic CO₂ Emissions. *Science*, 300(5625), 1538 LP – 1542. <https://doi.org/10.1126/science.1083592>
- Jansson, J. K., Hofmockel, K. S. (2020). Soil microbiomes and climate change. *Nature Reviews Microbiology*, 18, 35–46. <https://doi.org/10.1038/s41579-019-0265-7>
- Jarvis, P., Rey, A., Petsikos, C., Wingate, L., Rayment, M., Pereira, J., Banza, J., David, F., Miglietta, F., Borghetti, M., Manca, F., Valentini, R. (2007). Drying and wetting of Mediterranean soils stimulates decomposition and carbon dioxide emission: the “Birch effect.” *Tree Physiology*, 27, 929–940. <https://doi.org/10.1093/treephys/27.7.929>
- Jensen, M., Michelsen, A., Gashaw, M. (2001). Responses in plant, soil inorganic and microbial nutrient pools to experimental fire, ash and biomass addition in a woodland savanna. *Oecologia*, 128, 85–93. <https://doi.org/10.1007/s004420000627>
- Jones, D. L., Murphy, D. V., Khalid, M., Ahmad, W., Edwards-Jones, G., DeLuca, T. H. (2011). Short-term biochar-induced increase in soil CO₂ release is both biotically and abiotically mediated. *Soil Biology and Biochemistry*, 43, 1723–1731. <https://doi.org/10.1016/j.soilbio.2011.04.018>
- Jones, M. W., Santín, C., van der Werf, G. R., Doerr, S. H. (2019). Global fire emissions buffered by the production of pyrogenic carbon. *Nature Geoscience*, 12, 742–747. <https://doi.org/10.1038/s41561-019-0403-x>
- Jordán, A., González, F. A., Zavala, L. M. (2010). Re-establishment of soil water repellency after

- destruction by intense burning in a Mediterranean heathland (SW Spain). *Hydrological Processes*, 24, 736–748. <https://doi.org/https://doi.org/10.1002/hyp.7519>
- Jordán, A., Zavala, L. M., Mataix-Solera, J., Nava, A. L., Alanís, N. (2011). Effect of fire severity on water repellency and aggregate stability on Mexican volcanic soils. *CATENA*, 84, 136–147. <https://doi.org/https://doi.org/10.1016/j.catena.2010.10.007>
- Karhu, K., Auffret, M. D., Dungait, J. A. J., Hopkins, D. W., Prosser, J. I., Singh, B. K., Hartley, I. P. (2014). Temperature sensitivity of soil respiration rates enhanced by microbial community response. *Nature*, 513, 81–84. <https://doi.org/10.1038/nature13604>
- Kim, D. G., Vargas, R., Bond-Lamberty, B., Turetsky, M. R. (2012). Effects of soil rewetting and thawing on soil gas fluxes: a review of current literature and suggestions for future research. *Biogeosciences*, 9, 2459–2483. <https://doi.org/10.5194/bg-9-2459-2012>
- King, A. W., Hayes, D. J., Huntzinger, D. N., West, T. O., Post, W. M. (2012). North American carbon dioxide sources and sinks: Magnitude, attribution, and uncertainty. *Frontiers in Ecology and the Environment*, 10, 512–519. <https://doi.org/10.1890/120066>
- Kirschbaum, M. U. F. (2010). The temperature dependence of organic matter decomposition: Seasonal temperature variations turn a sharp short-term temperature response into a more moderate annually averaged response. *Global Change Biology*, 16, 2117–2129. <https://doi.org/10.1111/j.1365-2486.2009.02093.x>
- Kutiel, P., Naveh, Z. (1987). Soil properties beneath *Pinus halepensis* and *Quercus calliprinos* trees on burned and unburned mixed forest on Mt. Carmel, Israel. *Forest Ecology and Management*, 20, 11–24. [https://doi.org/10.1016/0378-1127\(87\)90147-2](https://doi.org/10.1016/0378-1127(87)90147-2)
- Kutílek, M. (2004). Soil hydraulic properties as related to soil structure. *Soil and Tillage Research*, 79, 175–184. <https://doi.org/10.1016/j.still.2004.07.006>
- Kuzyakov, Y. (2006). Sources of CO₂ efflux from soil and review of partitioning methods. *Soil Biology and Biochemistry*, 38, 425–448. <https://doi.org/10.1016/j.soilbio.2005.08.020>
- Kuzyakov, Yakov, Subbotina, I., Chen, H., Bogomolova, I., Xu, X. (2009). Black carbon decomposition and incorporation into soil microbial biomass estimated by ¹⁴C labeling. *Soil Biology and Biochemistry*, 41, 210–219. <https://doi.org/10.1016/j.soilbio.2008.10.016>
- Lado-Monserrat, L., Lull, C., Bautista, I., Lidón, A., Herrera, R. (2014). Soil moisture increment as a controlling variable of the “Birch effect”. Interactions with the pre-wetting soil

- moisture and litter addition. *Plant and Soil*, 379, 21–34. <https://doi.org/10.1007/s11104-014-2037-5>
- Lal, R. (2003). Global Potential of Soil Carbon Sequestration to Mitigate the Greenhouse Effect. *Critical Reviews in Plant Sciences*, 22, 151–184. <https://doi.org/10.1080/713610854>
- Lal, Rattan. (2008). Soil carbon stocks under present and future climate with specific reference to European ecoregions. *Nutrient Cycling in Agroecosystems*, 81, 113–127. <https://doi.org/10.1007/s10705-007-9147-x>
- Lal, Rattan. (2015). Restoring Soil Quality to Mitigate Soil Degradation. *Sustainability*, 7, 5875–5895. <https://doi.org/10.3390/su7055875>
- Lamparter, A., Bachmann, J., Goebel, M.-O., Woche, S. K. (2009). Carbon mineralization in soil: Impact of wetting–drying, aggregation and water repellency. *Geoderma*, 150, 324–333. <https://doi.org/10.1016/j.geoderma.2009.02.014>
- Lajtha, K., Bailey, V., McFarlane, K., Paustian, K., Bachelet, D., Abramoff, R., ... Zhu, Z. (2018). *Chapter 12: Soils. Second state of the carbon cycle report*. U.S. Global Change Research Program. Retrieved from <https://doi.org/10.7930/SOCCR2.2018.Ch12>
- Leighton-Boyce, G., Doerr, S. H., Shakesby, R. A., Walsh, R. P. D. (2007). Quantifying the impact of soil water repellency on overland flow generation and erosion: a new approach using rainfall simulation and wetting agent on in situ soil. *Hydrological Processes*, 21, 2337–2345. <https://doi.org/10.1002/hyp.6744>
- Leon, E., Vargas, R., Bullock, S., Lopez, E., Rodrigo, A., La, N., Jr, S. (2014). Hot spots, hot moments, and spatio-temporal controls on soil CO₂ efflux in a water-limited ecosystem. *Soil Biology and Biochemistry*, 77, 12–21. <https://doi.org/10.1016/j.soilbio.2014.05.029>
- Lewis, C. R. (2019). *The effect of rewetting with surfactant (Aquatrols®) on soil microbial communities*. Swansea University, BSc dissertation thesis.
- Liu, X., Wan, S., Su, B., Hui, D., Luo, Y. (2002). Response of soil CO₂ efflux to water manipulation in a tallgrass prairie ecosystem. *Plant and Soil*, 240, 213–223. <https://doi.org/https://doi.org/10.1023/A:1015744126533>
- Liu, Y., He, N., Wen, X., Xu, L., Sun, X., Yu, G., Schipper, L. A. (2018). The optimum temperature of soil microbial respiration: Patterns and controls. *Soil Biology and Biochemistry*, 121, 35–42. <https://doi.org/10.1016/j.soilbio.2018.02.019>

- Liu, Z., Rahav, M., Wallach, R. (2019). Spatial variation of soil water repellency in a commercial orchard irrigated with treated wastewater. *Geoderma*, 333, 214–224. <https://doi.org/10.1016/j.geoderma.2018.07.021>
- Longdoz, B., Yernaux, M., Aubinet, M. (2000). Soil CO₂ efflux measurements in mixed forest: impact of chamber disturbance, spatial variability and seasonal evolution. *Global Change Biology*, 6, 907–917. <https://doi.org/10.1046/j.1365-2486.2000.00369.x>
- Lozano, E., Jiménez-Pinilla, P., Mataix-Solera, J., Arcenegui, V., Mataix-Beneyto, J. (2016). Sensitivity of glomalin-related soil protein to wildfires: Immediate and medium-term changes. *Science of The Total Environment*, 572, 1238–1243. <https://doi.org/https://doi.org/10.1016/j.scitotenv.2015.08.071>
- Luo, Y., Wan, S., Hui, D., Wallace, L. L. (2001). Acclimatization of soil respiration to warming in a tall grass prairie. *Nature*, 413, 622–625. <https://doi.org/10.1038/35098065>
- Maestrini, B., Abiven, S., Singh, N., Bird, J., Torn, M. S., Schmidt, M. W. I. (2014). Carbon losses from pyrolysed and original wood in a forest soil under natural and increased N deposition. *Biogeosciences*, 11, 5199–5213. <https://doi.org/10.5194/bg-11-5199-2014>
- Maier, M., Schack-Kirchner, H., Aubinet, M., Goffin, S., Longdoz, B., & Parent, F. (2012). Turbulence Effect on Gas Transport in Three Contrasting Forest Soils. *Soil Science Society of America Journal*, 76, 1518. <https://doi.org/10.2136/sssaj2011.0376>
- Maier, M., Schack-Kirchner, H., Hildebrand, E. E., Holst, J. (2010). Pore-space CO₂ dynamics in a deep, well-aerated soil. *European Journal of Soil Science*, 61, 877–887. <https://doi.org/10.1111/j.1365-2389.2010.01287.x>
- Maier, M., Schack-Kirchner, H., Hildebrand, E. E., Schindler, D. (2011). Soil CO₂ efflux vs. soil respiration: implications for flux models. *Agricultural and Forest Meteorology*, 151, 1723–1730. <https://doi.org/10.1016/j.agrformet.2011.07.006>
- Malvar, M. C., Prats, S. A., Nunes, J. P., Keizer, J. J. (2011). Post-fire overland flow generation and inter-rill erosion under simulated rainfall in two eucalypt stands in north-central Portugal. *Environmental Research*, 111, 222–236. <https://doi.org/10.1016/j.envres.2010.09.003>
- Marañón-Jiménez, S., Castro, J., Kowalski, A. S., Serrano-Ortiz, P., Reverter, B. R., Sánchez-Cañete, E. P., Zamora, R. (2011). Post-fire soil respiration in relation to burnt wood management in a Mediterranean mountain ecosystem. *Forest Ecology and Management*,

261, 1436–1447. <https://doi.org/10.1016/j.foreco.2011.01.030>

- Martin, D. A., Moody, J. A. (2001). Comparison of soil infiltration rates in burned and unburned mountainous watersheds. *Hydrological Processes*, 15, 2893–2903. <https://doi.org/https://doi.org/10.1002/hyp.380>
- Massman, W. J., Frank, J. M., Reisch, N. B. (2008). Long-term impacts of prescribed burns on soil thermal conductivity and soil heating at a Colorado Rocky Mountain site: a data/model fusion study. *International Journal of Wildland Fire*, 17, 131–146. Retrieved from <https://doi.org/10.1071/WF06118>
- Masson-Demotte, V., Zhai, P., Pörtner, H. O., Roberts, D., Skea, J., Shukla, P. R., Pirani, A., Moufouma-Okia, C., Péan, C., Pidcock, R., Connors, S., Matthews, J. B. R., Chen, T., Zhou, X., Gomis, M. I., Lonnoy, E., Maycock, T., Tignor, M., Waterfield, T. (2018). *Global warming of 1.5 °C. An IPCC Special Report on the impacts of global warming of 1.5 °C above pre-industrial levels and related global greenhouse gas emission pathways, in the context of strengthening the global response to the threat of climate change*. Retrieved from <https://www.ipcc.ch/sr15/>
- Mataix-Solera, J., Cerdà, A., Arcenegui, V., Jordán, A., Zavala, L. M. (2011). Fire effects on soil aggregation: A review, *Earth-Science Review*, 109, 44–60. <https://doi.org/10.1016/j.earscirev.2011.08.002>
- Mataix-Solera, J., Doerr, S. H. (2004). Hydrophobicity and aggregate stability in calcareous topsoils from fire-affected pine forests in southeastern Spain. *Geoderma*, 118, 77–88. [https://doi.org/https://doi.org/10.1016/S0016-7061\(03\)00185-X](https://doi.org/https://doi.org/10.1016/S0016-7061(03)00185-X)
- Mataix-Solera, J., Gómez, I., Navarro-Pedreño, J., Guerrero, C., Moral, R. (2002). Soil organic matter and aggregates affected by wildfire in a *Pinus halepensis* forest in a Mediterranean environment. *International Journal of Wildland Fire*, 11, 107–114. Retrieved from <https://doi.org/10.1071/WF02020>
- Mataix-Solera, J., Guerrero, C., Garcia-Orenes, F., Barcenas, G. M., Torres, M. P. (2009). Forest fire effects on soil microbiology. In *Fire effects on soils and restoration strategies*. <https://doi.org/10.1201/9781439843338-c5>
- Meigs, G. W., Donato, D. C., Campbell, J. L., Jonathan, G., Law, B. E. (2009). Forest fire impacts on carbon uptake, storage and emission: the role of burn severity in the Eastern Cascades, Oregon. *Ecosystems*, 12, 1246–1267. <https://doi.org/10.1007/s10021-009-9285-x>

- Meisner, A., Bååth, E., Rousk, J. (2013). Microbial growth responses upon rewetting soil dried for four days or one year. *Soil Biology and Biochemistry*, *66*, 188–192. <https://doi.org/10.1016/j.soilbio.2013.07.014>
- Meisner, A., Leizeaga, A., Rousk, J., Bååth, E. (2017). Partial drying accelerates bacterial growth recovery to rewetting. *Soil Biology and Biochemistry*, *112*, 269–276. <https://doi.org/10.1016/j.soilbio.2017.05.016>
- Meisner, A., Rousk, J., Bååth, E. (2015). Prolonged drought changes the bacterial growth response to rewetting. *Soil Biology and Biochemistry*, *88*, 314–322. <https://doi.org/10.1016/j.soilbio.2015.06.002>
- Melillo, J. M., Steudler, P. A., Aber, J. D., Newkirk, K., Lux, H., Bowles, F. P., Morrisseau, S. (2002). Soil warming and carbon-cycle feedbacks to the climate system. *Science*, *298*, 2173–2176. <https://doi.org/10.1126/science.1074153>
- Merino, A., Chávez-Vergara, B., Salgado, J., Fonturbel, M. T., García-Oliva, F., Vega, J. A. (2015). Variability in the composition of charred litter generated by wildfire in different ecosystems. *Catena*, *133*, 52–63. <https://doi.org/10.1016/j.catena.2015.04.016>
- Miesel, J. R., Hockaday, W. C., Kolka, R. K., Townsend, P. A. (2015). Soil organic matter composition and quality across fire severity gradients in coniferous and deciduous forests of the southern boreal region. *Journal of Geophysical Research: Biogeosciences*, *120*, 1124–1141. <https://doi.org/10.1002/2015JG002959>
- Miller, A. E., Schimel, J. P., Meixner, T., Sickman, J. O., Melack, J. M. (2005). Episodic rewetting enhances carbon and nitrogen release from chaparral soils. *Soil Biology and Biochemistry*, *37*, 2195–2204. <https://doi.org/10.1016/j.soilbio.2005.03.021>
- Moody, J. A., Shakesby, R. A., Robichaud, P. R., Cannon, S. H., Martin, D. A. (2013). Current research issues related to post-wildfire runoff and erosion processes. *Earth Science Reviews*, *122*, 10–37. <https://doi.org/10.1016/j.earscirev.2013.03.004>
- Moore, P. A., Lukenbach, M. C., Kettridge, N., Petrone, R. M., Devito, K. J., Waddington, J. M. (2017). Peatland water repellency: Importance of soil water content, moss species, and burn severity. *Journal of Hydrology*, *554*, 656–665. <https://doi.org/10.1016/j.jhydrol.2017.09.036>
- Moyano, F. E., Manzoni, S., Chenu, C. (2013). Responses of soil heterotrophic respiration to moisture availability: an exploration of processes and models. *Soil Biology and*

Biochemistry, 59, 72–85. <https://doi.org/10.1016/j.soilbio.2013.01.002>

- Muhr, J., Borken, W. (2009). Delayed recovery of soil respiration after wetting of dry soil further reduces C losses from a Norway spruce forest soil. *Journal of Geophysical Research*, 114, G04023. <https://doi.org/10.1029/2009JG000998>
- Muhr, J., Franke, J., Borken, W. (2010). Drying–rewetting events reduce C and N losses from a Norway spruce forest floor. *Soil Biology and Biochemistry*, 42, 1303–1312. <https://doi.org/10.1016/j.soilbio.2010.03.024>
- Muhr, J., Goldberg, S. D., Borken, W., Gebauer, G. (2008). Repeated drying-rewetting cycles and their effects on the emission of CO₂, N₂O, NO, and CH₄ in a forest soil. In *Journal of Plant Nutrition and Soil Science*, 171, 719–728. <https://doi.org/10.1002/jpln.200700302>
- Munson, S. M., Benton, T. J., Lauenroth, W. K., Burke, I. C. (2010). Soil carbon flux following pulse precipitation events in the shortgrass steppe. *Ecological Research*, 25, 205–211. <https://doi.org/10.1007/s11284-009-0651-0>
- Muñoz-Rojas, M., Erickson, T. E., Martini, D., Dixon, K. W., Merritt, D. J. (2016). Soil physicochemical and microbiological indicators of short, medium and long term post-fire recovery in semi-arid ecosystems. *Ecological Indicators*, 63, 14–22. <https://doi.org/10.1016/j.ecolind.2015.11.038>
- Müller, K., Deurer, M., Kawamoto, K., Kuroda, T., Subedi, S., Hiradate, S., Komatsu, T., Clothier, B. E. (2014). A new method to quantify how water repellency compromises soils' filtering function. *European Journal of Soil Science*, 65, 348–359. <https://doi.org/10.1111/ejss.12136>
- Naisse, C., Girardin, C., Davasse, B., Chabbi, A., Rumpel, C. (2015). Effect of biochar addition on C mineralisation and soil organic matter priming in two subsoil horizons. *Journal of Soils and Sediments*, 15, 825–832. <https://doi.org/10.1007/s11368-014-1002-5>
- Neary, D. G., Klopatek, C. C., DeBano, L. F., Ffolliott, P. F. (1999). Fire effects on belowground sustainability: a review and synthesis. *Forest Ecology and Management*, 122, 51–71. [https://doi.org/https://doi.org/10.1016/S0378-1127\(99\)00032-8](https://doi.org/https://doi.org/10.1016/S0378-1127(99)00032-8)
- Norman, J. M., Garcia, R., Verma, S. B. (1992). Soil surface CO₂ fluxes and the carbon budget of a grassland. *Journal of Geophysical Research: Atmospheres*, 97, 18845–18853. <https://doi.org/10.1029/92JD01348>

- Novara, A., Gristina, L., Bodi, M. B., Cerdà, A. (2011). The impact of fire on redistribution of soil organic matter on a Mediterranean hillslope under maquia vegetation type. *Land Degradation and Development*, 22, 530–536. <https://doi.org/10.1002/ldr.1027>
- Novara, A., Gristina, L., Rühl, J., Pasta, S., D'Angelo, G., La Mantia, T., Pereira, P. (2013). Grassland fire effect on soil organic carbon reservoirs in a semiarid environment. *Solid Earth*, 4, 381–385. <https://doi.org/10.5194/se-4-381-2013>
- Nyman, P., Sheridan, G., Smith, H., Lane, P. (2013). Modeling the effects of surface storage, macropore flow and water repellency on infiltration after wildfire. *Journal of Hydrology*, 513, 301–313. <https://doi.org/10.1016/J.JHYDROL.2014.02.044>
- Oertel, C., Matschullat, J., Zurba, K., Zimmermann, F., Erasmi, S. (2016). Greenhouse gas emissions from soils. A review. *Chemie Der Erde*, 76, 327–352. <https://doi.org/10.1016/j.chemer.2016.04.002>
- Or, D., Smets, B. F., Wraith, J. M., Dechesne, A., Friedman, S. P. (2007). Physical constraints affecting bacterial habitats and activity in unsaturated porous media - a review. *Advances in Water Resources*, 30, 1505–1527. <https://doi.org/10.1016/j.advwatres.2006.05.025>
- Osborn, J. F., Pelishek, R. E., Krammes, J. S., Letey, J. (1964). Soil Wettability as a Factor in Erodibility. *Soil Science Society of America Journal*, 28(2), 294–295. <https://doi.org/https://doi.org/10.2136/sssaj1964.03615995002800020050x>
- Öztürk, M., Hakeem, K. R., Faridah-Hanum, I., Efe, R. (2015). *Climate change impacts on high-altitude ecosystems*. Springer.
- Qi, Y., & Xu, M. (2001). Separating the effects of moisture and temperature on soil CO₂ efflux in a coniferous forest in the Sierra Nevada mountains. *Plant and Soil*, 237, 15–23. <https://doi.org/10.1023/A:1013368800287>
- Parker, L. W., Miller, J., Steinberger, Y., Whitford, W. G. (1983). Soil respiration in a chihuahuan desert rangeland. *Soil Biology and Biochemistry*, 15, 303–309. [https://doi.org/https://doi.org/10.1016/0038-0717\(83\)90075-5](https://doi.org/https://doi.org/10.1016/0038-0717(83)90075-5)
- Pellegrini, A. F. A., Ahlström, A., Hobbie, S. E., Reich, P. B., Nieradzik, L. P., Staver, A. C., Jackson, R. B. (2018). Fire frequency drives decadal changes in soil carbon and nitrogen and ecosystem productivity. *Nature*, 553, 194–198. <https://doi.org/10.1038/nature24668>
- Pereira, P., Úbeda, X., Martin, D. A. (2012). Fire severity effects on ash chemical composition

and water-extractable elements. *Geoderma*, 191, 105–114.
<https://doi.org/10.1016/j.geoderma.2012.02.005>

Perkiömäki, J., Kiikkilä, O., Moilanen, M., Issakainen, J., Tervahauta, A., Fritze, H. (2003). Cadmium-containing wood ash in a pine forest: Effects on humus microflora and cadmium concentrations in mushrooms, berries, and needles. *Canadian Journal of Forest Research*, 33, 2443–2451. <https://doi.org/10.1139/x03-169>

Pietikäinen, J., Pettersson, M., Bååth, E. (2005). Comparison of temperature effects on soil respiration and bacterial and fungal growth rates. *FEMS Microbiology Ecology*, 52, 49–58. <https://doi.org/10.1016/j.femsec.2004.10.002>

Pinto, A. S., Bustamante, M. M. C., Kisselle, K., Burke, R., Zepp, R., Viana, L. T., Varella, R. F., Molina, M. (2002). Soil emissions of N₂O, NO, and CO₂ in Brazilian Savannas: Effects of vegetation type, seasonality, and prescribed fires. *Journal of Geophysical Research*, 107, 1–9. <https://doi.org/10.1029/2001jd000342>

Placella, S. A., Brodie, E. L., Firestone, M. K. (2012). Rainfall-induced carbon dioxide pulses result from sequential resuscitation of phylogenetically clustered microbial groups. *Proceedings of the National Academy of Sciences of the United States of America*, 109, 10931–10936. <https://doi.org/10.1073/pnas.1204306109>

Pressler, Y., Moore, J. C., Cotrufo, M. F. (2019). Belowground community responses to fire: meta-analysis reveals contrasting responses of soil microorganisms and mesofauna. *Oikos*, 128, 309–327. <https://doi.org/10.1111/oik.05738>

Prieto-Fernández, A., Acea, M. J., Carballas, T. (1998). Soil microbial and extractable C and N after wildfire. *Biology and Fertility of Soils*, 27, 132–142. <https://doi.org/10.1007/s003740050411>

Raison, R. J. (1979). Modification of the soil environment by vegetation fires, with particular reference to nitrogen transformations: A review. *Plant and Soil*, 51, 73–108. <https://doi.org/10.1007/BF02205929>

Raison, R. J., McGarity, J. W. (1980). Effects of ash, heat, and the ash-heat interaction on biological activities in two contrasting soils - I. Respiration rate. *Plant and Soil*, 55, 363–376. <https://doi.org/10.1007/BF02182697>

Ravikovitch, P. I., Bogan, B. W., Neimark, A. V. (2005). Nitrogen and carbon dioxide adsorption by soils. *Environmental Science and Technology*, 39, 4990–4995.

<https://doi.org/10.1021/es048307b>

- Redeker, K. R., Baird, A. J., Teh, Y. A. (2015). Quantifying wind and pressure effects on trace gas fluxes across the soil-atmosphere interface. *Biogeosciences*, *12*, 7423–7434. <https://doi.org/10.5194/bg-12-7423-2015>
- Reichstein, M., Bahn, M., Ciais, P., Frank, D., Mahecha, M. D., Seneviratne, S. I., Wattenbach, M. (2013). Climate extremes and the carbon cycle. *Nature*, *500*, 287–295. <https://doi.org/10.1038/nature12350>
- Rey, A. (2015). Mind the gap: non-biological processes contributing to soil CO₂ efflux. *Global Change Biology*, *21*, 1752–1761. <https://doi.org/10.1111/gcb.12821>
- Rey, A., Beilelli-Marchesini, L., Were, A., Serrano-ortiz, P., Etiope, G., Papale, D., Pegoraro, E. (2012). Wind as a main driver of the net ecosystem carbon balance of a semiarid Mediterranean steppe in the South East of Spain. *Global Change Biology*, *18*, 539–554. <https://doi.org/10.1111/j.1365-2486.2011.02534.x>
- Rey, A., Oyonarte, C., Morán-López, T., Raimundo, J., Pegoraro, E. (2017). Changes in soil moisture predict soil carbon losses upon rewetting in a perennial semiarid steppe in SE Spain. *Geoderma*, *287*, 135–146. <https://doi.org/10.1016/j.geoderma.2016.06.025>
- Rhoades, C. C., Nunes, J. P., Silins, U., Doerr, S. H. (2019). The influence of wildfire on water quality and watershed processes: New insights and remaining challenges. *International Journal of Wildland Fire*, *28*, 721–725. https://doi.org/10.1071/WFv28n10_FO
- Ritsema, C. J., Dekker, L. W. (1994). How water moves in a water repellent sandy soil: 2. Dynamics of fingered flow. *Water Resour. Res.*, *30*, 2519–2531.
- Ritsema, C. J., Dekker, L. W. (2000). Preferential flow in water repellent sandy soils: principles and modeling implications. *Journal of Hydrology*, *231–232*, 308–319. [https://doi.org/10.1016/S0022-1694\(00\)00203-1](https://doi.org/10.1016/S0022-1694(00)00203-1)
- Riveros-Iregui, D. A., McGlynn, B. L., Epstein, H. E., Welsch, D. L. (2008). Interpretation and evaluation of combined measurement techniques for soil CO₂ efflux: Discrete surface chambers and continuous soil CO₂ concentration probes. *Journal of Geophysical Research*, *113*, G04027. <https://doi.org/10.1029/2008JG000811>
- Robinson, D. A., Hopmans, J. W., Filipovic, V., van der Ploeg, M., Lebron, I., Jones, S. B., Reinsch, S., Jarvis, N., Tuller, M. (2019). Global environmental changes impact soil hydraulic functions through biophysical feedbacks. *Global Change Biology*, *25*, 1895–

1904. <https://doi.org/10.1111/gcb.14626>

- Robinson, D. A., Jones, S. B., Lebron, I., Reinsch, S., Domínguez, M. T., Smith, A. R., Emmett, B. A. (2016). Experimental evidence for drought induced alternative stable states of soil moisture. *Scientific Reports*, 6, 20018. <https://doi.org/10.1038/srep20018>
- Rochette, P., & Hutchinson, G. L. (2005). Measurement of Soil Respiration in situ: Chamber Techniques. Retrieved from <http://digitalcommons.unl.edu/usdaarsfacpub>
- Rogers, B. M., Balch, J. K., Goetz, S. J., Lehmann, C. E. R., Turetsky, M. (2020). Focus on changing fire regimes: interactions with climate, ecosystems, and society. *Environmental Research Letters*, 15, 30201. <https://doi.org/10.1088/1748-9326/ab6d3a>
- Rutledge, S., Campbell, D. I., Baldocchi, D., Schipper, L. A. (2010). Photodegradation leads to increased carbon dioxide losses from terrestrial organic matter. *Global Change Biology*, 16, 3065–3074. <https://doi.org/10.1111/j.1365-2486.2009.02149.x>
- Salazar, A., Sulman, B. N., Dukes, J. S. (2018). Microbial dormancy promotes microbial biomass and respiration across pulses of drying-wetting stress. *Soil Biology and Biochemistry*, 116, 237–244. <https://doi.org/10.1016/j.soilbio.2017.10.017>
- Sánchez-García, C., Santín, C., Doerr, S. H., Strydom, T., Urbanek, E. (*In submission*). Wildland fire ash enhances short-term CO₂ flux from soil in a Southern African savannah.
- Sánchez-García, C., Doerr, S. H., Urbanek, E. (2020a). The effect of water repellency on the short-term release of CO₂ upon soil wetting. *Geoderma*, 375, 114481. <https://doi.org/10.1016/j.geoderma.2020.114481>
- Sánchez-García, C., Oliveira, B. R. F., Keizer, J. J., Doerr, S. H., Urbanek, E. (2020b). Water repellency reduces soil CO₂ efflux upon rewetting. *Science of The Total Environment*, 708, 135014. <https://doi.org/10.1016/J.SCITOTENV.2019.135014>
- Santín, C., Doerr, S. H. (2016). Fire effects on soils: The human dimension. *Philosophical Transactions of the Royal Society B: Biological Sciences*, 371, 28–34. <https://doi.org/10.1098/rstb.2015.0171>
- Santín, C., Doerr, S. (2018). Chapter 7 - Carbon. In *Fire effects on soil properties* (pp. 115–128). CSIRO Publishing.
- Santín, C., Doerr, S. H., Kane, E. S., Masiello, C. A., Ohlson, M., de la Rosa, J. M., Dittmar, T. (2016). Towards a global assessment of pyrogenic carbon from vegetation fires. *Global Change Biology*, 22, 76–91. <https://doi.org/10.1111/gcb.12985>

- Santín, C., Doerr, S. H., Jones, M. H., Merino, A., Warneke, C., Roberts, J. M. (2020). The relevance of pyrogenic carbon for carbon budgets from fires: insights from the FIREX experiment. *Global Biogeochemical Cycles*, (C), 1–17. <https://doi.org/10.1029/2020gb006647>
- Santín, C., Doerr, S. H., Merino, A., Bryant, R., Loader, N. J. (2016). Forest floor chemical transformations in a boreal forest fire and their correlations with temperature and heating duration. *Geoderma*, 264, 71–80. <https://doi.org/10.1016/j.geoderma.2015.09.021>
- Santín, C., Doerr, S. H., Merino, A., Bucheli, T. D., Bryant, R., Ascough, P., Gao, X., Masiello, C. A. (2017). Carbon sequestration potential and physicochemical properties differ between wildfire charcoals and slow-pyrolysis biochars. *Scientific Reports*, 7, 1–11. <https://doi.org/10.1038/s41598-017-10455-2>
- Santín, C., Doerr, S. H., Otero, X. L., Chafer, C. J. (2015). Quantity, composition and water contamination potential of ash produced under different wildfire severities. *Environmental Research*, 142, 297–308. <https://doi.org/10.1016/j.envres.2015.06.041>
- Santín, C., Doerr, S. H., Preston, C. M., González-Rodríguez, G. (2015). Pyrogenic organic matter production from wildfires: a missing sink in the global carbon cycle. *Global Change Biology*, 21, 1621–1633. <https://doi.org/10.1111/gcb.12800>
- Santín, C., Doerr, S. H., Shakesby, R. A., Bryant, R., Sheridan, G. J., Lane, P. N. J., Bell, T. L. (2012). Carbon loads, forms and sequestration potential within ash deposits produced by wildfire: New insights from the 2009 “Black Saturday” fires, Australia. *European Journal of Forest Research*, 131, 1245–1253. <https://doi.org/10.1007/s10342-012-0595-8>
- Savage, S. M. (1974). Mechanism of Fire-Induced Water Repellency in Soil. *Soil Science Society of America Journal*, 38, 652–657. <https://doi.org/https://doi.org/10.2136/sssaj1974.03615995003800040033x>
- Scharlemann, J. P. W., Tanner, E. V. J., Hiederer, R., Kapos, V. (2014). Global soil carbon: understanding and managing the largest terrestrial carbon pool. *Carbon Management*, 5, 81–91. <https://doi.org/10.4155/cmt.13.77>
- Schimel, J. P. (2018). Life in Dry Soils: Effects of Drought on Soil Microbial Communities and Processes. *Annual Review of Ecology, Evolution, and Systematics*, 49, 409–432. <https://doi.org/10.1146/annurev-ecolsys-110617-062614>

- Schindlbacher, A., Wunderlich, S., Borke, W., Kitzler, B., Zechmeister-Boltenstern, S., Jandl, R. (2012). Soil respiration under climate change: prolonged summer drought offsets soil warming effects. *Global Change Biology*, 18, 2270–2279. <https://doi.org/10.1111/j.1365-2486.2012.02696.x>
- Schlesinger, W. H., Andrews, J. A. (2000). Soil respiration and the global carbon cycle. *Biogeochemistry*, 48, 7–20. <https://doi.org/10.1023/A:1006247623877>
- Schymanski, S., Grahm, L., Or, D. (2017). The physical origins of rapid soil CO₂ release following wetting. Presented at the EGU General Assembly 23-28 April 2017, Vienna.
- Seaton, F. M., Jones, D. L., Creer, S., George, P. B. L., Smart, S. M., Lebron, I., Barret, G., Emmett, B. A., Robinson, D. A. (2019). Plant and soil communities are associated with the response of soil water repellency to environmental stress. *Science of The Total Environment*, 687, 929–938. <https://doi.org/10.1016/J.SCITOTENV.2019.06.052>
- Serrano-Ortiz, P., Roland, M., Sanchez-Moral, S., Janssens, I. A., Domingo, F., Godd ris, Y., Kowalski, A. S. (2010). Hidden, abiotic CO₂ flows and gaseous reservoirs in the terrestrial carbon cycle: Review and perspectives. *Agricultural and Forest Meteorology*, 150, 321–329. <https://doi.org/10.1016/j.agrformet.2010.01.002>
- Shackleton, C. M., Scholes, R. J. (2000). Impact of fire frequency on woody community structure and soil nutrients in the Kruger National Park. *Koedoe*, 43, 75–81. <https://doi.org/10.4102/koedoe.v43i1.210>
- Shakesby, R. A., Bento, C. P. M., Ferreira, C. S. S., Ferreira, A. J. D., Stoof, C. R., Urbanek, E., Walsh, R. P. D. (2015). Impacts of prescribed fire on soil loss and soil quality: An assessment based on an experimentally-burned catchment in central Portugal. *Catena*, 128, 278–293. <https://doi.org/10.1016/j.catena.2013.03.012>
- Shakesby, R. A., Doerr, S. H. (2006). Wildfire as a hydrological and geomorphological agent. *Earth-Science Reviews*, 74, 269–307. <https://doi.org/10.1016/j.earscirev.2005.10.006>
- Shakesby, R. A., Doerr, S. H., Walsh, R. P. D. (2000). The erosional impact of soil hydrophobicity: Current problems and future research directions. *Journal of Hydrology*, 231–232, 178–191. [https://doi.org/10.1016/S0022-1694\(00\)00193-1](https://doi.org/10.1016/S0022-1694(00)00193-1)
- Shakesby, Richard A., Bento, C. P. M., Ferreira, C. S. S., Ferreira, A. J. D., Stoof, C. R., Urbanek, E., Walsh, R. P. D. (2015). Impacts of prescribed fire on soil loss and soil quality: An

- assessment based on an experimentally-burned catchment in central Portugal. *Catena*, 128, 278–293. <https://doi.org/10.1016/j.catena.2013.03.012>
- Singh, B. P., de Courcelles, V. R., Adams, M. A. (2011). Soil Health and Climate Change. Chapter 7: Soil Respiration in Future Global Change Scenarios. *Soil Biology*, 29, 131–153. <https://doi.org/10.1007/978-3-642-20256-8>
- Singh, R. S. (1994). Changes in soil nutrients following burning of dry tropical savanna. *International Journal of Wildland Fire*, 4, 187–194. <https://doi.org/10.1071/WF9940187>
- Smit, I. P. J., Asner, G. P. (2012). Roads increase woody cover under varying geological, rainfall and fire regimes in African savanna. *Journal of Arid Environments*, 80, 74–80. <https://doi.org/https://doi.org/10.1016/j.jaridenv.2011.11.026>
- Smit, I. P. J., Asner, G. P., Govender, N., Kennedy-Bowdoin, T., Knapp, D. E., Jacobson, J. (2010). Effects of fire on woody vegetation structure in African savanna. *Ecological Applications*, 20, 1865–1875. <https://doi.org/10.1890/09-0929.1>
- Smith, A. P., Bond-Lamberty, B., Benscoter, B. W., Tfaily, M. M., Hinkle, C. R., Liu, C., Bailey, V. L. (2017). Shifts in pore connectivity from precipitation versus groundwater rewetting increases soil carbon loss after drought. *Nature Communications*, 8, 1–11. <https://doi.org/10.1038/s41467-017-01320-x>
- Smith, K. A., Ball, T., Conen, F., Dobbie, K. E., Massheder, J., Rey, A. (2003). Exchange of greenhouse gases between soil and atmosphere: interactions of soil physical factors and biological processes. *European Journal of Soil Science*, 54, 779–791. <https://doi.org/10.1046/j.1365-2389.2003.00567.x>
- Smith, J. L., Collins, H. P., Bailey, V. L. (2010). The effect of young biochar on soil respiration. *Soil Biology and Biochemistry*, 42, 2345–2347. <https://doi.org/10.1016/j.soilbio.2010.09.013>
- Song, J., Liu, Z., Zhang, Y., Yan, T., Shen, Z., Piao, S. (2019). Effects of wildfire on soil respiration and its heterotrophic and autotrophic components in a montane coniferous forest, 12, 336–345. <https://doi.org/10.1093/jpe/rty031>
- Soto, B., Benito, E., Diaz-Fierros, F. (1991). Heat-Induced Degradation Processes in Forest Soils. *International Journal of Wildland Fire*, 1. <https://doi.org/10.1071/WF9910147>

- Sowerby, A., Emmett, B. A., Tietema, A., Beier, C. (2008). Contrasting effects of repeated summer drought on soil carbon efflux in hydric and mesic heathland soils. *Global Change Biology*, *14*, 2388–2404. <https://doi.org/10.1111/j.1365-2486.2008.01643.x>
- Spohn, M., Schleuss, P. M. (2019). Addition of inorganic phosphorus to soil leads to desorption of organic compounds and thus to increased soil respiration. *Soil Biology and Biochemistry*, *130*, 220–226. <https://doi.org/10.1016/j.soilbio.2018.12.018>
- Sponseller, R. A. (2007). Precipitation pulses and soil CO₂ flux in a Sonoran Desert ecosystem. *Global Change Biology*, *13*, 426–436. <https://doi.org/10.1111/j.1365-2486.2006.01307.x>
- Startsev, V. V., Dymov, A. A., Prokushkin, A. S. (2017). Soils of postpyrogenic larch stands in Central Siberia: Morphology, physicochemical properties, and specificity of soil organic matter. *Eurasian Soil Science*, *50*, 885–897. <https://doi.org/10.1134/S1064229317080117>
- Stockmann, U., Adams, M. A., Crawford, J. W., Field, D. J., Henakaarchchi, N., Jenkins, M., Minasny, B., McBratney, A. B., de Courcelles, V. R., Singh, K., Wheeler, I., Abbott, K., Angers, D. A., Baldock, J., Bird, M., Brookes, P. C., Chenu, C., Jastrow, J. D., Lal, R., Lehmann, J., O'Donnell, A. G., Parton, W. J., Whitehead, D., Zimmermann, M. (2013). The knowns, known unknowns and unknowns of sequestration of soil organic carbon. *Ecosystems and Environment*, *164*, 80–99. <http://dx.doi.org/10.1016/j.agee.2012.10.001>
- Stoof, C. R., Wesseling, J. G., Ritsema, C. J. (2010). Effects of fire and ash on soil water retention. *Geoderma*, *159*, 276–285. <https://doi.org/10.1016/j.geoderma.2010.08.002>
- Subke, J. A., Inghima, I., Cotrufo, M. F. (2006). Trends and methodological impacts in soil CO₂ efflux partitioning: A metaanalytical review. *Global Change Biology*. Blackwell Publishing Ltd. <https://doi.org/10.1111/j.1365-2486.2006.01117.x>
- Tecon, R., Or, D. (2017). Biophysical processes supporting the diversity of microbial life in soil. *FEMS Microbiology Reviews*, *41*, 599–623. <https://doi.org/10.1093/femsre/fux039>
- Thomas, A. D., Dougill, A. J., Elliott, D. R., Mairs, H. (2014). Seasonal differences in soil CO₂ efflux and carbon storage in Ntwetwe Pan, Makgadikgadi Basin, Botswana. *Geoderma*, *219–220*, 72–81. <https://doi.org/10.1016/j.geoderma.2013.12.028>
- Thomas, A. D., Hoon, S. R. (2010). Carbon dioxide fluxes from biologically-crusted Kalahari Sands after simulated wetting. *Journal of Arid Environments*, *74*, 131–139. <https://doi.org/10.1016/j.jaridenv.2009.07.005>

- Trenberth, K. E., Dai, A., van der Schrier, G., Jones, P. D., Barichivich, J., Briffa, K. R., Sheffield, J. (2013). Global warming and changes in drought. *Nature Climate Change*, 4, 17. <https://doi.org/https://doi.org/10.1038/nclimate2067>
- Úbeda, X. (1999). Structural changes on soils after forest fires. In *Extended Abstracts of 6th International Meeting of Soils with Mediterranean Type of Climate*. (pp. 793–796). Barcelona, Spain: Universitat de Barcelona.
- Ulery, A. L., Graham, R. C. (1993). Forest Fire Effects on Soil Color and Texture. *Soil Science Society of America Journal*, 57, 135–140. <https://doi.org/https://doi.org/10.2136/sssaj1993.03615995005700010026x>
- Urbanek, E., Bodi, M., Doerr, S. H., Shakesby, R. A. (2010). Influence of Initial Water Content on the Wettability of Autoclaved Soils. *Soil Science Society of America Journal*, 74, 2086–2088. <https://doi.org/10.2136/sssaj2010.0164N>
- Urbanek, E., Doerr, S. H. (2017). CO₂ efflux from soils with seasonal water repellency. *Biogeosciences*, 14, 4781–4794. <https://doi.org/https://doi.org/10.5194/bg-14-4781-2017>
- Urbanek, E., Hallett, P., Feeney, D., Horn, R. (2007). Water repellency and distribution of hydrophilic and hydrophobic compounds in soil aggregates from different tillage systems. *Geoderma*, 140, 147–155. <https://doi.org/10.1016/j.geoderma.2007.04.001>
- Urbanek, E., Shakesby, R. A. (2009). Impact of stone content on water movement in water-repellent sand. *European Journal of Soil Science*, 60, 412–419. <https://doi.org/10.1111/j.1365-2389.2009.01128.x>
- Urbanek, E., Walsh, R. P. D., Shakesby, R. A. (2015). Patterns of soil water repellency change with wetting and drying: The influence of cracks, roots and drainage conditions. *Hydrological Processes*, 29, 2799–2813. <https://doi.org/10.1002/hyp.10404>
- Van Der Werf, G. R., Randerson, J. T., Giglio, L., Van Leeuwen, T. T., Chen, Y., Rogers, B. M., Mu, M., Van Markle, M. J. E., Morton, D. C., Collatz, G. J., Yokelson, R. J., Kasibhatla, P. S. (2017). Global fire emissions estimates during 1997–2016. *Earth System Science Data*, 9, 697–720. <https://doi.org/10.5194/essd-9-697-2017>
- van Reeuwijk, L. P. (2002). *Procedures for soil analysis* (Sixth). Wageningen: ISRIC, FAO.
- van Straaten, O., Doamba, S. W. M. F., Corre, M. D., Veldkamp, E. (2019). Impacts of burning

- on soil trace gas fluxes in two wooded savanna sites in Burkina Faso. *Journal of Arid Environments*, 165, 132–140. <https://doi.org/10.1016/j.jaridenv.2019.02.013>
- Valzano, F. P., Greene, R. S. B., Murphy, B. W. (1997). Direct effects of stubble burning on soil hydraulic and physical properties in a direct drill tillage system. *Soil and Tillage Research*, 42, 209–219. [https://doi.org/https://doi.org/10.1016/S0167-1987\(96\)01101-4](https://doi.org/https://doi.org/10.1016/S0167-1987(96)01101-4)
- Vargas, R., Collins, S. L., Thomey, M. L., Johson, J. E., Brown, R. F., Natvig, D. O, Friggens, M. T. (2012). Precipitation variability and fire influence the temporal dynamics of soil CO₂ efflux in an arid grassland. *Global Change Biology*, 18, 1401–1411. <https://doi.org/10.1111/j.1365-2486.2011.02628.x>
- Vargas, R, Detto, M., Baldocchi, D. (2010). Multiscale analysis of temporal variability of soil CO₂ production as influenced by weather and vegetation. *Global Change*. Retrieved from <http://onlinelibrary.wiley.com/doi/10.1111/j.1365-2486.2009.02111.x/full>
- Venter, F. J., Govender, N. (2012). A geomorphic and soil description of the long-term fire experiment in the Kruger National Park, South Africa. *Koedoe; Vol 54, No 1*. Retrieved from <https://koedoe.co.za/index.php/koedoe/article/view/1037>
- Vega, J. A., Fontúrbel, T., Merino, A., Fernández, C., Ferreira, A., Jiménez, E. (2013). Testing the ability of visual indicators of soil burn severity to reflect changes in soil chemical and microbial properties in pine forests and shrubland. *Plant and Soil*, 369(1), 73–91. <https://doi.org/10.1007/s11104-012-1532-9>
- Vicca, S., Bahn, M., Estiarte, M., Van Loon, E. E., Vargas, R., Alberti, G., Ambus, P., Arain, M. A., Beier, C., Bentley, L. P., Borken, W., Buchmann, N., Collins, S. L., De Dato, G., Dukes, J. S., Escolar, C., Fay, P., Guidolotti, G., Hanson, P. J., Kahmen, A., Kröel-Dulay, G., Ladreiter-Knauss, T., Larsen, K. S., Lellei-Kovacs, E., Lebrija-Trejos, E., Maestre, F. T., Marhan, S., Marshall, M., Meir, P., Miao, Y., Muhr, J., Niklaus, P. A., Ogaya, R., Peñuelas, J., Poll, C., Rustad, L. E., Savage, K., Schindlbacher, A., Schmidt, I. K., Smith, A. R., Sotta, E. D., Suseela, V., Tietema, A., Van Gestel, N., Van Straaten, O., Wan, S., Weber, U., Janssens, I. A. (2014). Can current moisture responses predict soil CO₂ efflux under altered precipitation regimes? A synthesis of manipulation experiments. *Biogeosciences*, 11, 2991–3013. <https://doi.org/10.5194/bg-11-2991-2014>
- Vlamiš, J., Gowans, K. D. (1961). Availability of Nitrogen, Phosphorus, and Sulfur after Brush Burning. *Journal of Range Management*, 14, 38. <https://doi.org/10.2307/3894829>

- Wang, X., Cammeraat, E. L. H., Romeijn, P., Kalbitz, K. (2014). Soil Organic Carbon Redistribution by Water Erosion – The Role of CO₂ Emissions for the Carbon Budget. *PLOS ONE*, 9, e96299. Retrieved from <https://doi.org/10.1371/journal.pone.0096299>
- Wang, Q., He, N., Liu, Y., Li, M., Xu, L. (2016). Strong pulse effects of precipitation events on soil microbial respiration in temperate forests. *Geoderma*, 275, 67–73. <https://doi.org/10.1016/j.geoderma.2016.04.016>
- Wang, Z., Wu, Q., Wu, L., Ritsema, C., Dekker, L., Feyen, J. (2000). Effects of soil water repellency on infiltration rate and flow instability. *Journal of Hydrology*, 231–232, 265–276. [https://doi.org/10.1016/S0022-1694\(00\)00200-6](https://doi.org/10.1016/S0022-1694(00)00200-6)
- Waring, B. G., Powers, J. S. (2016). Unraveling the mechanisms underlying pulse dynamics of soil respiration in tropical dry forests. *Environmental Research Letters*, 11. <https://doi.org/10.1088/1748-9326/11/10/105005>
- Wei, F., Wang, S., Fu, B., Brandt, M., Pan, N., Wang, C., Fensholt, R. (2020). Nonlinear dynamics of fires in Africa over recent decades controlled by precipitation. *Global Change Biology*, 26, 4495–4505. <https://doi.org/10.1111/gcb.15190>
- White, I., Colomera, P. M., Philip, J. R. (1977). Experimental Studies of Wetting Front Instability Induced by Gradual Change of Pressure Gradient and by Heterogeneous Porous Media1. *Soil Science Society of America Journal*, 41, 483–489. <https://doi.org/10.2136/sssaj1977.03615995004100030010x>
- Woods, S. W., Balfour, V. N. (2008). The effect of ash on runoff and erosion after a severe forest wildfire, Montana, USA. *International Journal of Wildland Fire*, 17(5), 535–548. <https://doi.org/10.1071/WF07040>
- Woods, S. W., Balfour, V. N. (2010). The effects of soil texture and ash thickness on the post-fire hydrological response from ash-covered soils. *Journal of Hydrology*, 393(3–4), 274–286. <https://doi.org/10.1016/j.jhydrol.2010.08.025>
- Wofford, P., Vidrio, E. (2015). *Procedure for Determining Soil Particle Density Using Gay-Lussac Specific-Gravity Bottles*. Sacramento.
- Wüthrich, C., Schaub, D., Weber, M., Marxer, P., Conedera, M. (2002). Soil respiration and soil microbial biomass after fire in a sweet chestnut forest in southern Switzerland. *Catena*, 48, 201–215. [https://doi.org/10.1016/S0341-8162\(01\)00191-6](https://doi.org/10.1016/S0341-8162(01)00191-6)

- Xiang, S. R., Doyle, A., Holden, P. A., Schimel, J. P. (2008). Drying and rewetting effects on C and N mineralization and microbial activity in surface and subsurface California grassland soils. *Soil Biology and Biochemistry*, *40*, 2281–2289. <https://doi.org/10.1016/j.soilbio.2008.05.004>
- Zepp, G., Miller, L., Burke, A., Parsons, D. A. B., Scholes, M. C., Service, P. (1996). Effects of moisture and burning on soil-atmosphere exchange of trace carbon gases in a southern African savanna. *Journal of Geophysical Research*, *101*, 23699–23706. <https://doi.org/10.1029/95JD01371>
- Zhuravleva, A. I., Myakshina, T. N., Blagodatskaya, E. V. (2011). The effect of pyrogenically modified substrates on mineralizing activity and growth strategies of microorganisms of grey forest soil. *Microbiology*, *80*, 194–204. <https://doi.org/10.1134/S0026261711020202>
- Zimmermann, M., Bird, M. I., Wurster, C., Saiz, G., Goodrick, I., Barta, J., Capek, P., Santruckova, H., Smernik, R. (2012). Rapid degradation of pyrogenic carbon. *Global Change Biology*, *18*, 3306–3316. <https://doi.org/10.1111/j.1365-2486.2012.02796.x>
- Zimmermann, S., Frey, B. (2002). Soil respiration and microbial properties in an acid forest soil: Effects of wood ash. *Soil Biology and Biochemistry*. [https://doi.org/10.1016/S0038-0717\(02\)00160-8](https://doi.org/10.1016/S0038-0717(02)00160-8)
- Zubkova, M., Boschetti, L., Abatzoglou, J. T., Giglio, L. (2019). Changes in Fire Activity in Africa from 2002 to 2016 and Their Potential Drivers. *Geophysical Research Letters*, *46*, 7643–7653. <https://doi.org/10.1029/2019GL083469>